Vortex bound states in conventional and topological superconductors

Hai-Hu Wen

Physics Department, Nanjing University, China

XXVI Int. Summer School "Nicolas Cabrera"
Madrid, Sept. 8-13, 2019

Outline of the lecture

- **Introduction**
- **Caroli-de Gennes-Matricon states and possible Majorana modes in vortex cores of $FeTe_{0.55}Se_{0.45}$**

  Nat. Commun. 9, 970(2018). arXiv.1909.01686
- **Nematic superconductivity and ZBCPs in $Sr_xBi_2Se_3$ and $Bi_2Te_3/FeTe_{0.55}Se_{0.45}$**

  Nat. Commun. 8, 14466 (2017).

  Sci. Adv. 4, eaat1084 (2018).
- **Concluding remarks**

Outline of the lecture

- **Introduction**
- Caroli-de Gennes-Matricon states and possible Majorana modes in vortex cores of $FeTe_{0.55}Se_{0.45}$

  Nat. Commun. 9, 970(2018). arXiv.1909.01686
- Nematic superconductivity in $Sr_xBi_2Se_3$ and $Bi_2Te_3/FeTe_{0.55}Se_{0.45}$

  Nat. Commun. 8, 14466 (2017).

  Sci. Adv. 4, eaat1084 (2018).
- Concluding remarks

Ginzburg-Landau theory

V. L. Ginzburg, L. D. Landau, Zh. Eksperim. I Teor. Fiz. 20, 1064(1950).

2003 Nobel Prize

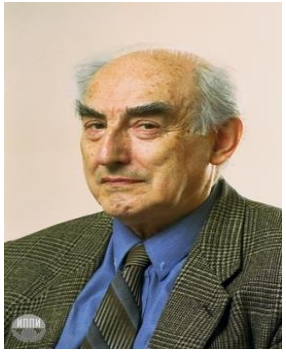

V. L. Ginzburg A. A. Abrikosov

$$\psi(r) = \psi_0 e^{i\varphi}$$

$$g_s(T,H) = f_n(T,0) + \alpha|\psi|^2 + \frac{\beta}{2}|\psi|^4 + \frac{1}{2m^*}|(-i\hbar\nabla - e^* A)\psi|^2 + \frac{1}{2\mu_0}B^2 - B \bullet H$$

GL-I

$$\alpha\psi + \beta|\psi|^2\psi + \frac{1}{2m^*}\left(\frac{\hbar}{i}\nabla - \frac{e^*}{c}\vec{A}\right)^2\psi = 0$$

$$\xi^2(T) = \frac{\hbar^2}{2m^*|\alpha(T)|}$$

GL-II

$$j_s = \frac{e^*\hbar}{2m^* i}(\psi^*\nabla\psi - \psi\nabla\psi^*) - \frac{e^{*2}}{m^* c}\psi^*\psi\vec{A}$$

$$= \frac{e^*}{m^*}|\psi|^2(\hbar\nabla\phi - \frac{e^{*2}}{m^*}\vec{A}) = e^*|\psi|^2\vec{v}_s$$

$$\lambda^2 = \frac{m^*}{\mu_0 e^{*2}|\psi_0|^2}$$

L. P. Gor'kov, JETP 9, 1364(1959). A.A.Abrikosov, JETP 5, 1174(1957).

Interface energy between N-SC areas

$$\sigma_{NS} = \int_{-\infty}^{\infty} [-\frac{\beta}{2}|\psi|^4 + \frac{(B-\mu_0 H_c)^2}{2\mu_0}]dx$$

$$\kappa = \frac{\lambda}{\xi}$$

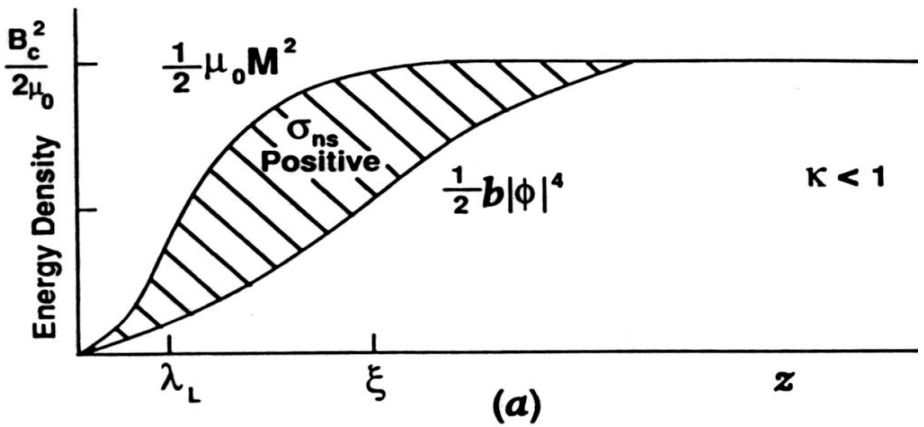

(a)

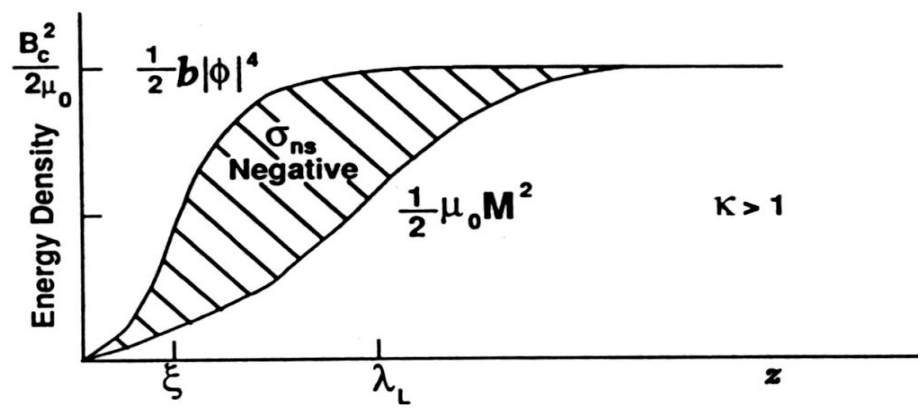

(b)

$$\kappa = \frac{1}{\sqrt{2}}, \quad \sigma = 0,$$

$$\kappa < \frac{1}{\sqrt{2}}, \quad \sigma > 0,$$

Type-I

$$\kappa > \frac{1}{\sqrt{2}}, \quad \sigma < 0,$$

Type-II

By solving the GL Equations in case of type-II SC, vortex lattice was predicted

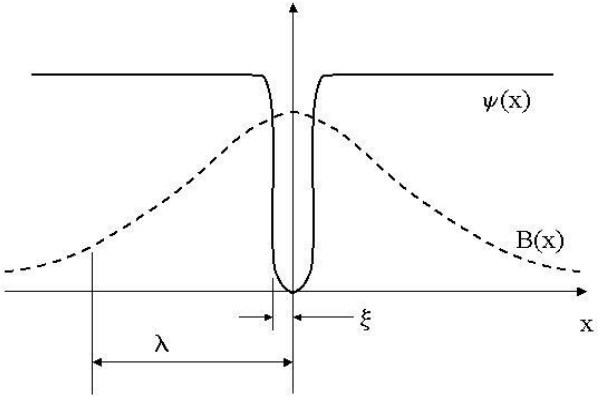

$$\Phi_0 = \frac{h}{2e}$$

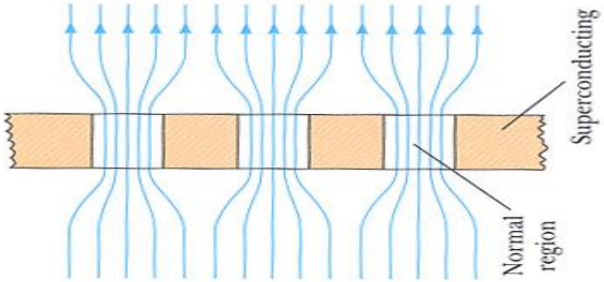

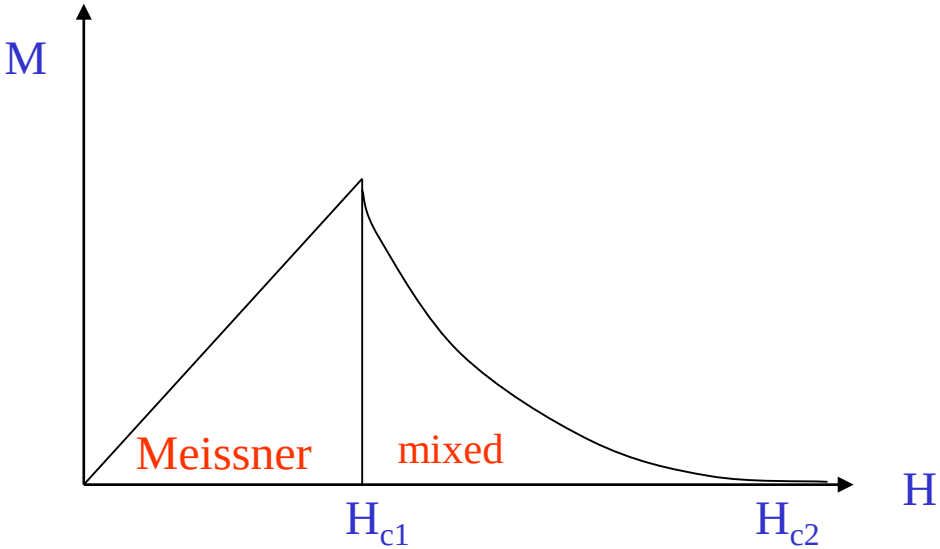

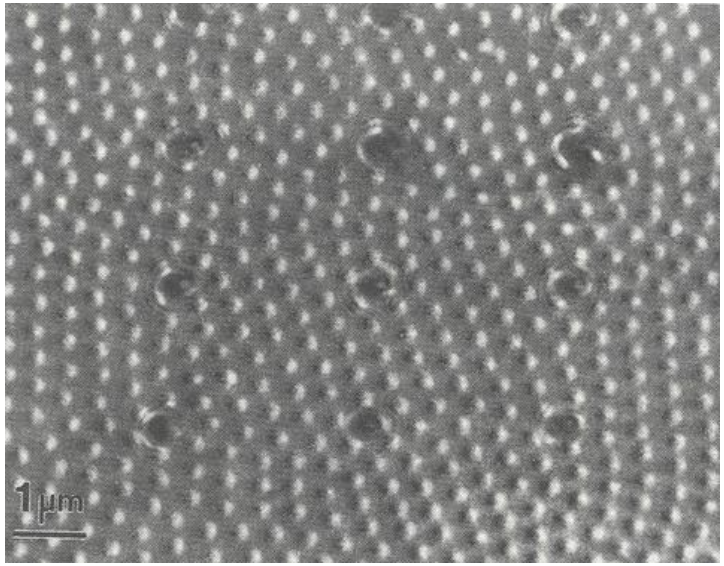

A.A.Abrikosov, JETP 5, 1174(1957).

Vortex structure of a single vortex

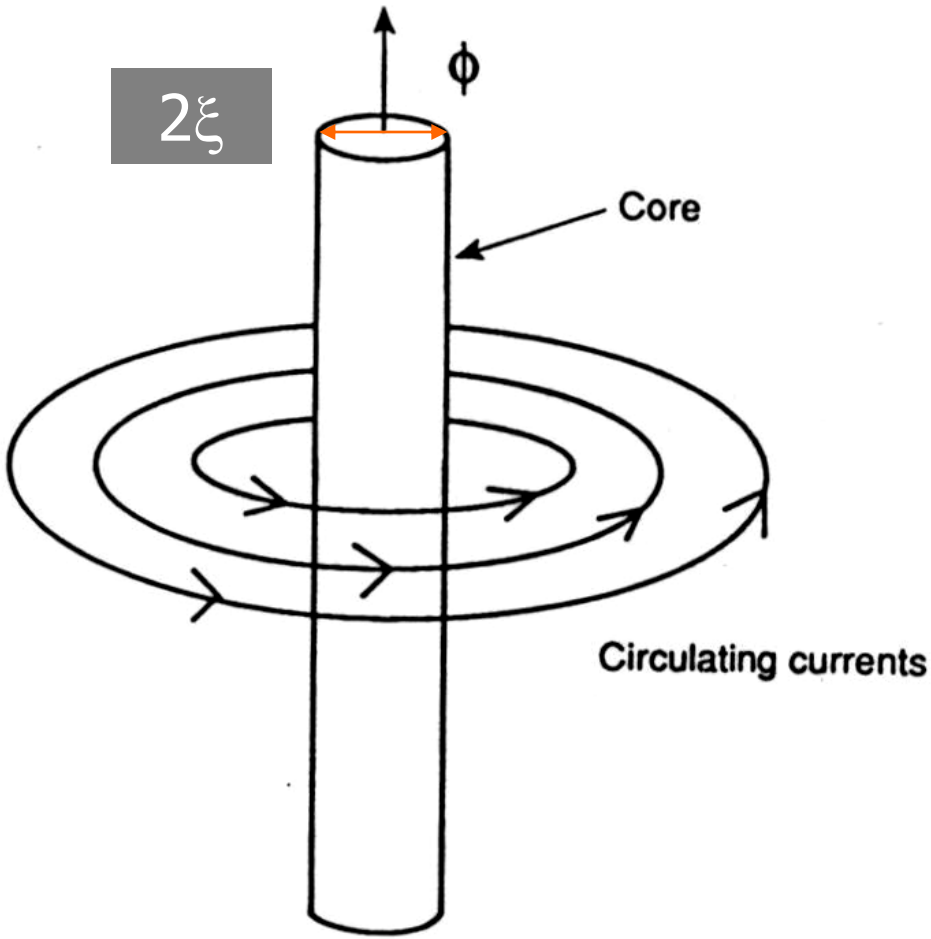

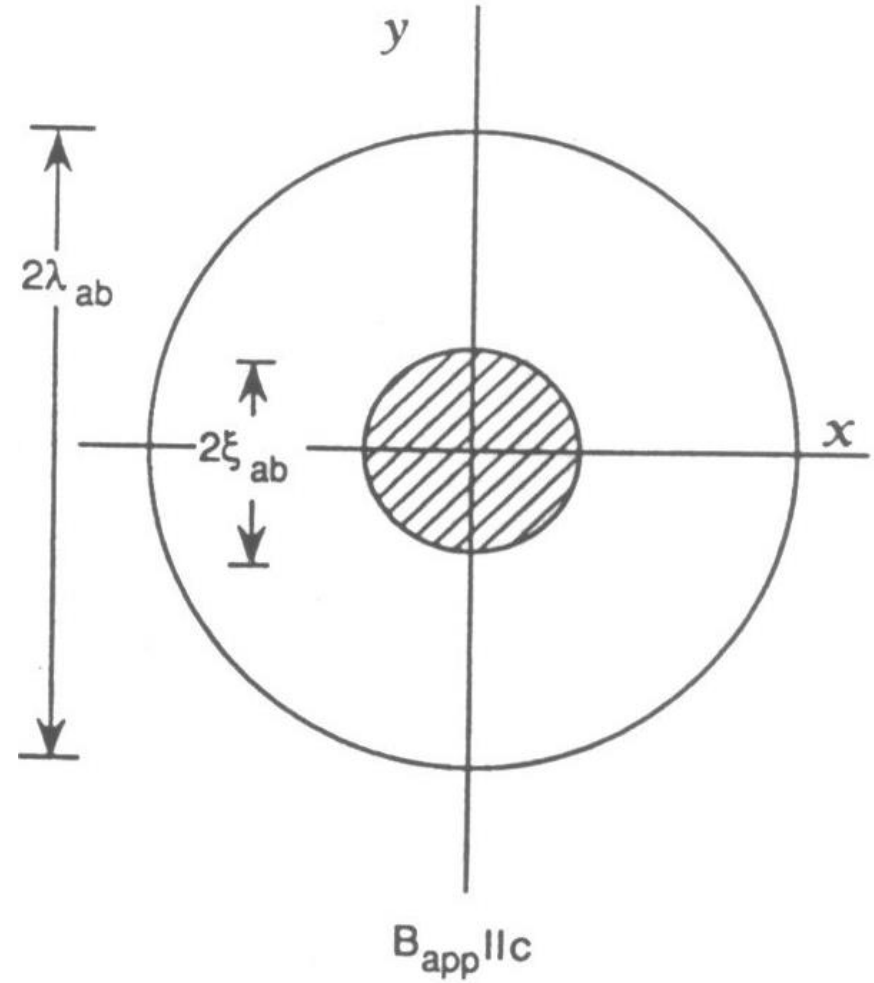

Bogoliubov QPs are confined with the vortex core with size of ξ, leading to the vortex bound states.

Outline of the lecture

- Introduction
- **Caroli-de Gennes-Matricon states and possible Majorana modes in vortex cores of $FeTe_{0.55}Se_{0.45}$**

  Nat. Commun. 9, 970(2018). arXiv.1909.01686
- Nematic superconductivity and ZBCPs in $Sr_xBi_2Se_3$ and $Bi_2Te_3/FeTe_{0.55}Se_{0.45}$

  Nat. Commun. 8, 14466 (2017).

  Sci. Adv. 4, eaat1084 (2018).
- Concluding remarks

Volume 9, number 4 PHYSICS LETTERS 1 May 1964

BOUND FERMION STATES ON A VORTEX LINE IN A TYPE II SUPERCONDUCTOR

C. CAROLI, P. G. DE GENNES, J. MATRICON
Service de Physique des Solides, Faculté des Sciences, Orsay (S & O)

Received 31 March 1964

This note discusses the excitations of low energy $\epsilon \ll \Delta_\infty$ (where Δ_∞ is the gap in zero field) which exist near an Abrikosov vortex line [1] in a pure superconductor of type II. The energy gap ϵ_0 for these excitations is very small $\epsilon_0 \sim \Delta_\infty^2/E_F$ where E_F is the Fermi energy. Above ϵ_0 the density of states is finite and comparable to that of a cylinder of normal metal of radius ξ (the coherence length). These low lying states will play a major role in the discussion of transport and relaxation phenomena in type II superconductors at low temperatures.

mean free path $l > \xi$

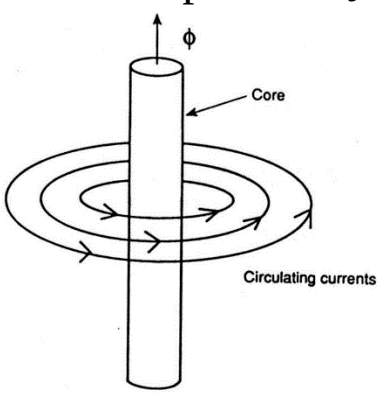

$$\epsilon(k,r) = \{\Delta_\infty^2 + \xi_k^2\}^{\frac{1}{2}} + \hbar v_S \cdot k$$

$$\epsilon u(r) = \left[\frac{1}{2m}\left(p - \frac{eA}{c}\right)^2 - E_F\right] u(r) + W(r)\, v(r) \,,$$

$$\epsilon v(r) = \left[-\frac{1}{2m}\left(p + \frac{eA}{c}\right)^2 + E_F\right] v(r) + W(r)\, u(r) \,.$$

$$W(r) = \Delta(r)\, e^{-i\theta}$$

$$E_\mu = \mu\Delta^2/E_F$$

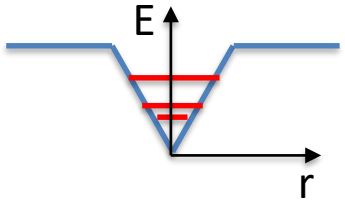

Discrete energy levels of CdGM bound states should be observed.

C. Caroli, P. G. de Gennes, J. J. Matricon, *J. Phys. Lett.* **9**, 307-309 (1964).

To observe the discrete CdGM states, it must be in the **Quantum Limit**

$$\frac{T}{T_c} \ll \frac{\Delta}{E_F} \sim \frac{1}{k_F \xi_0}$$

This is very hard in conventional supercond uctors, because Δ/E_F ~10^{-3}. Quantum limit w ould mean T≤ 10 mK.

2H-NbSe2; T ≈ 0.3 K *B* = 0.05 T

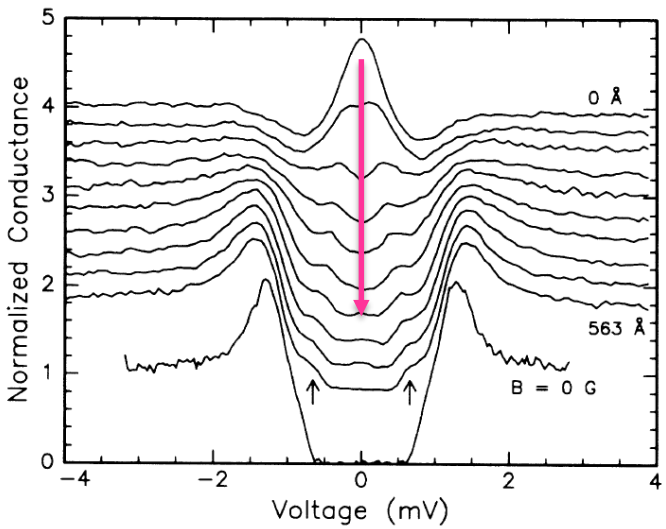

H. F. Hess, *et al.*, PRL 64, 2711 (1990).

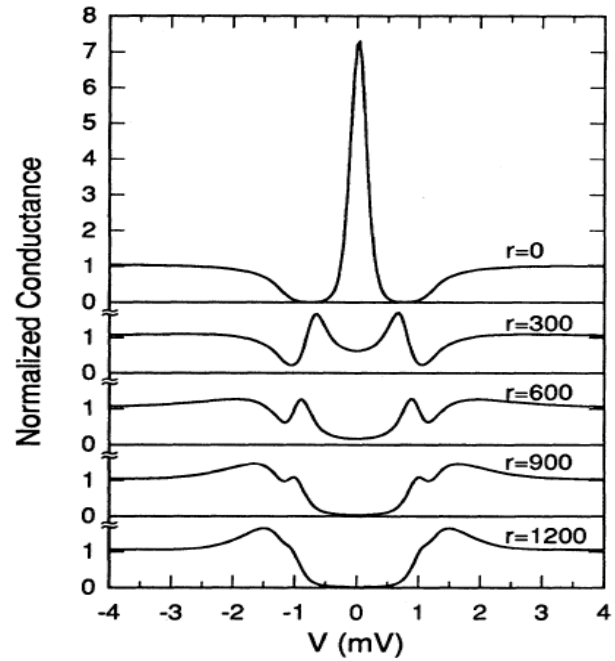

F. Gygi, and M. Schluter, PRB 43, 7609 (1991).

For 53 years, the discrete CdGM bound states with different energy levels have not been really observed!

$$E_{CdGM} = \mu \frac{\Delta^2}{E_F}$$

Low-Lying Quasiparticle Excitations around a Vortex Core in Quantum Limit

N. Hayashi, T. Isoshima, M. Ichioka, and K. Machida. Phys. Rev. Lett.80, 2921 (1998).

$$\left[\frac{-1}{2k_F\xi_0}\nabla^2 - E_F\right]u_j(\mathbf{r}) + \Delta(\mathbf{r})v_j(\mathbf{r}) = E_j u_j(\mathbf{r})$$

$$-\left[\frac{-1}{2k_F\xi_0}\nabla^2 - E_F\right]v_j(\mathbf{r}) + \Delta^*(\mathbf{r})u_j(\mathbf{r}) = E_j v_j(\mathbf{r})$$

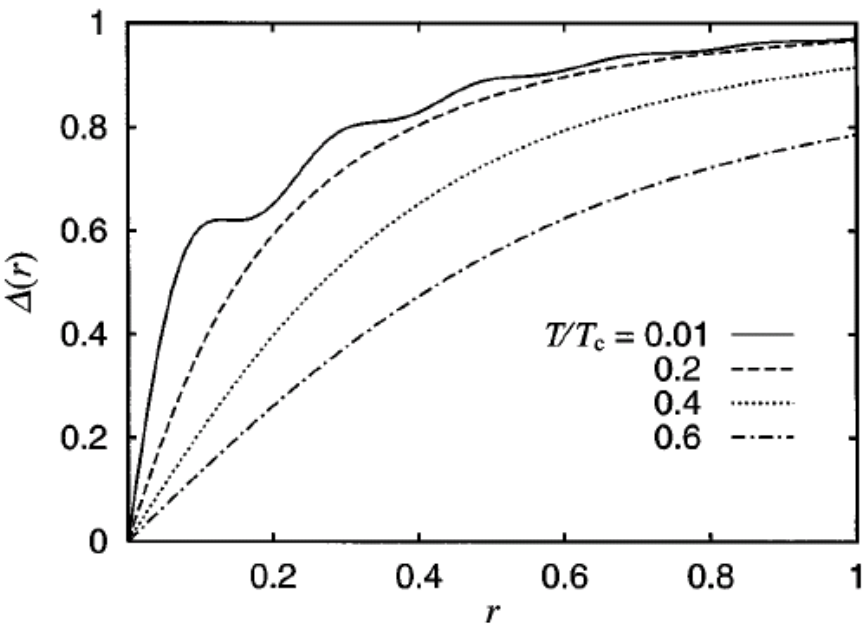

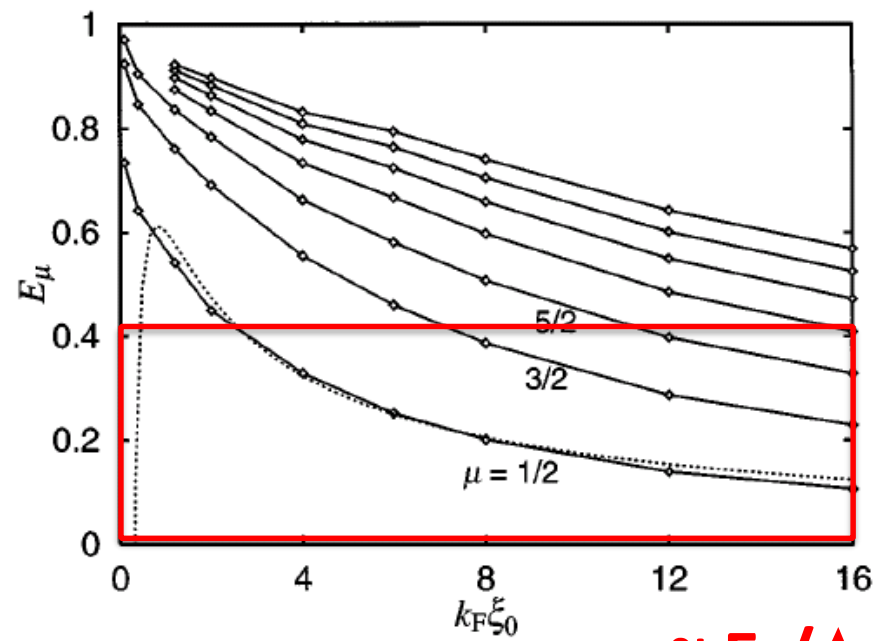

~ E_F/Δ

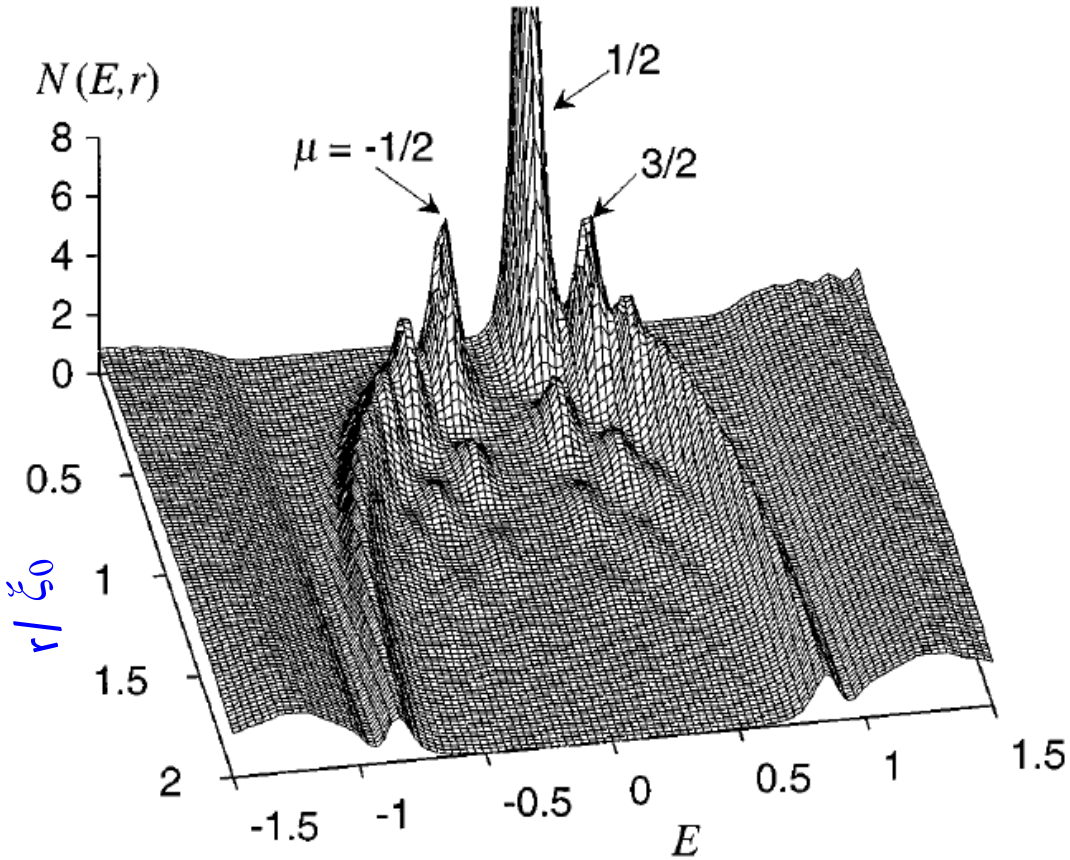

$$\frac{T}{T_c} \ll \frac{\Delta}{E_F} \sim \frac{1}{k_F \xi_0}$$

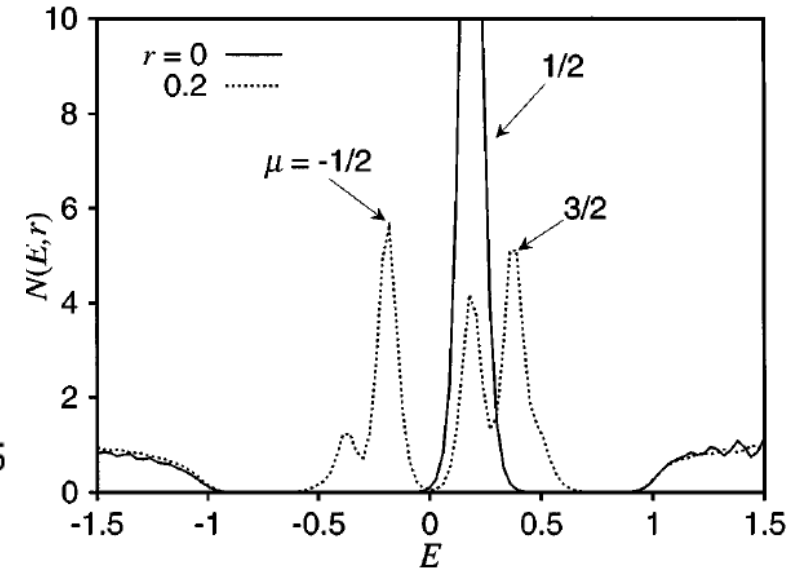

$$E_\mu = \mu\Delta^2/E_F$$

$$\mu = 1/2, 3/2, 5/2, \ldots$$

The particle-hole asymmetry in the vortex bound states in the quantum limit for single band.

N. Hayashi, T. Isoshima, M. Ichioka, and K. Machida, Phys. Rev. Lett. 80 2921 (2000).

Sub-gap states in cuprate

Revisiting the vortex-core tunnelling spectroscopy in $YBa_2Cu_3O_{7-\delta}$

Jens Bruér,[1] Ivan Maggio-Aprile,[1] Nathan Jenkins,[1] Zoran Ristić,[1] Andreas Erb,[2] Christophe Berthod,[1] Øystein Fischer,[1] and Christoph Renner[1,*]

PRL1995

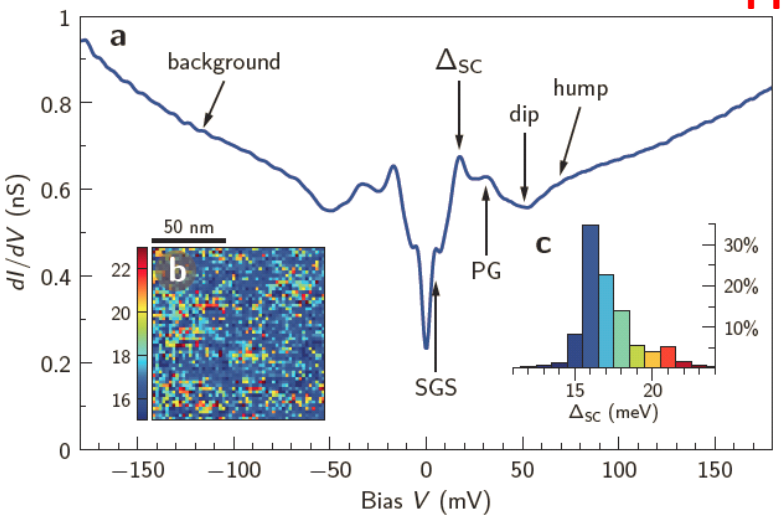

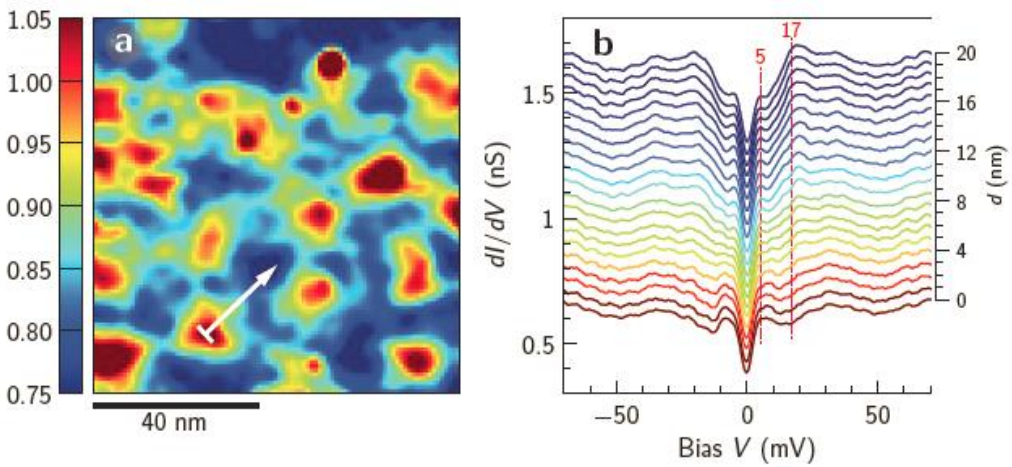

Nat. Commun. 7, 11139(2016).

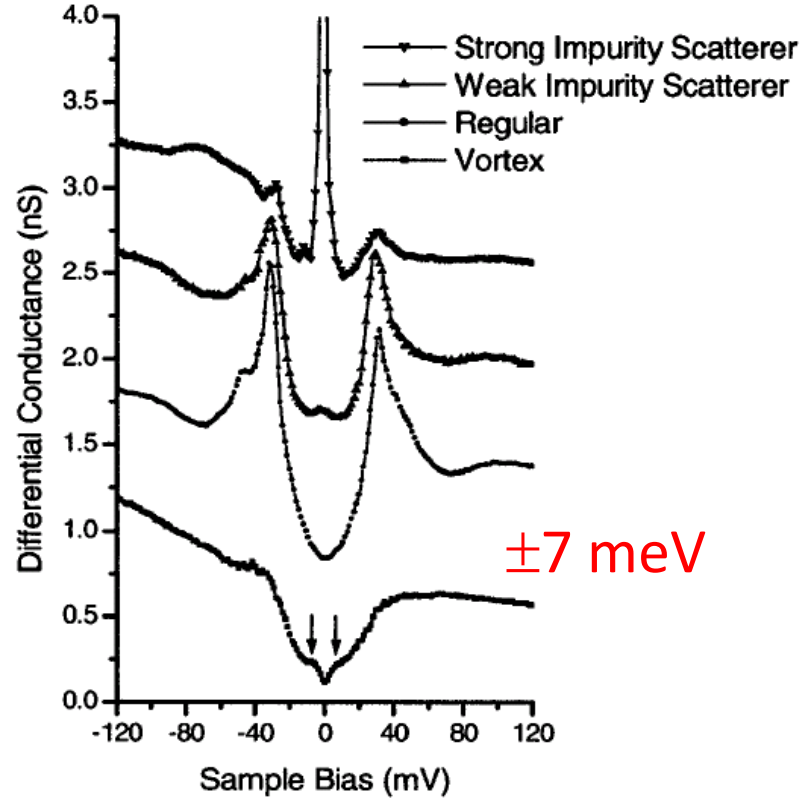

S. H. Pan et al., Nature 85, 1536(1996).

- **Two symmetric peaks around zero bias**
- **It appears inside and outside vortex core, could be competing order**
- **E_F not well defined in cuprates**

STM/STS measurements

$$I = \frac{4\pi e}{\hbar}\int_{-\infty}^{\infty}\left[\mathrm{f}(\varepsilon - eV) - \mathrm{f}(\varepsilon)\right]\rho_s(\varepsilon)\rho_t(\varepsilon - eV)\left|M\right|^2 \mathrm{d}\varepsilon$$

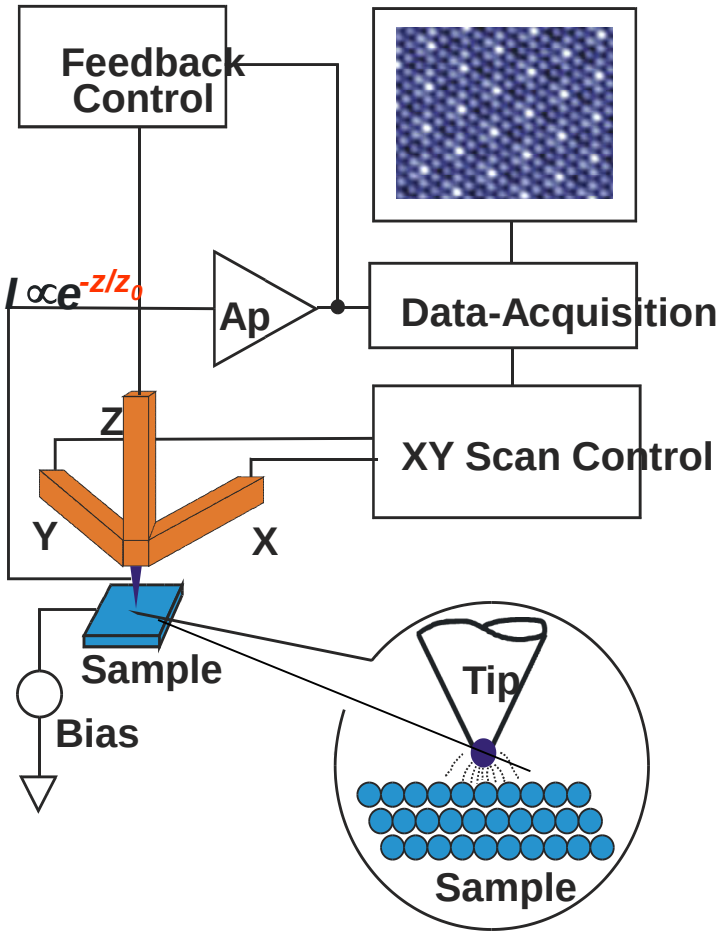

Spatial mapping

- **I/V → Image**
- **dI/dV → LDOS**
- **d^2I/dV^2 → interaction between the electrons and the bosonic excitations**
- **Fourier transform: from real space to momentum space**

$FeTe_{0.55}Se_{0.45}$

Post anneal the sample to achieve the best SC transition, before the STM study.

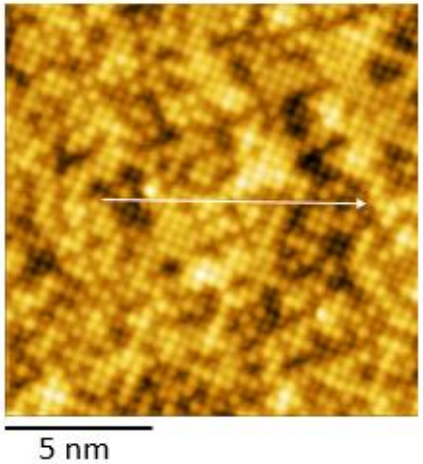

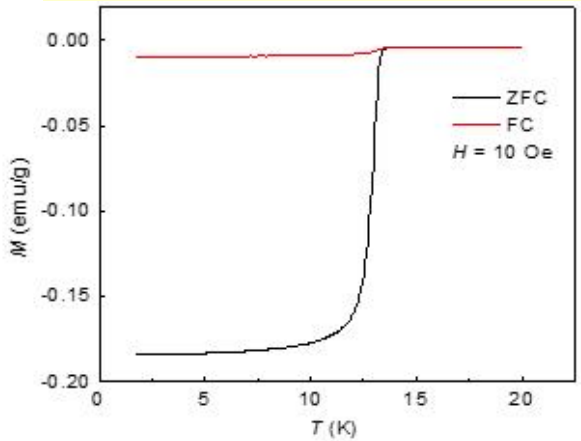

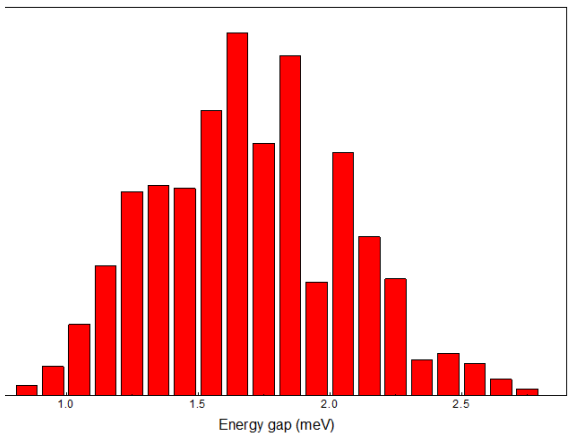

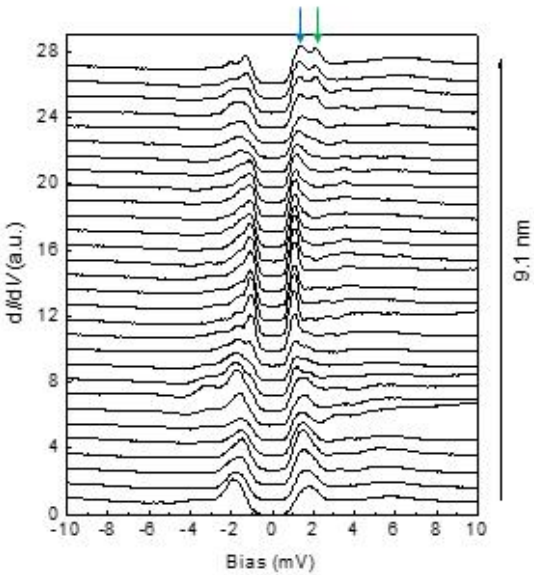

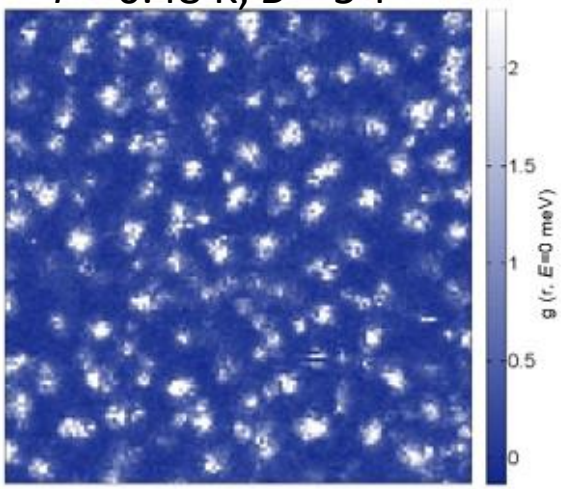

Full gap structure

It shows one or two coherence peaks

M. Y. Chen, et al.,
Nature Communications 9, 970 (2018).

Three discreet energy levels on positive bias (about 20% vortices)

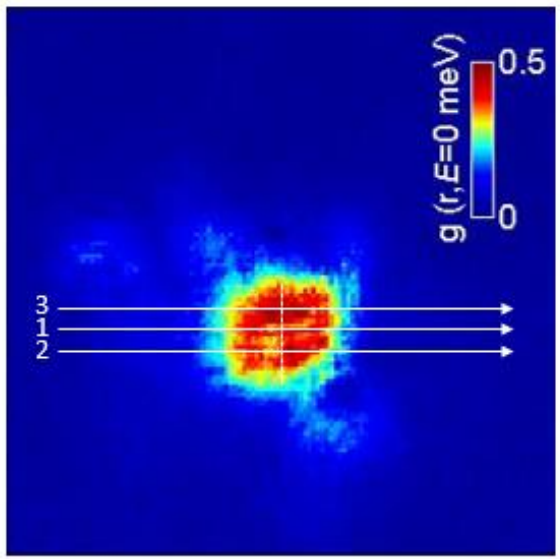

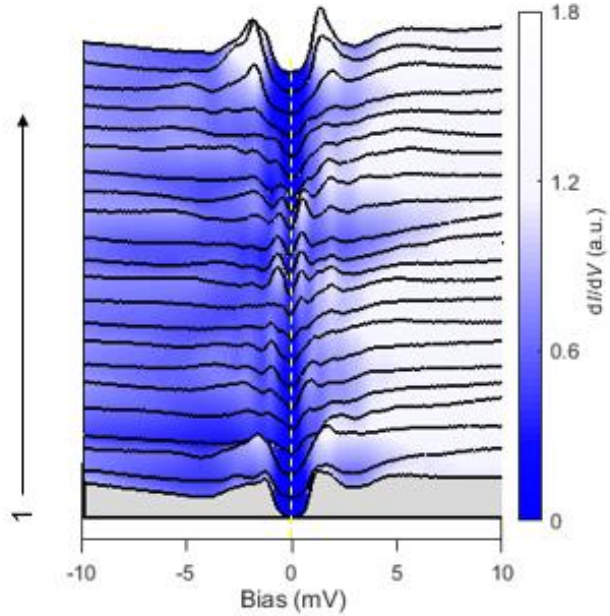

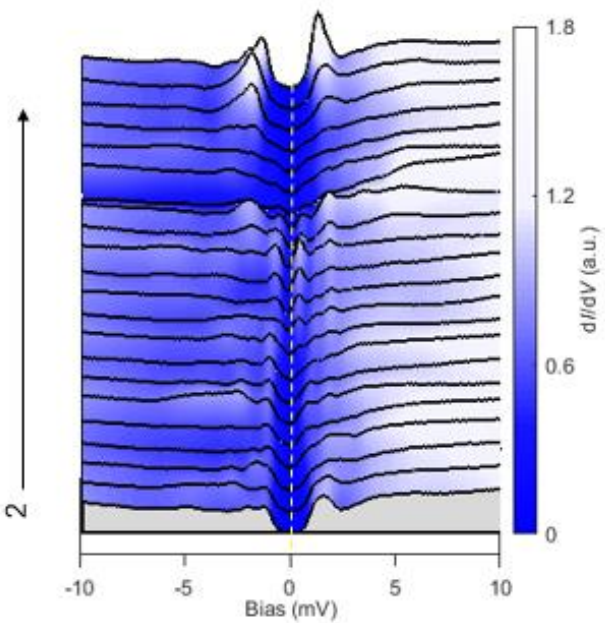

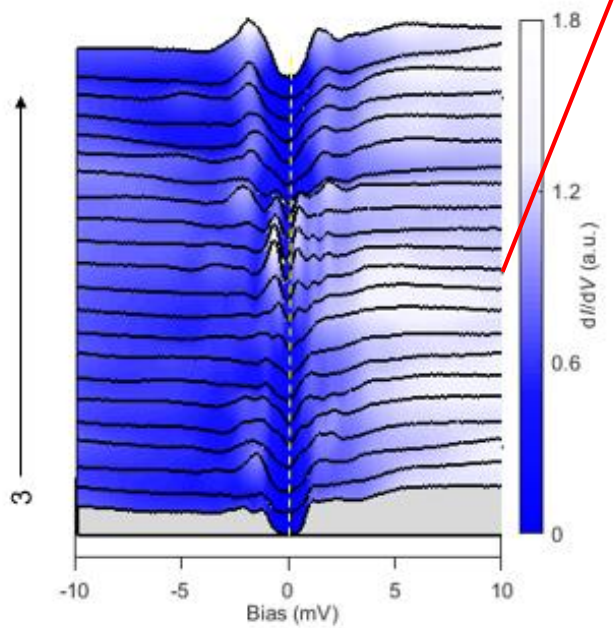

+0.45, +1.2, and +1.8 meV

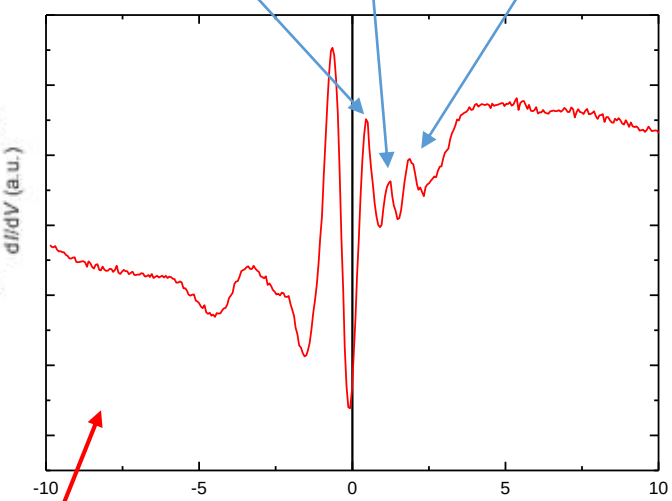

$E_{1/2}/E_{3/2}/E_{5/2}$

$=1/2.7/4.2$

$E_\mu = \mu\Delta^2/E_F$

$\mu = 1/2, 3/2, 5/2, \ldots$

M. Y. Chen, H. Yang, HHW et al. Nature Commun. 9, 970(2018).

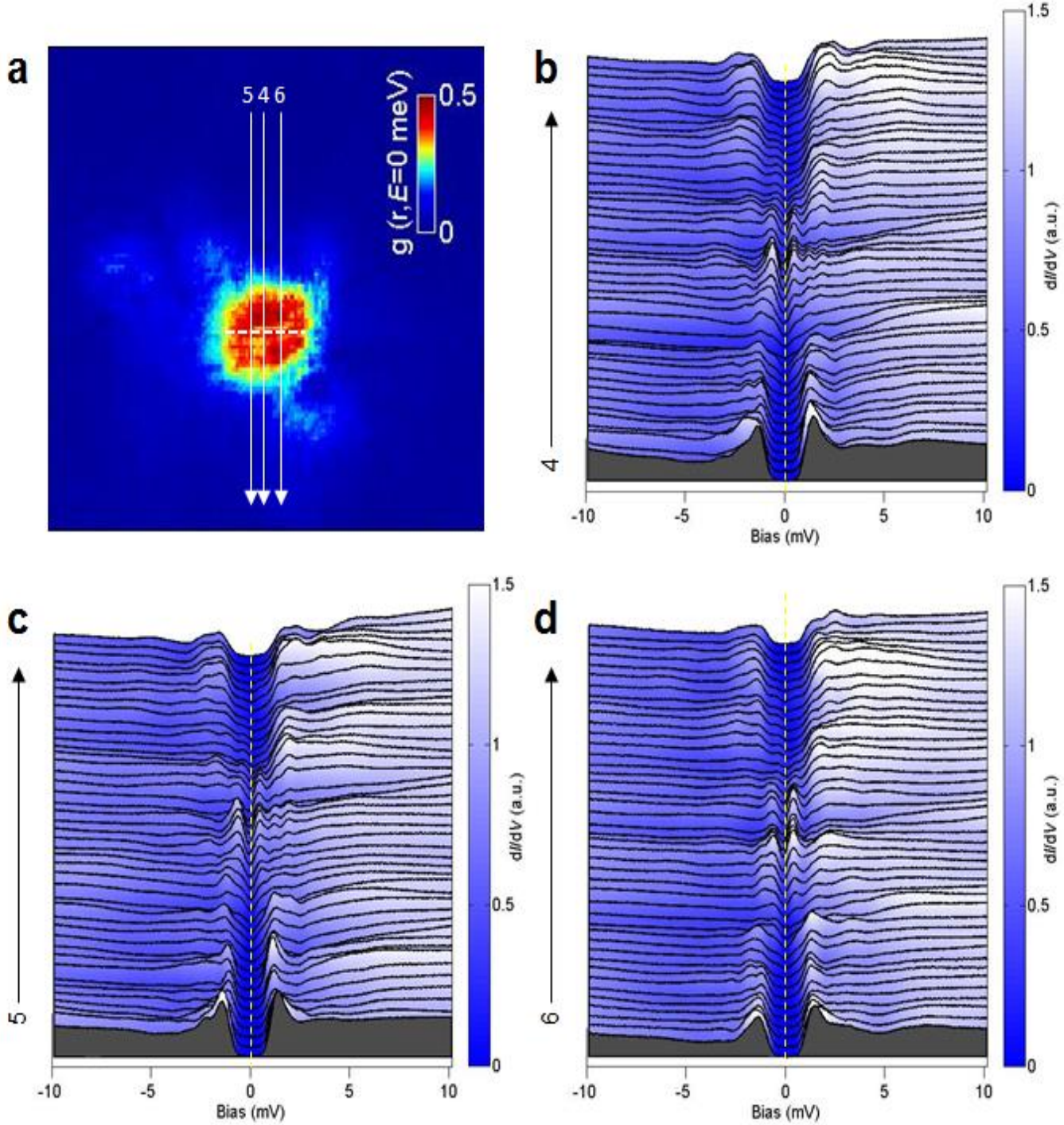
a
5 4 6
g (r,E=0 meV)
0.5
0
b
4
c
5
d
6
Bias (mV)
-10
-5
0
5
10
dI/dV (a.u.)
1.5
1
0.5
0

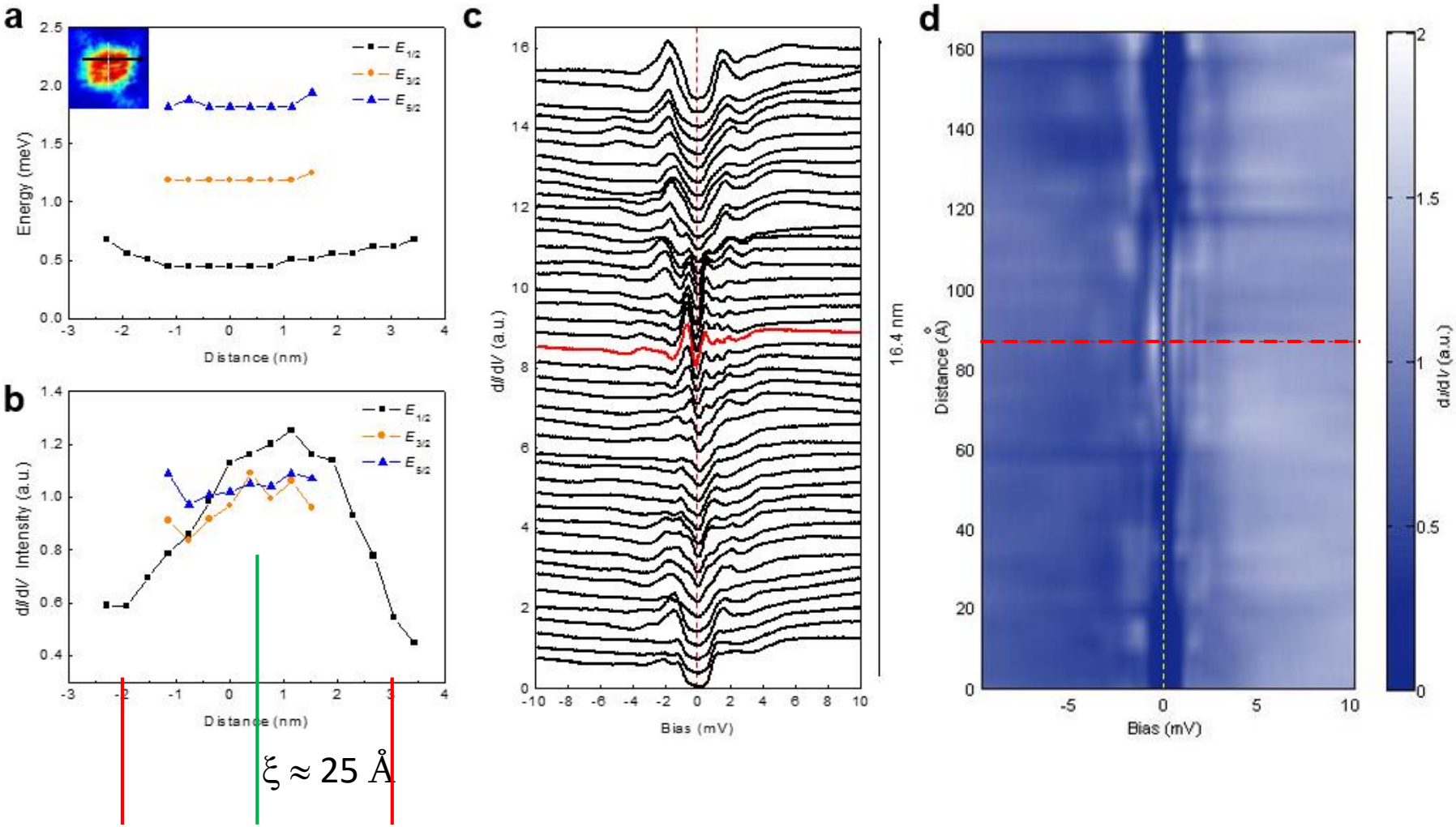

The peak position does not shift spatially until out of the vortex core region.

M. Y. Chen, H. Yang, HHW et al Nature Commun. 9, 970(2018).

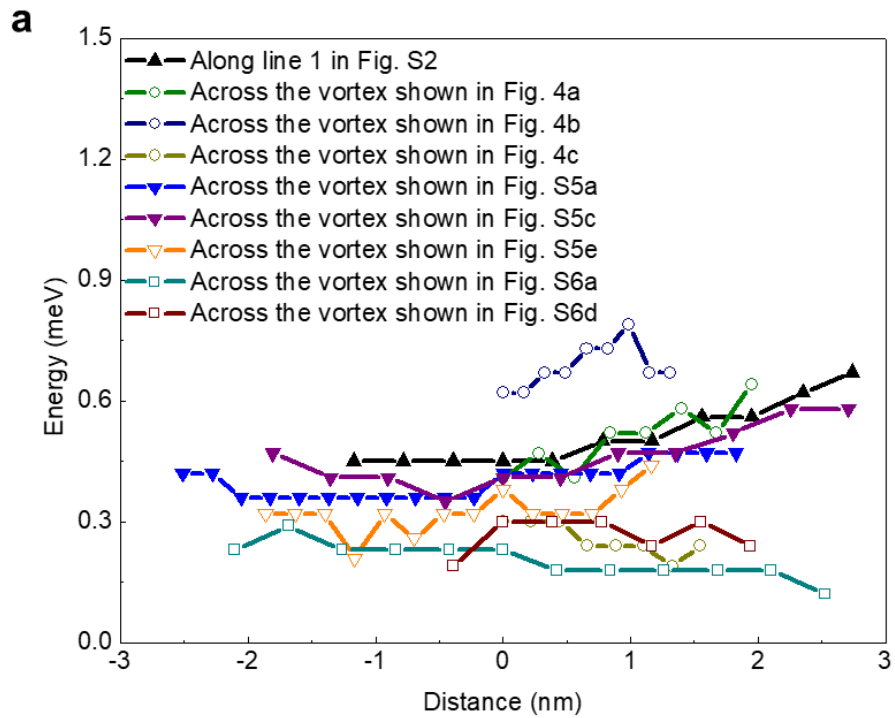

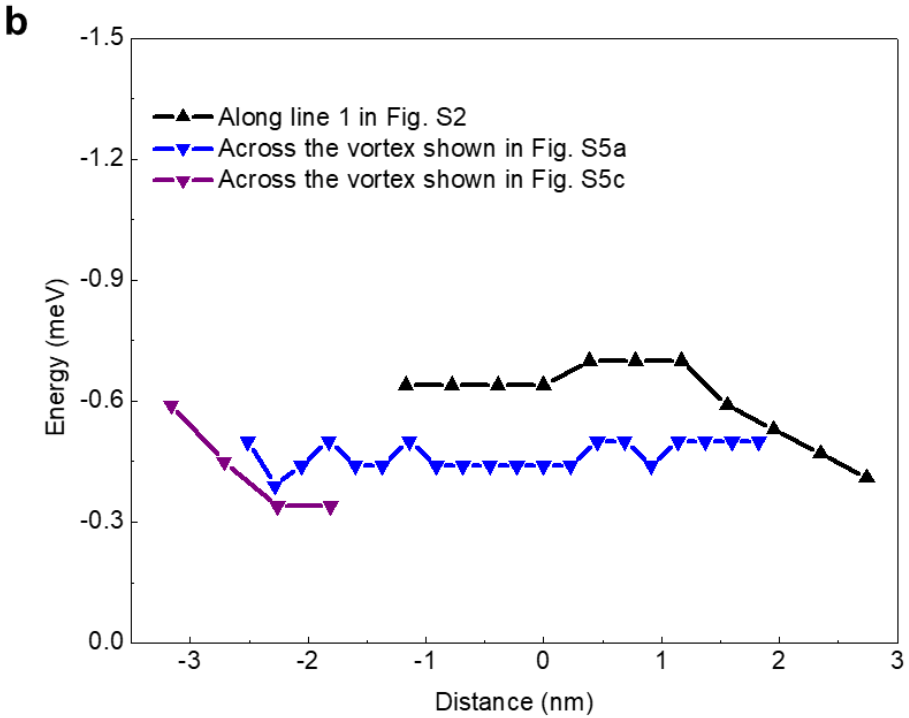

All peak energies of the 1st peak at (a) positive and (b) negative bias.

Taking the average value

$E_{1/2} = \Delta^2/2E_F \approx 0.45$ meV

Δ = 1.1 to 2.1 meV

E_F = 1.3 to 4.9 meV

Spatial evolution of the first level (μ=1/2) peak intensity

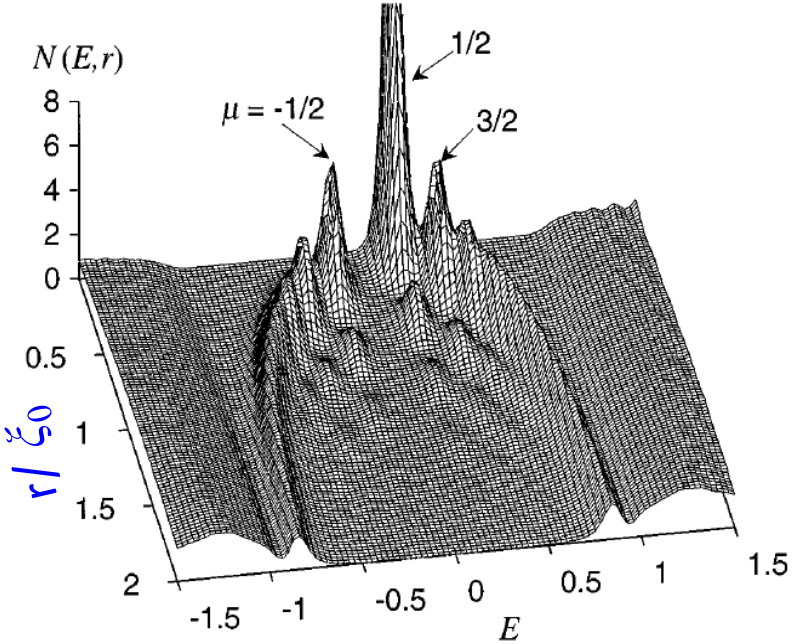

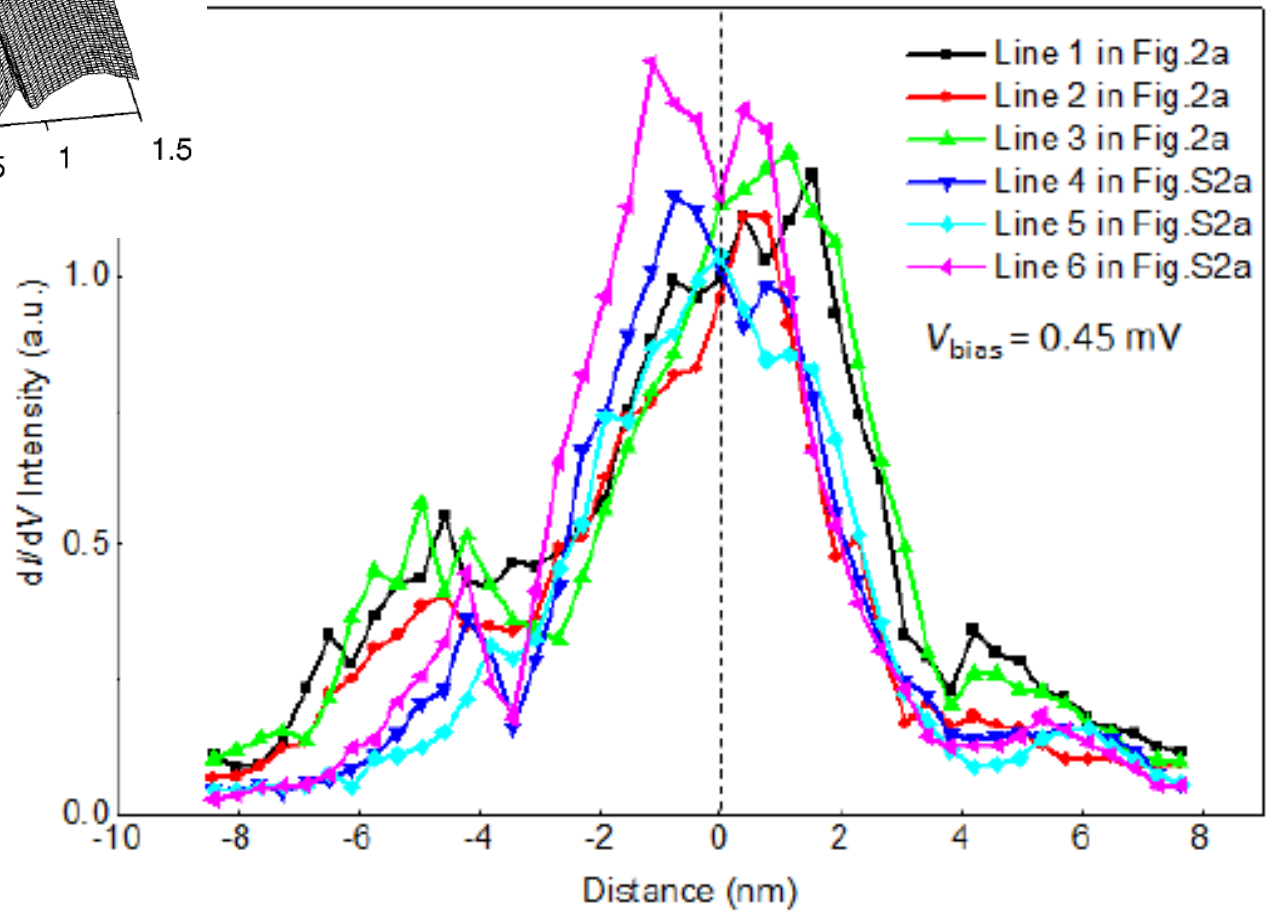

V_{bias}=0.45 mV

The possible nature of the asymmetry of the observed CdGM states

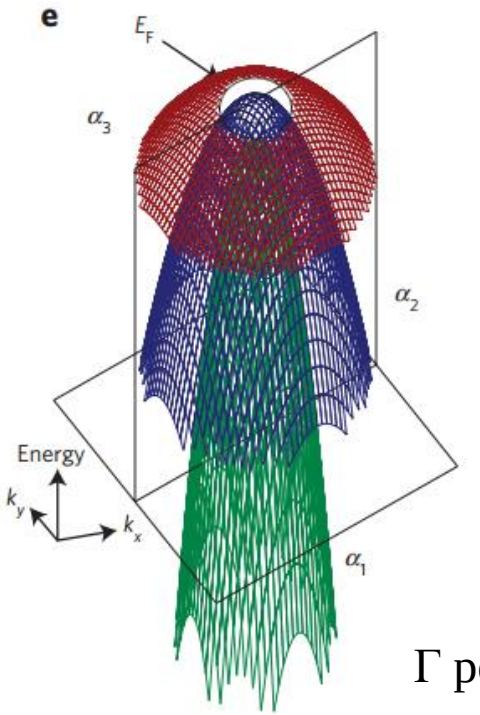

Γ point

hole band

Δ = 2 meV

E_F = 4 meV

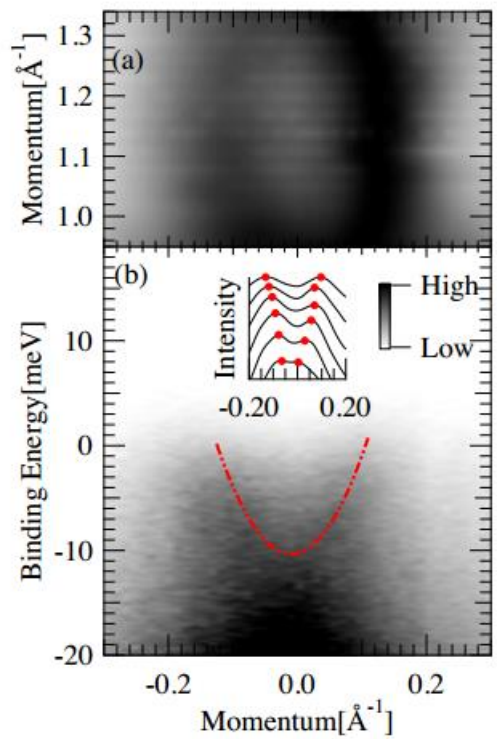

M point

electron band

Δ = 5 meV

E_F = 10 meV

The asymmetric spectrum and different features on the positive and negative energy si de are induced by the existence of shallow electron and hole bands with different Fermi energies

Lubashevsky, …,Kanigel A, Nat. Phys. 8, 309-312 (2012).

Some quantitative estimate:

$$\xi \approx \frac{\hbar v_F}{\pi \Delta_s} \qquad E_F = \frac{1}{2}\frac{\hbar^2 k_F^2}{2m} \qquad \frac{\Delta}{E_F} = \frac{4}{\pi}\frac{1}{\xi k_F} \approx \frac{1}{\xi k_F}$$

$$\frac{T}{T_c} << \frac{\Delta}{E_F} \approx \frac{1}{\xi k_F}$$

Quantum limit

T = 400 mK, and

$T/T_c \approx 0.03, \quad 1/k_F\xi_0 \approx 0.3$ to 0.6

Using ξ_0 = 25 Å, $k_F(\alpha\text{-}band)$ = 0.07 Å^{-1}, $k_F(\beta\text{-}band)$ = 0.12 Å^{-1}

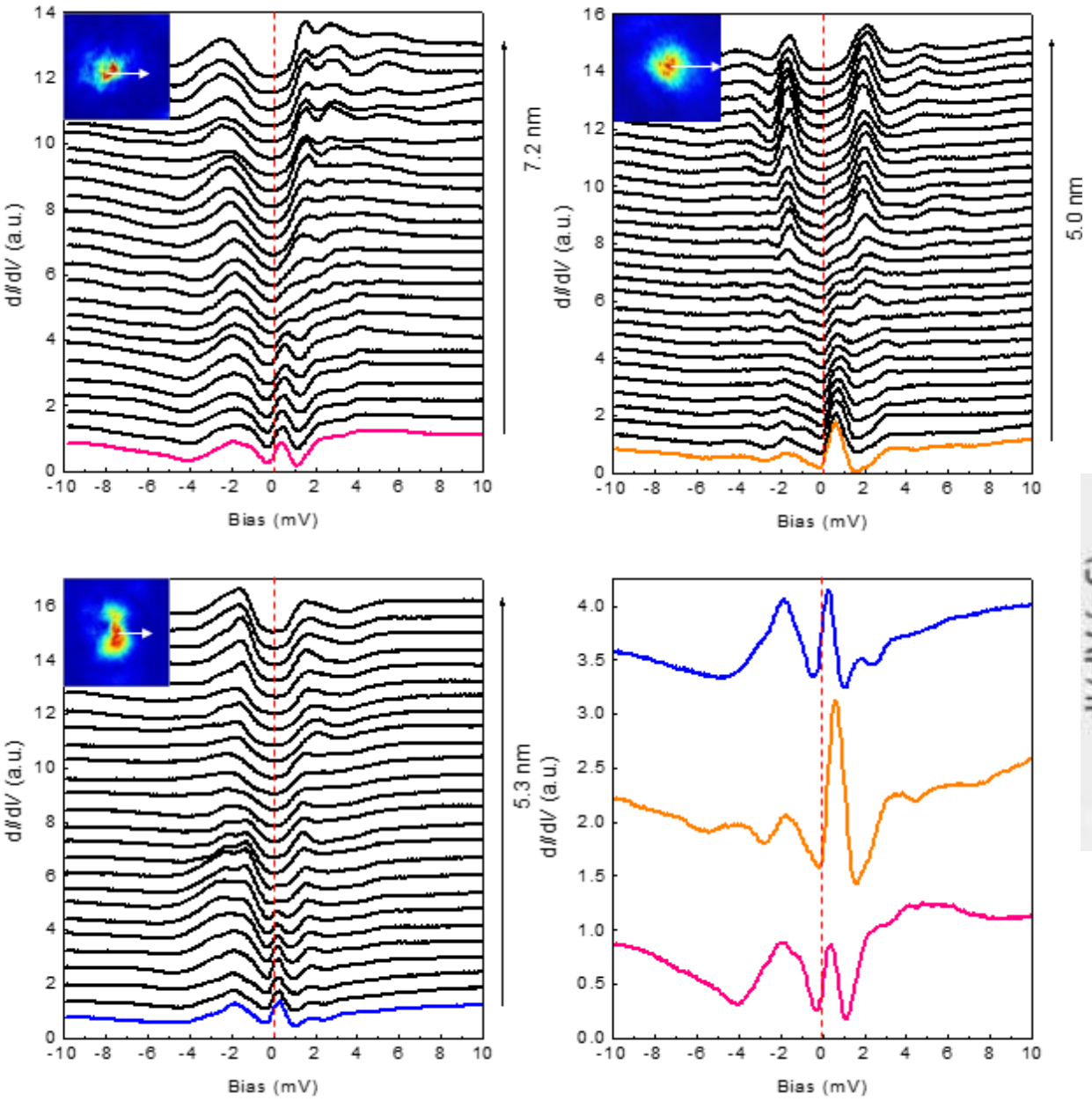

Some spectra (~40-50%) show a single peak near zero

$\mu_0 H = 4$ T

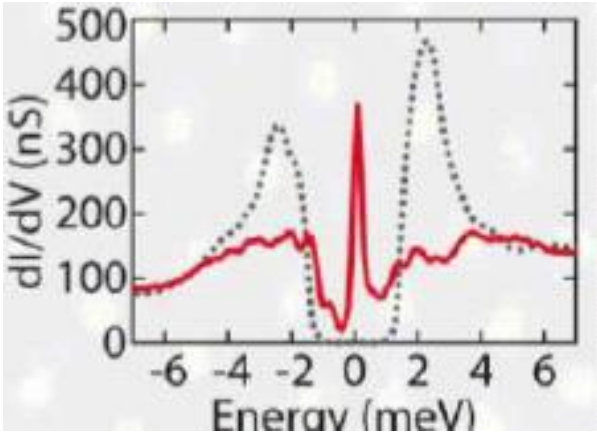

Freek Massee, et al. Science Advances 1, e1500033 (2015)

M. Y. Chen, H. Yang, HHW et al. Nature Commun. 9, 970(2018).

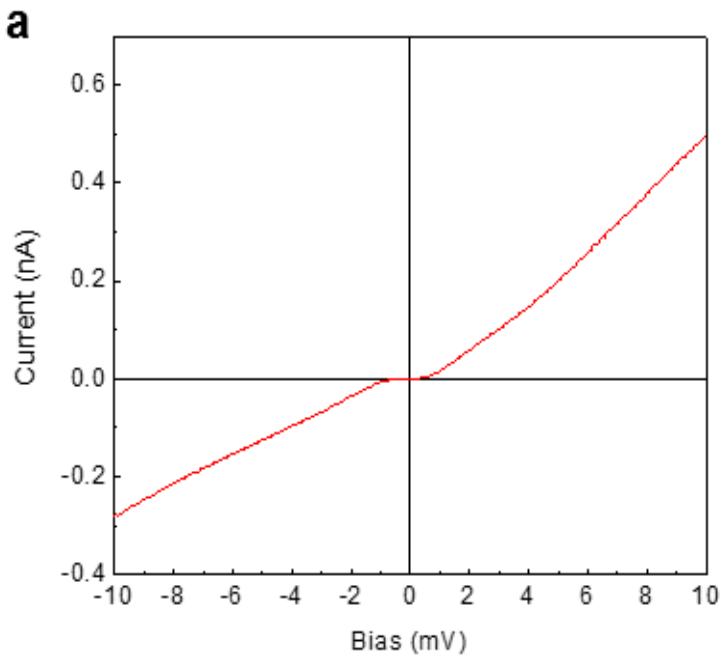

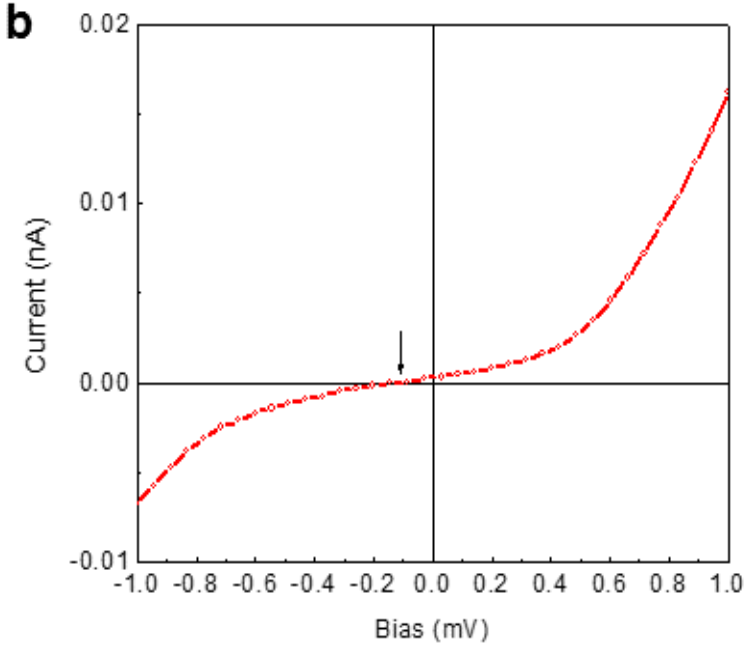

How to calibrate the zero bias.

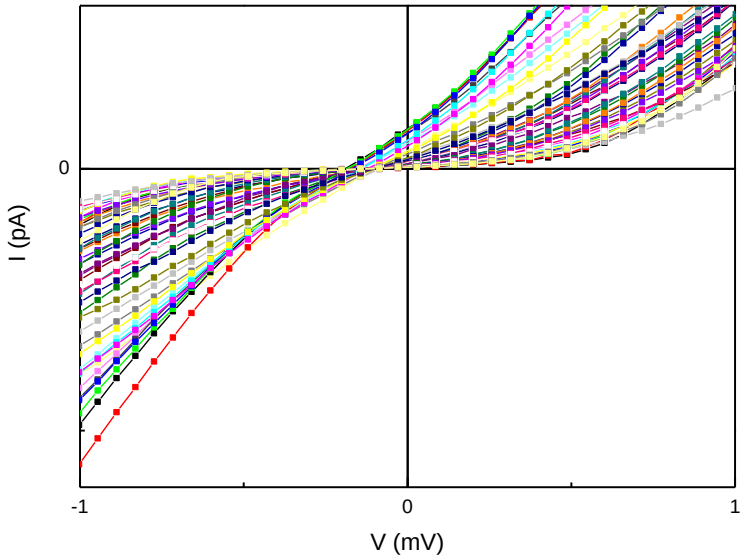

We have measured more than 30 vortices in total before Dec. 2017, about 20% of them show the discrete energy levels. Quite some vortices show the asymmetric single peak at a positive energy and near zero-bias.

Observation of pristine Majorana bound state in iron-based superconductor FeTe0.6Se0.4

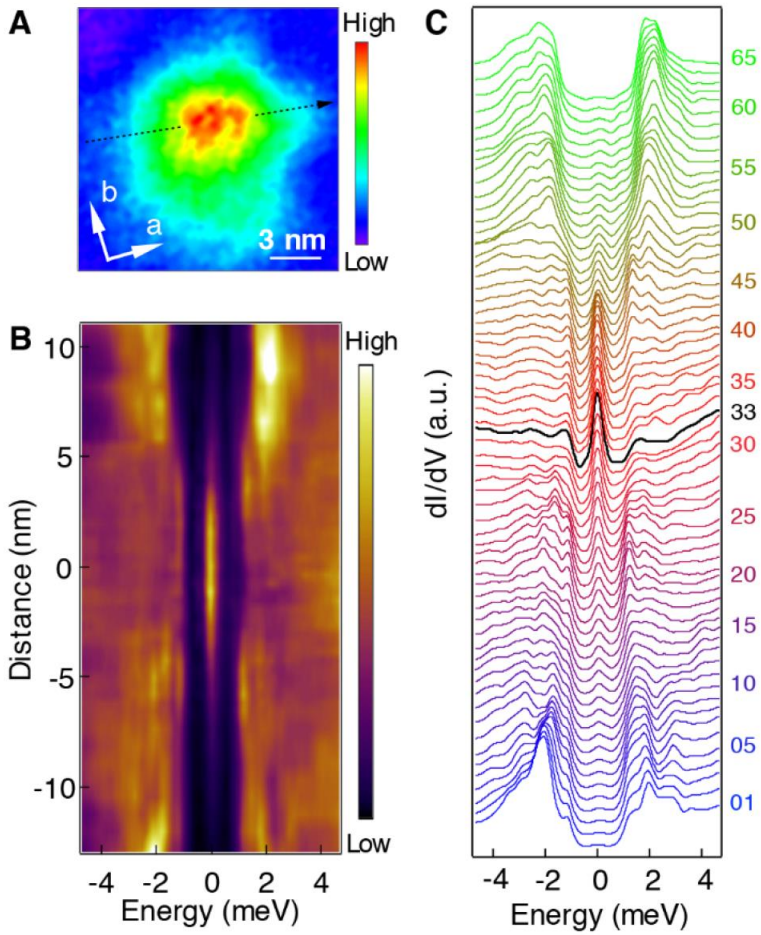

Dongfei Wang, Lingyuan Kong, Hong Ding*, and Hongjun Gao*, et al. Science, eaao1797 (2018)

Robust and clean Majorana zero mode in the vortex core of high-temperature superconductor (Li0.84Fe0.16)OHFeSe

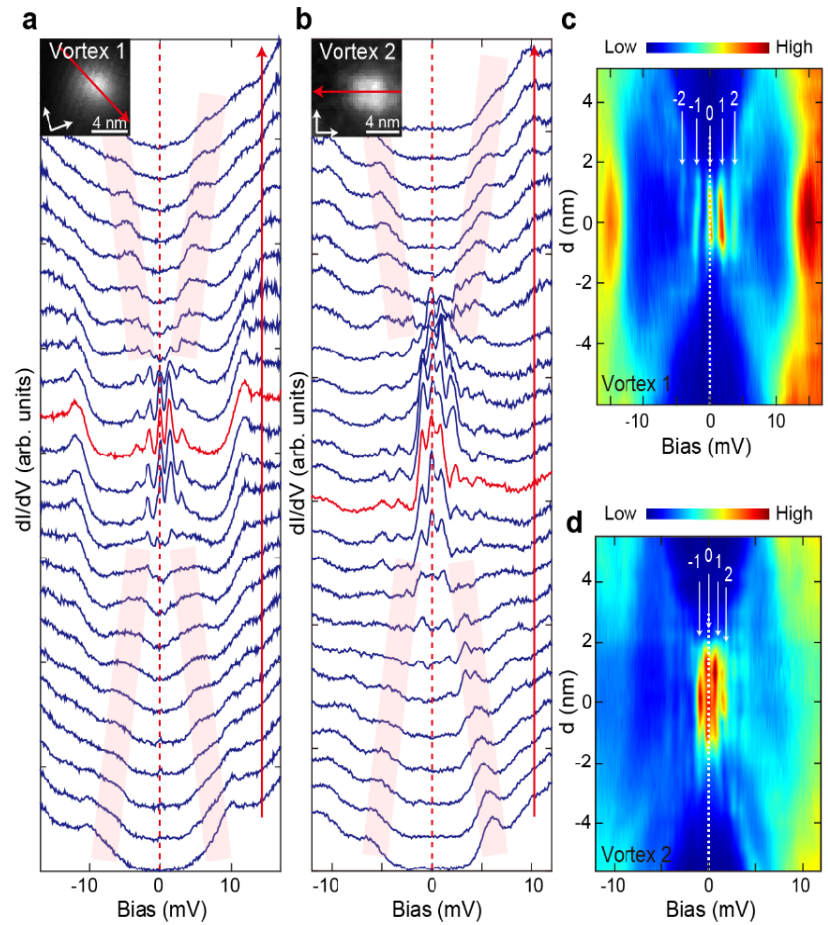

Q. Liu, C. Chen, T. Zhang*, D. L. Feng* et al., Phys. Rev. X 8, 041056 (2018)

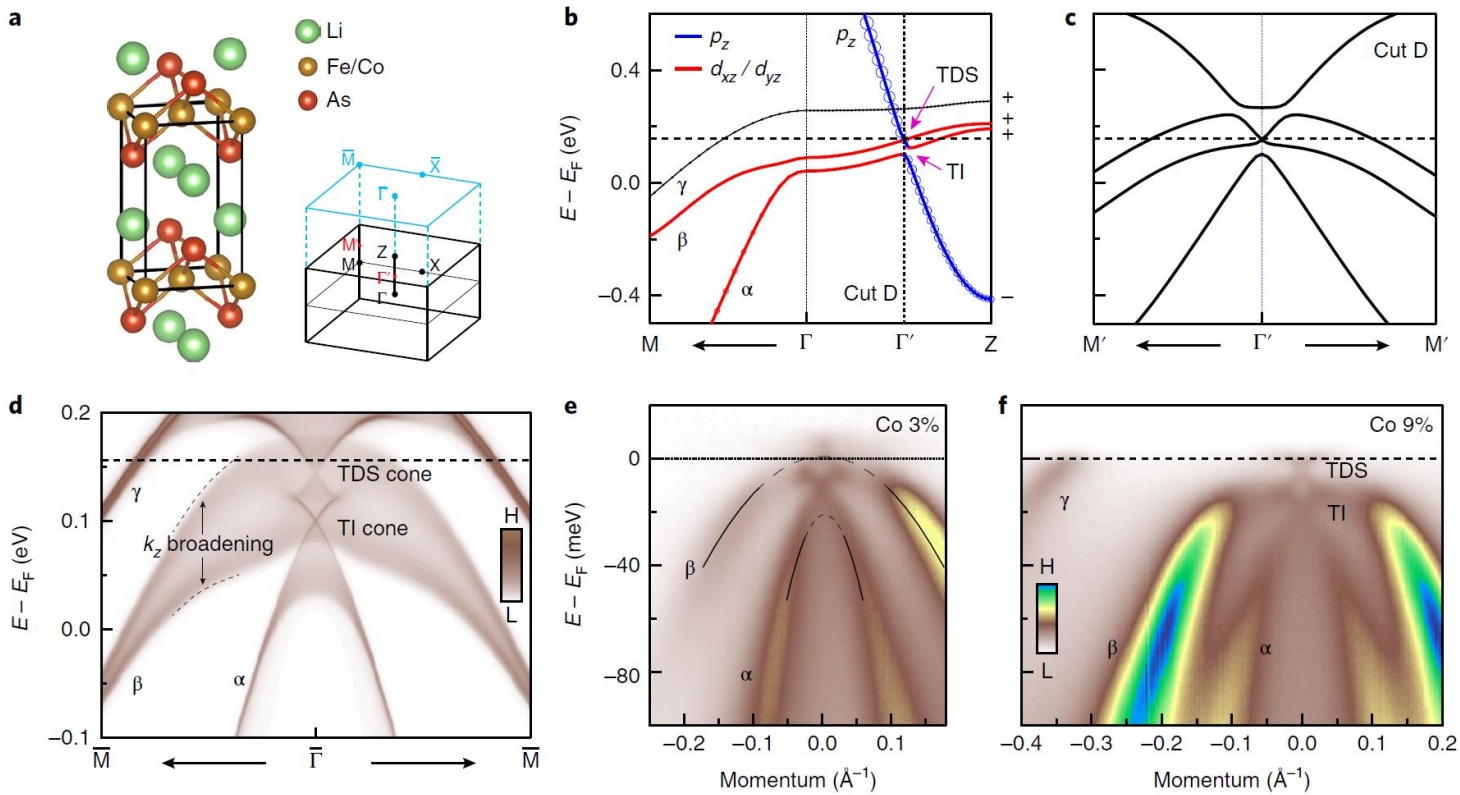

Theoretically it was proposed that the downward shifted p_z band due to the Te substitution will cross the d_{xz} band near Fermi energy. Because of the strong spin-orbital coupling effect and the parity feature of these bands, a topological surface state exists with a spin-helical texture.

- X. Wu, S. Qin, Y. Liang, H. Fan, and J. Hu, Phys. Rev. B 93, 115129 (2016).
- P. Zhang, ··· H. Ding, and S. Shin, Science 360, 182 (2018).

How to reconcile with the IOP and RIKEN data in $FeTe_{0.6}Se_{0.4}$?

Check with more vortices

200x200 nm^2

0.5 T

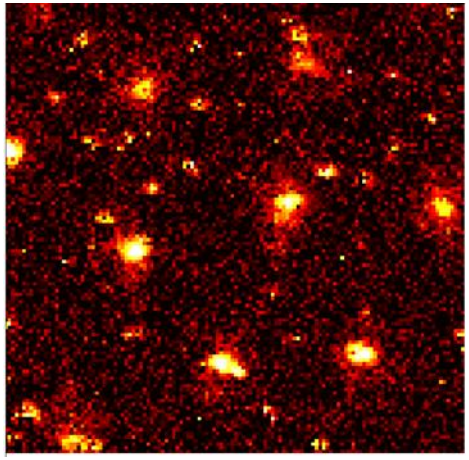

1.0 T

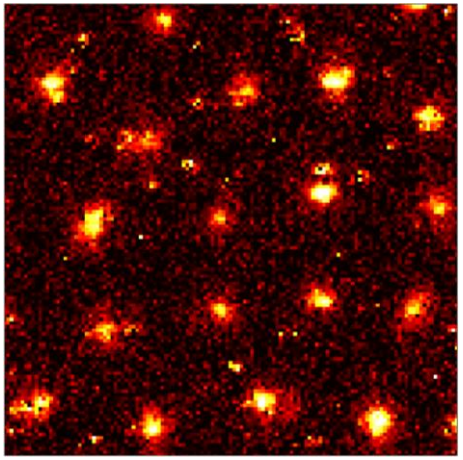

2.0 T

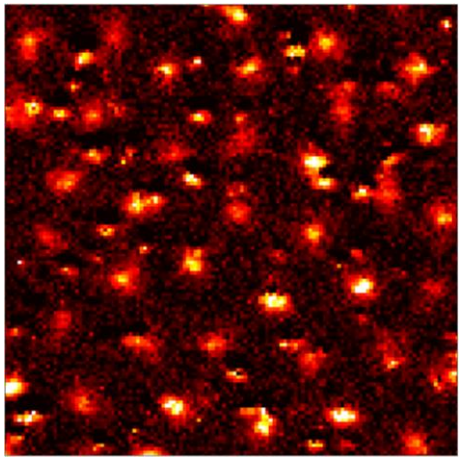

4.0 T

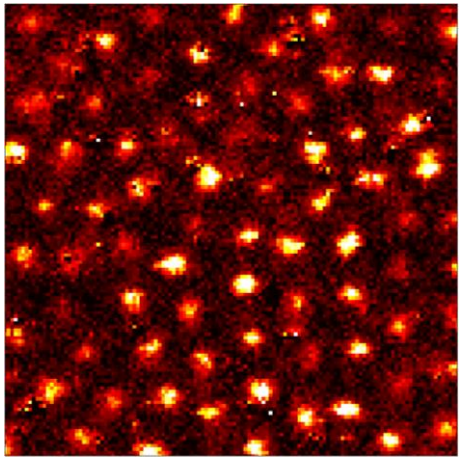

6.0 T

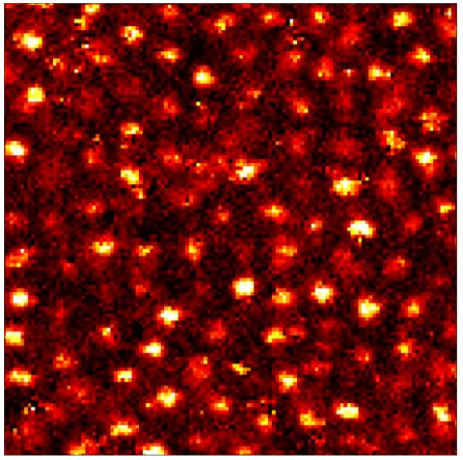

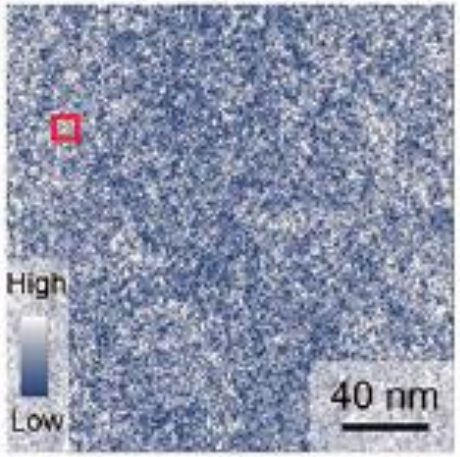

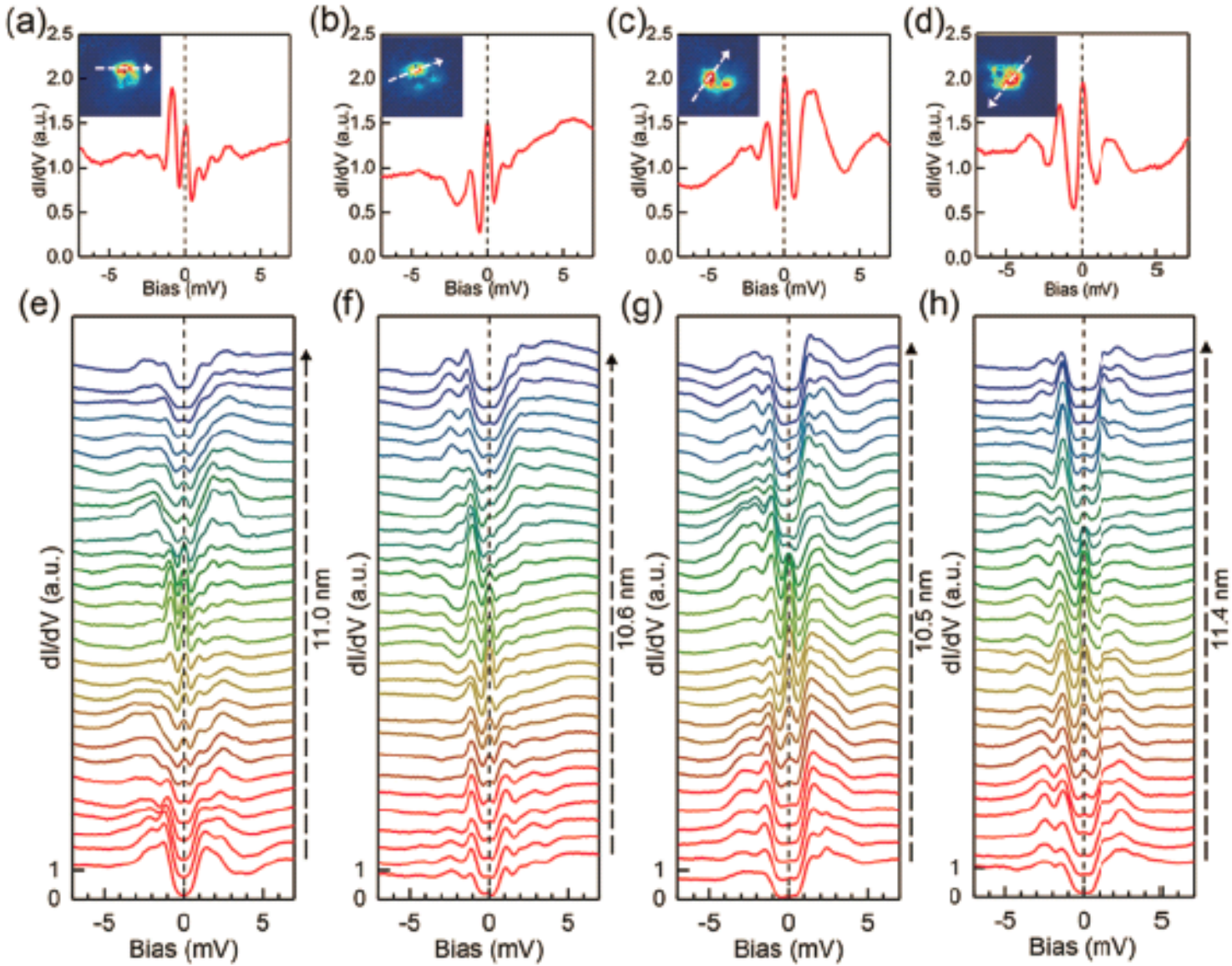

Some typical vortices with the ZBCP

X. Y. Chen et al., arXiv.1909.01686

In the same area we measured the vortex core states under different magnetic fields, and try to have statistics on the probability of the ZBCP (criterion: peak within ±0.1meV)

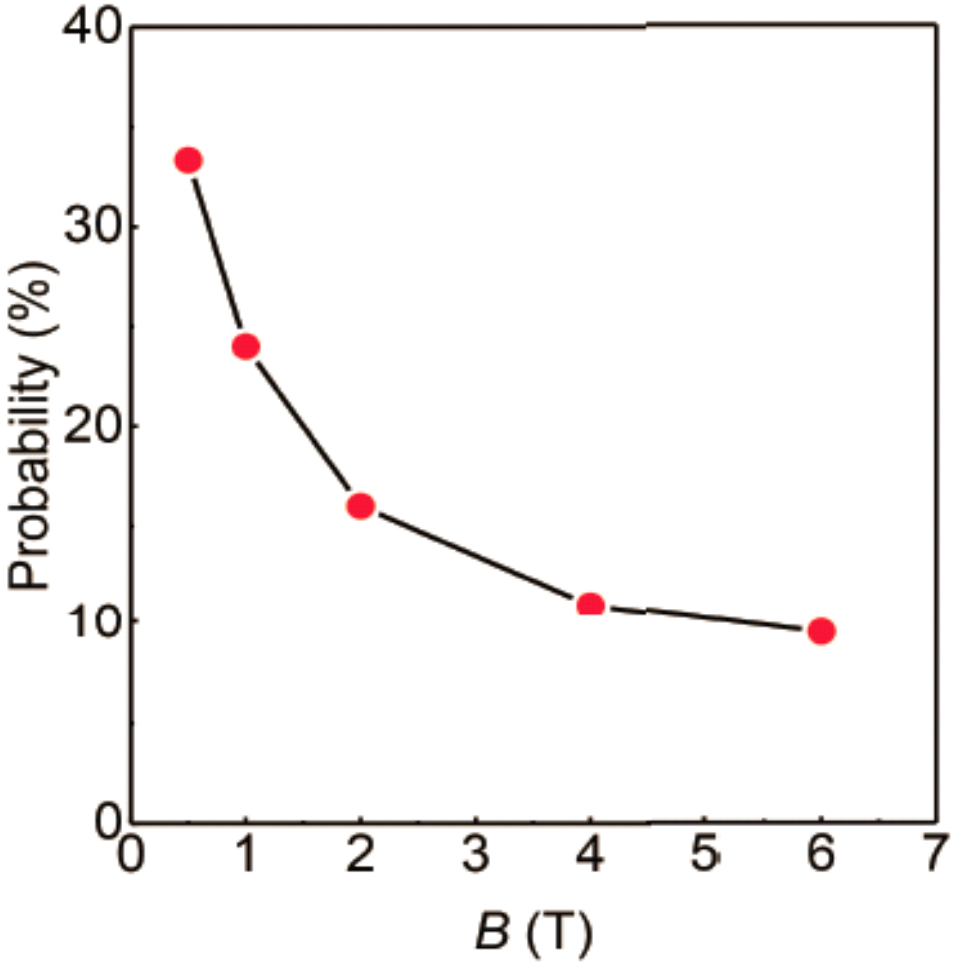

0.5 T	5/15
1 T	8/33
2 T	21/120
4 T	18/160
6 T	23/240

Xiaoyu Chen, HHW et al.
arXiv.1909.01686

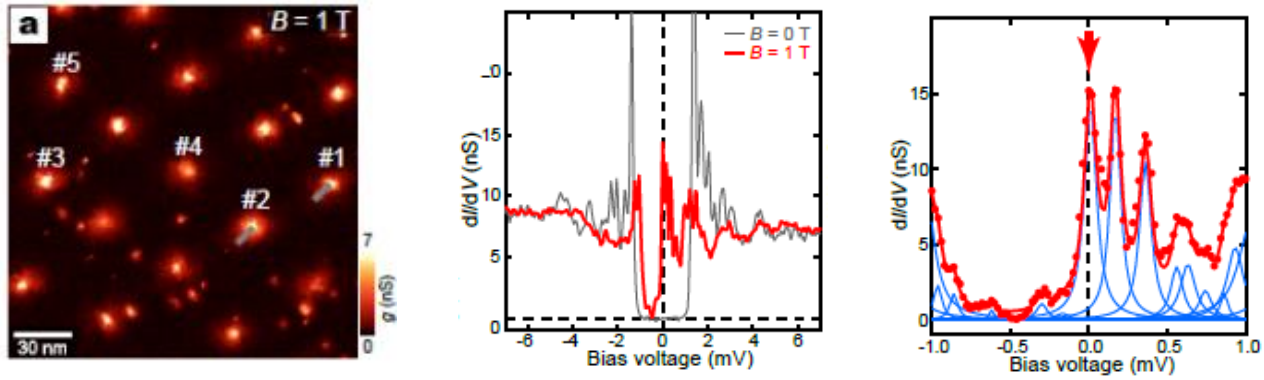

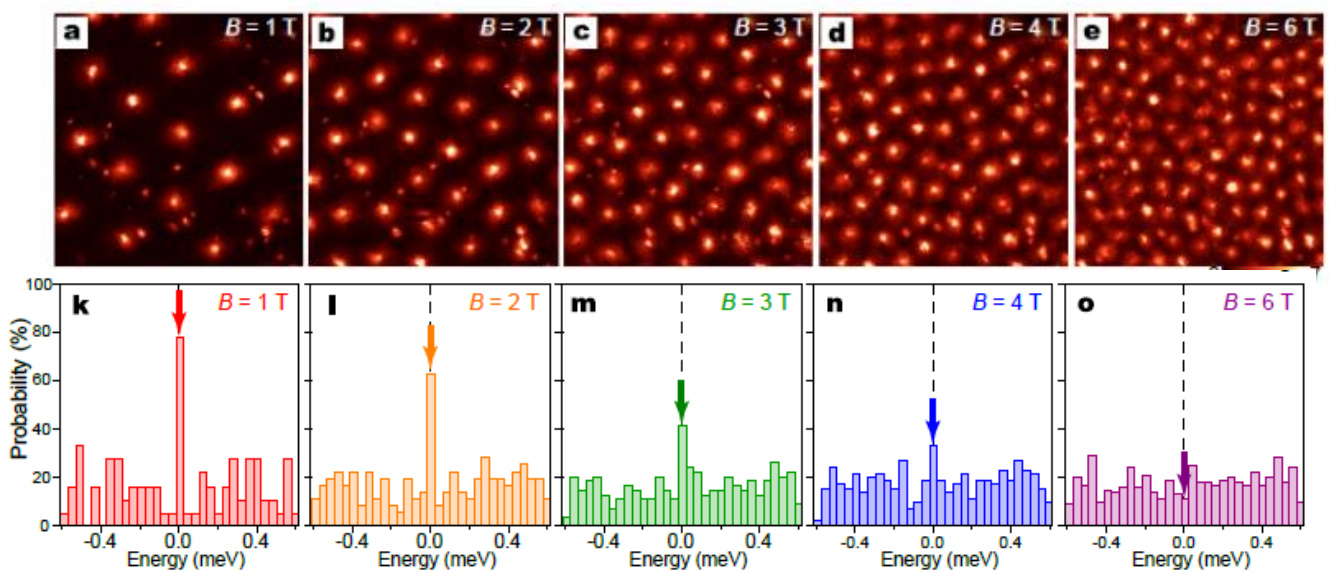

T Machida, T. Hanaguri, et.al
Nat. Material. 18, 811(2019).

The higher percentage is probably due to

- More Te concentration in their samples
- Lower temperature with higher energy resolution

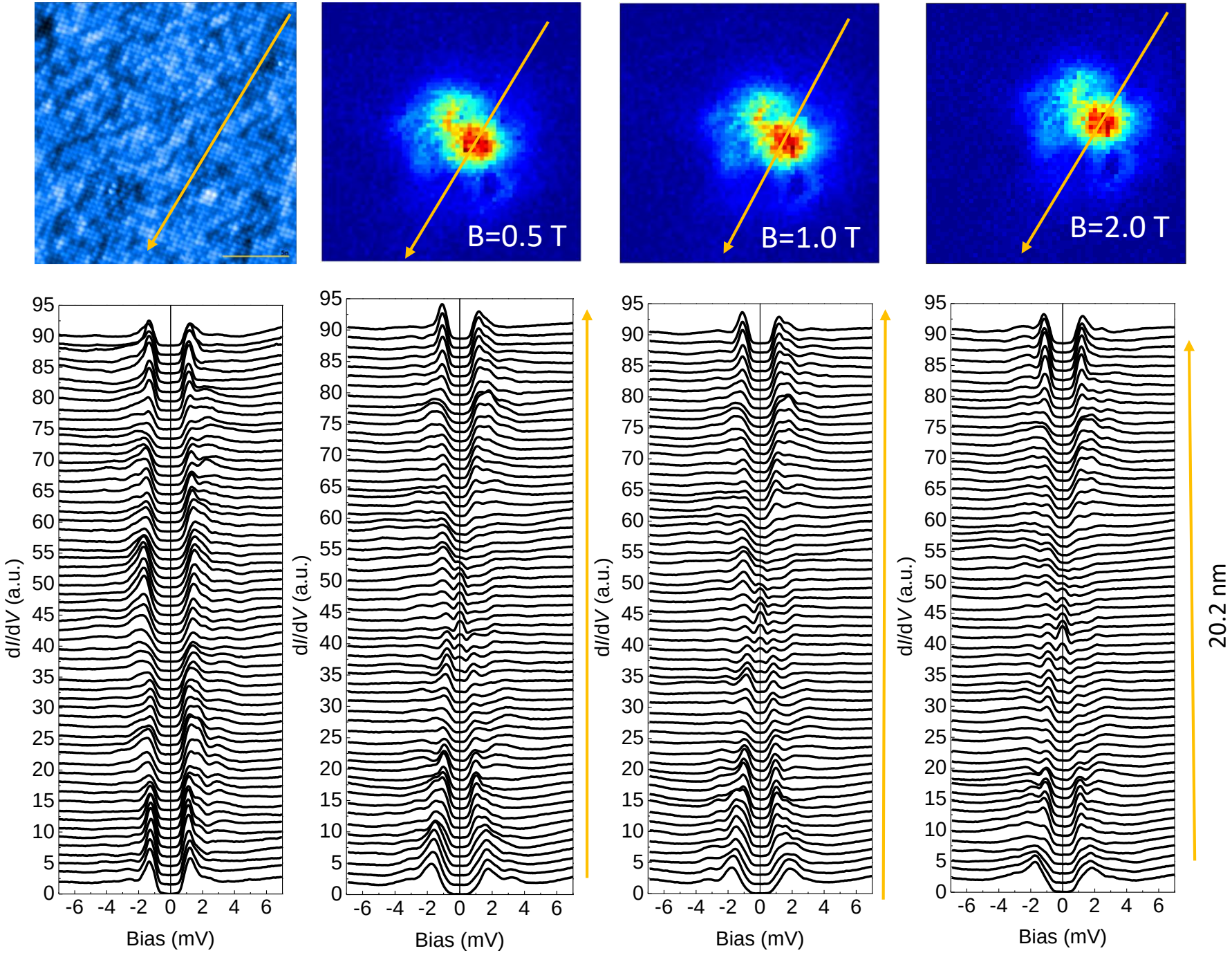

S2

Magnetic field dependence of the ZBCP

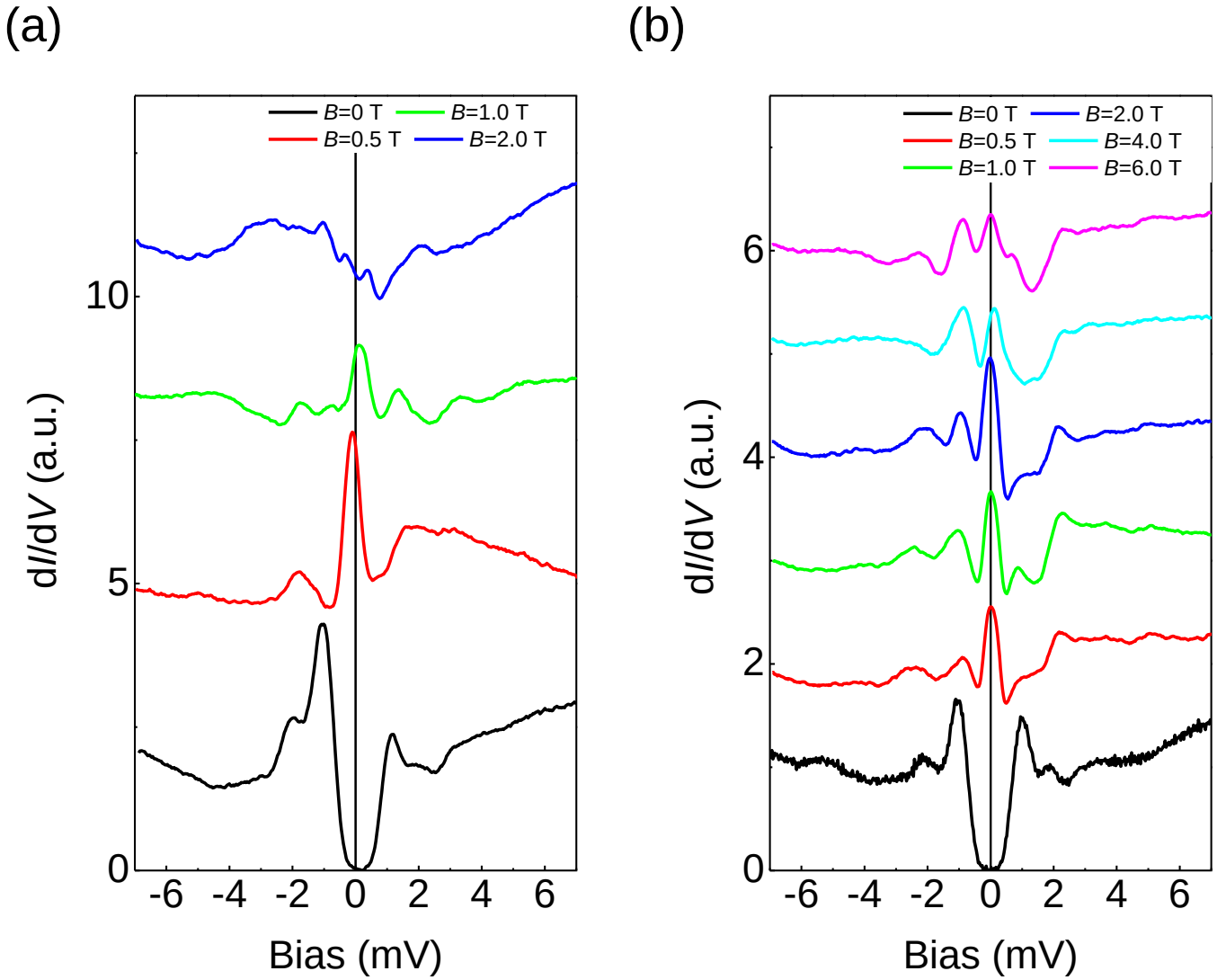

The ZBCP could be due to Majorana mode.

The split by field could be induced by the interaction.

Some times the zero-bias peak (Majorana-mode) appears at high magnetic field, for example at B = 6.0 T

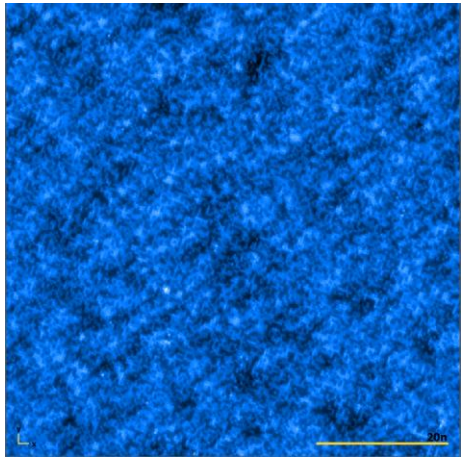

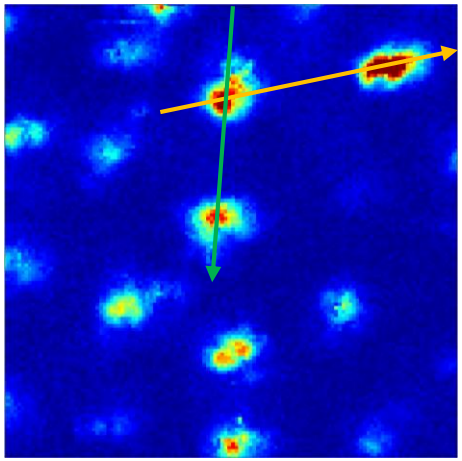

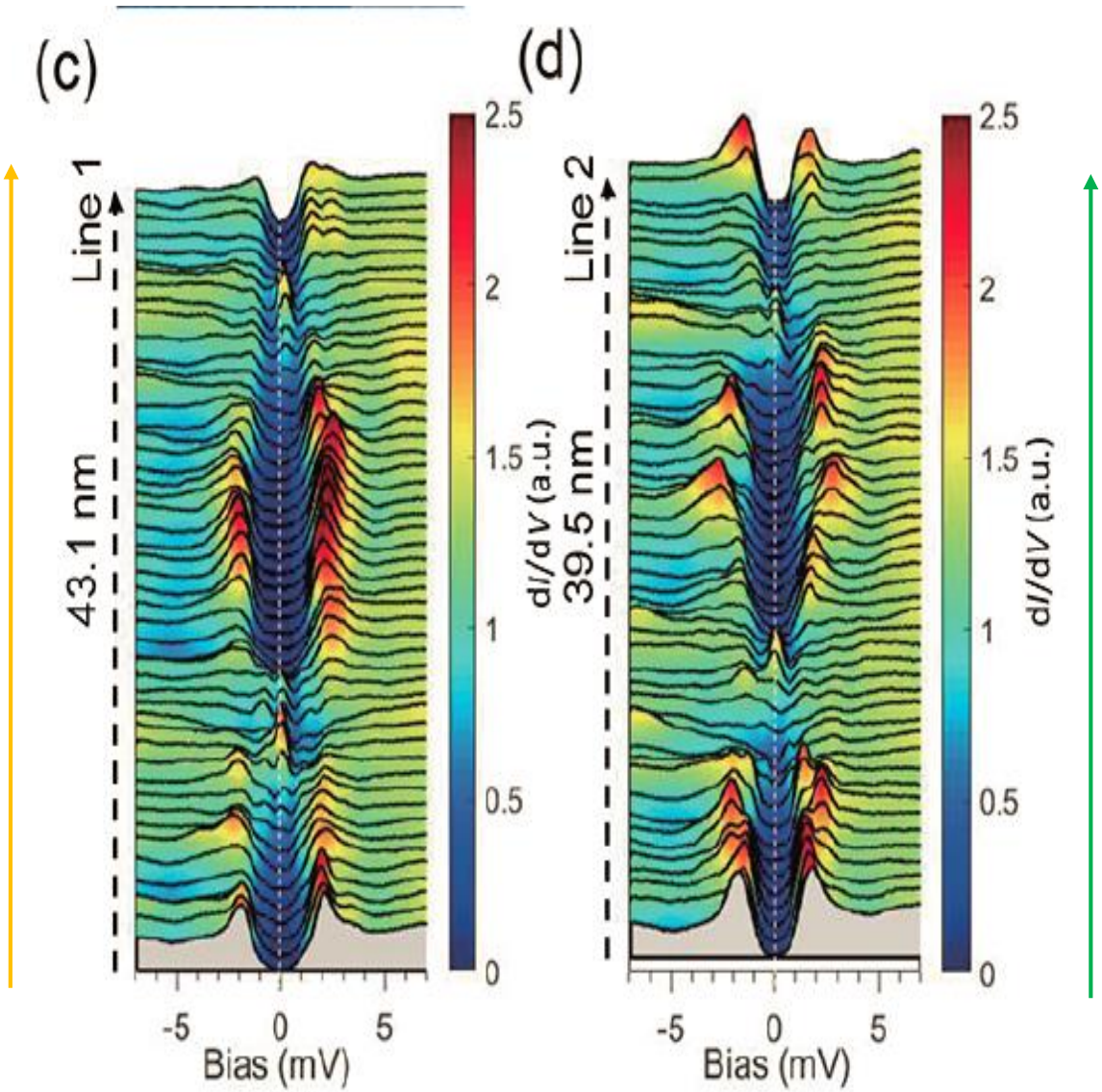

The ZBCP is very fragile to thermal effect, disappears at about 4K.

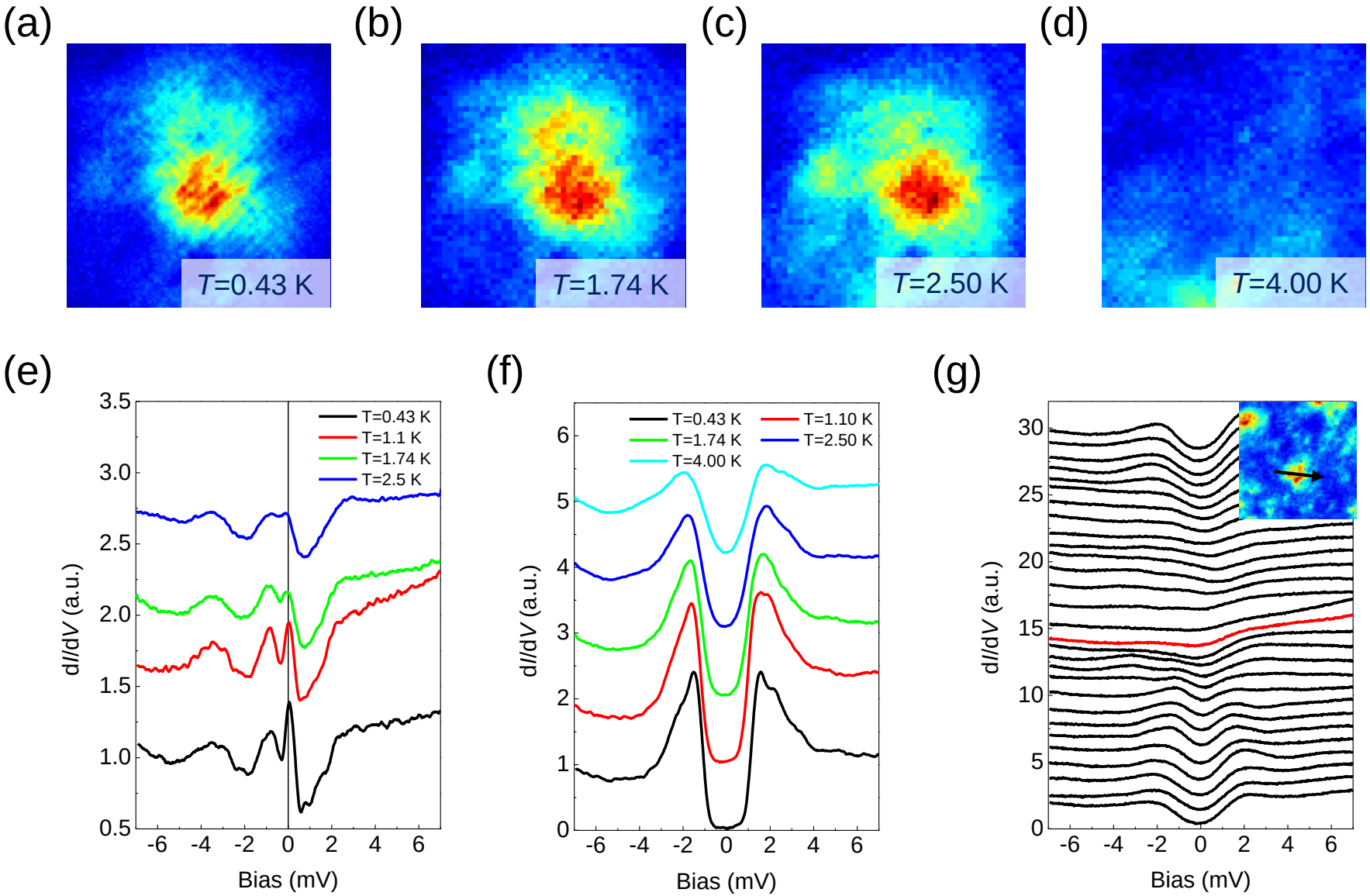

Xiaoyu Chen, HHW et al. arXiv.1909.01686

Vortices with zero energy modes

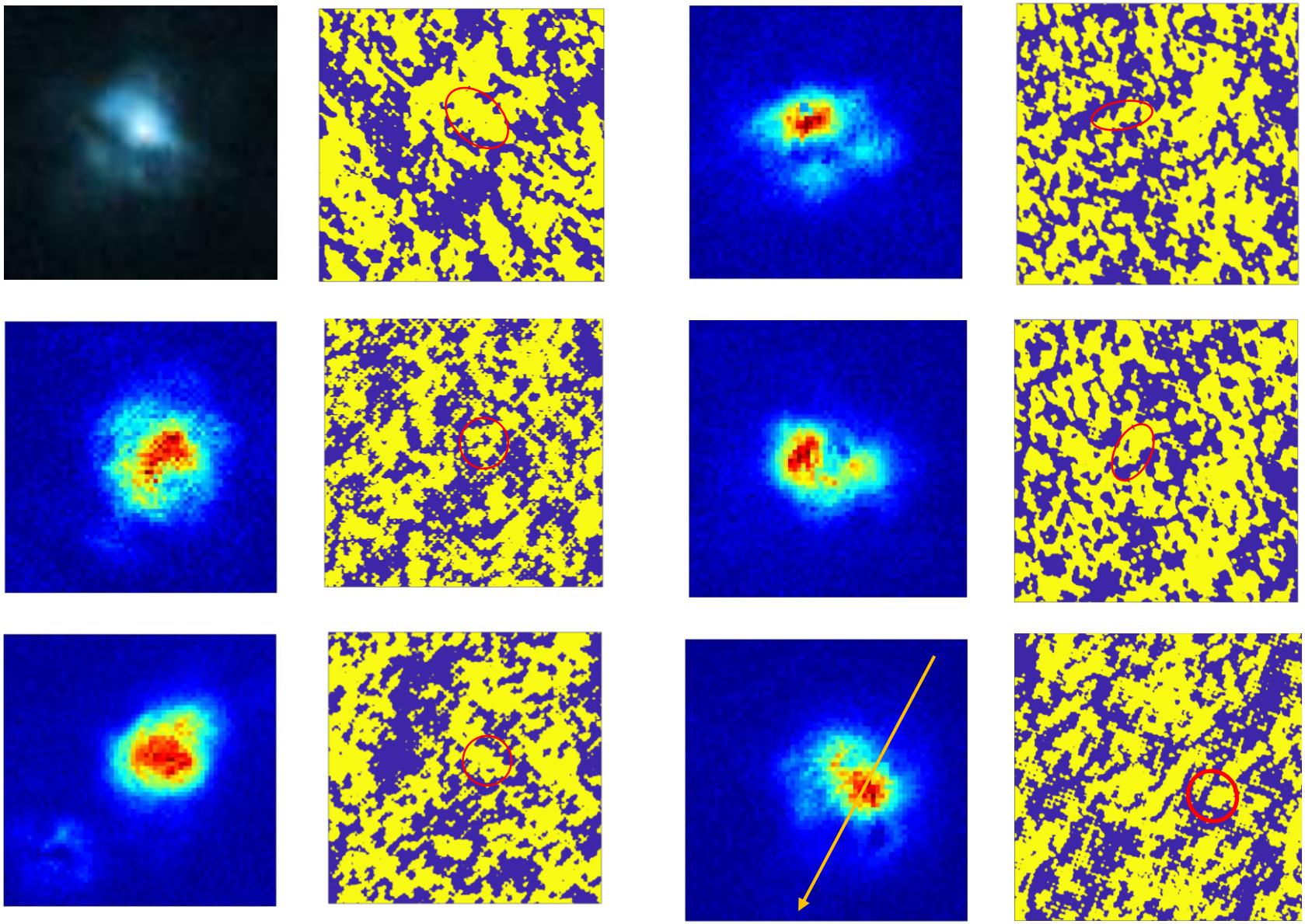

Vortices without zero energy modes

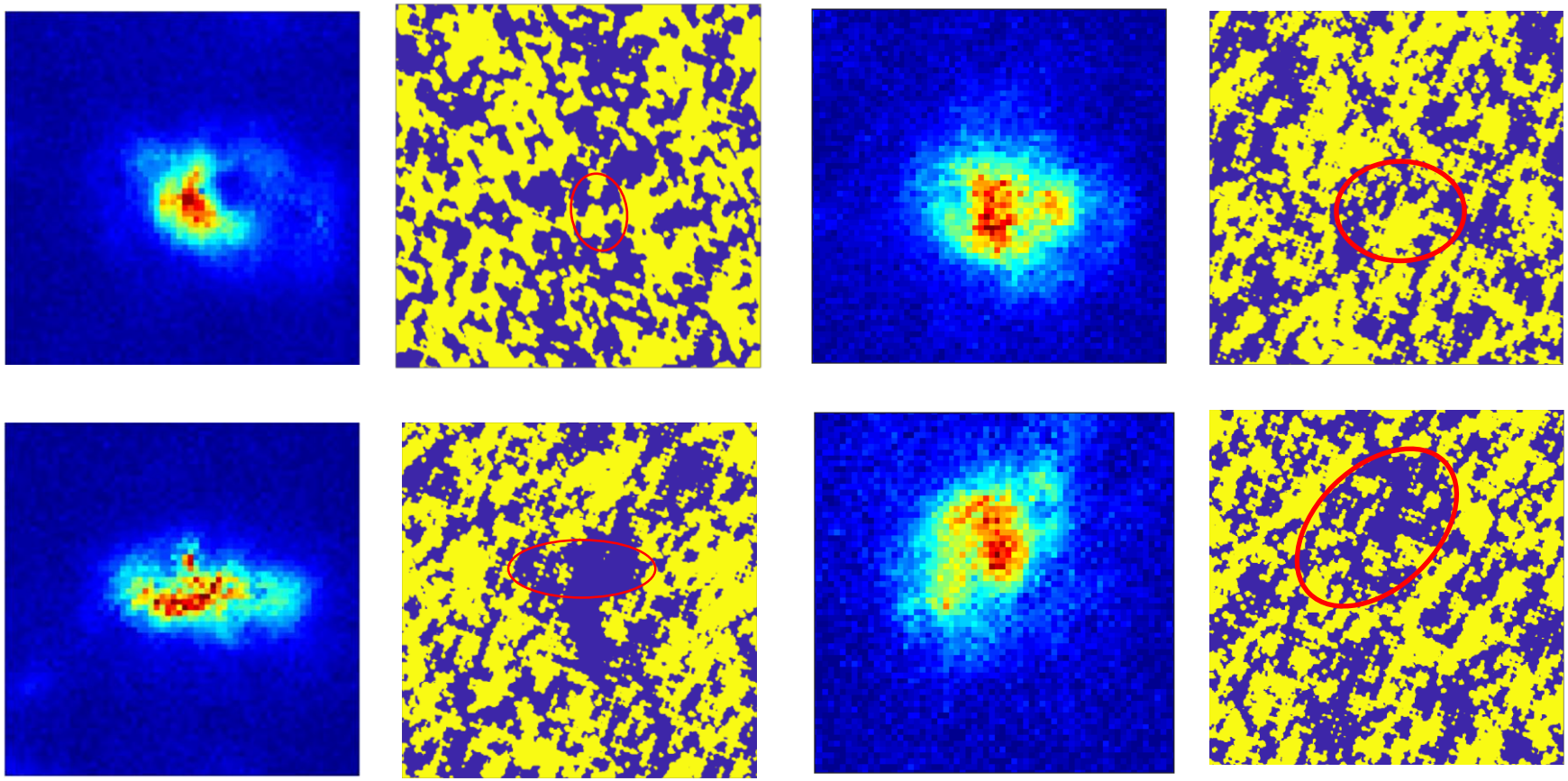

No clear correlation between the appearance of Majorana modes and local surface concentration of Te/Se.

Concluding remarks

- Discrete energy levels of Caroli-de Gennes-Martricon states have been observed in some vortex cores of $FeTe_{0.55}Se_{0.45}$($E_{1/2}$, $E_{3/2}$, $E_{5/2}$) in the quantum limit due to small Fermi energy, small value of E_F/Δ would imply the BCS-BEC crossover.

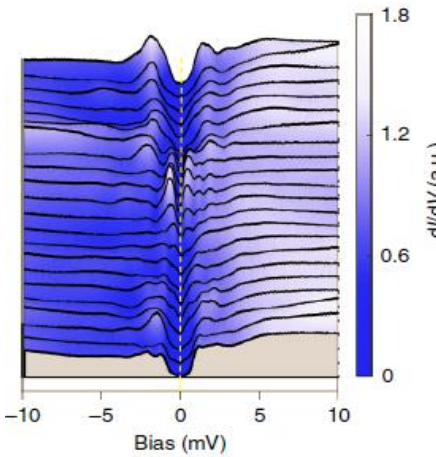

- In some vortices of Fe(Te,Se), we confirmed the ZBCP which does not behave as the usual CdGM states. This could be due to the Majorana mode, or due to the multiband effect. The ZBCP has sensitive temperature, magnetic field and environment dependence.

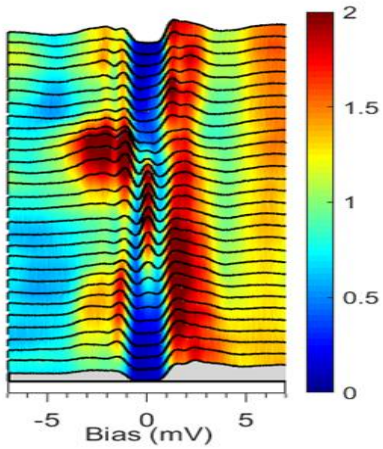

- M. Y. Chen, H. Yang, HHW et al., Nature Commun. 9, 970(2018).
- X. Y. Chen, H. Yang, HHW et al., arXiv. 1909.01686.

Outline of the lecture

- Introduction
- Caroli-de Gennes-Matricon states and possible Majorana modes in vortex cores of $FeTe_{0.55}Se_{0.45}$

  Nat. Commun. 9, 970(2018). arXiv.1909.01686
- **Nematic superconductivity and ZBCPs in $Sr_xBi_2Se_3$ and $Bi_2Te_3/FeTe_{0.55}Se_{0.45}$**

  Nat. Commun. 8, 14466 (2017).

  Sci. Adv. 4, eaat1084 (2018).
- Concluding remarks

Topological superconductor (TSC):

- 3D TSCs: Possess a pairing gap with odd parity in the bulk; Gapless surface states consisting of Majorana fermions; Within the vortex core there is Majorana mode (zero energy mode)
- 2D TSCs: Spin helical edge state, a finite DOS at zero energy
- 1D TSCs: helical SC chain, MZMs show at the two terminals

- M. Z. Hasan, C. L. Kane, *Rev. Mod. Phys.* **82**, 3045-3067 (2010)
- X. L. Qi & S. C. Zhang, RMP **83**, 1057 (2011)
- M. Sato, Y. Ando, *Rep. Prog. Phys.* **80**, 076501 (2017)

Majorana Feimion: $\gamma = \gamma^{+}$, non-abelian statistics

Some routes toward a TSC:

1. Proximity effect: nanowire/SC, TI/SC heterostructure: $Bi_2Se_3/NbSe_2$, Bi_2Se_3/Bi2212
2. Dope a TI: $Cu_xBi_2Se_3$, $Sr_xBi_2Se_3$, $Sn_{1-x}In_xTe$
3. Superconductor with topological band structure itself Fe(Te,Se)
4. Pressurize a TI: Bi_2Se_3, Bi_2Te_3, Sb_2Se_3, Sb_2Te

Majorana fermions in 1D system

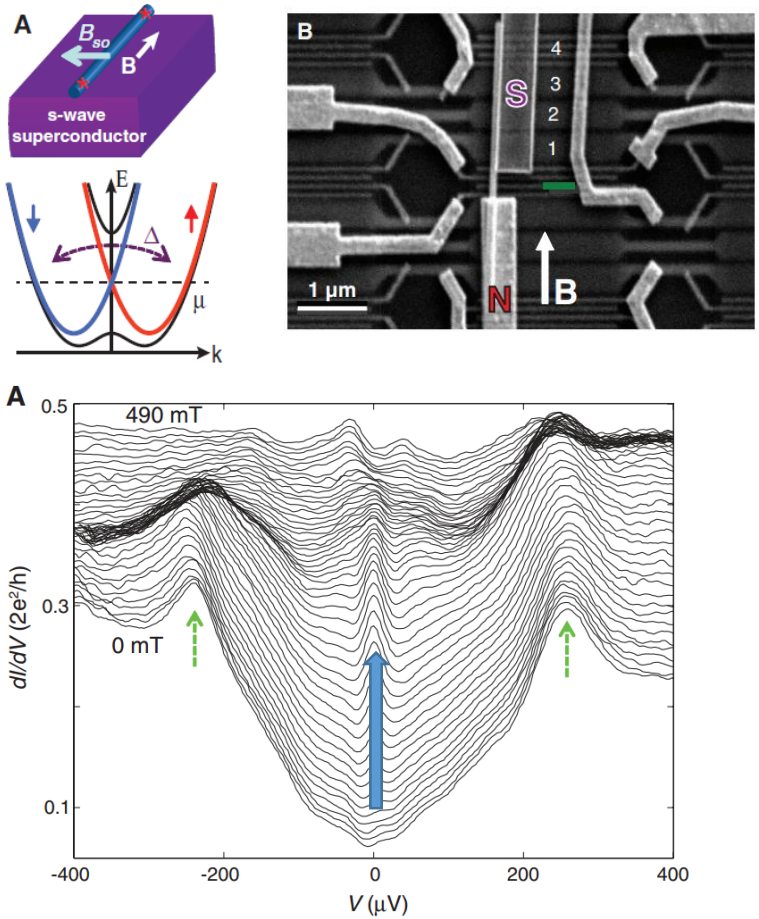

Zero-bias conduction peak

V. Mourik et al., Science 336, 1003–1007 (2012).

Majorana quasi-particle

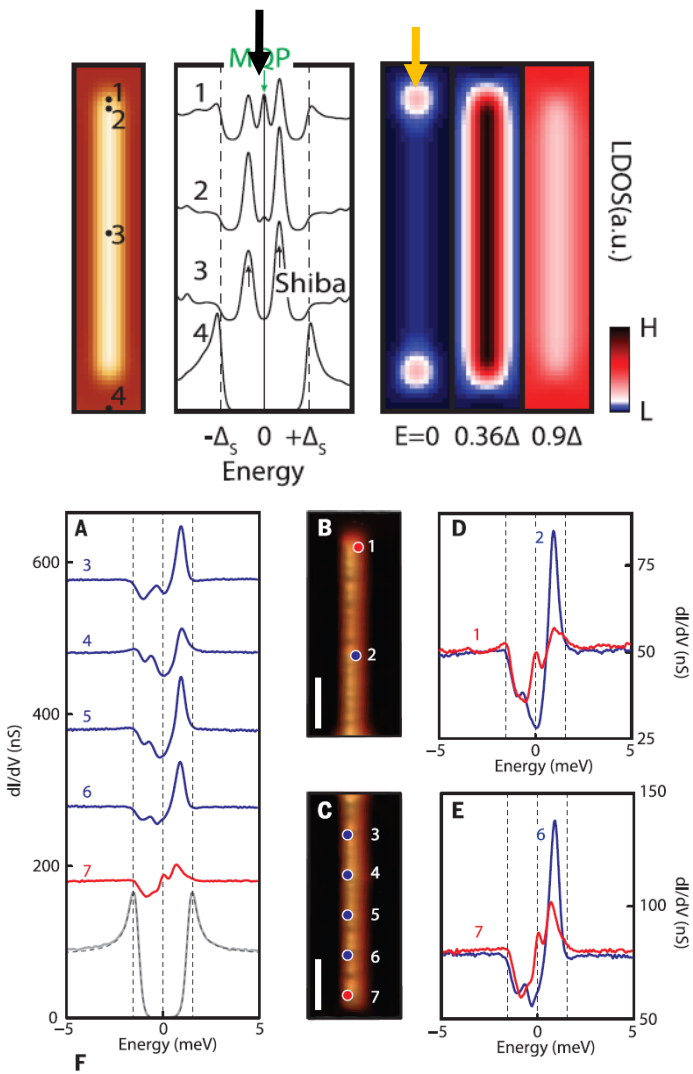

Stevan Nadj-Perge et al. *Science* **346**, 602-607 (2014).

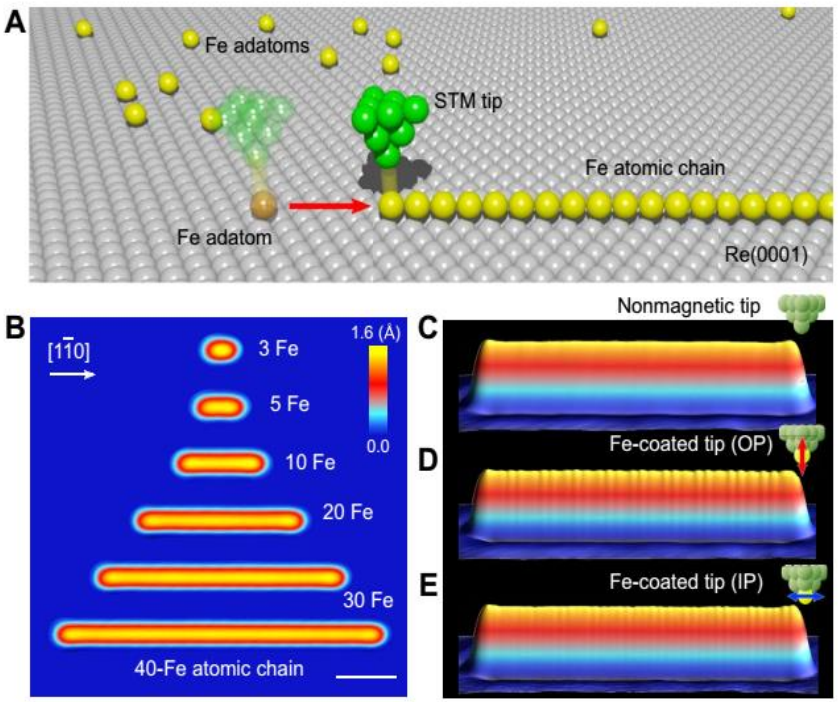

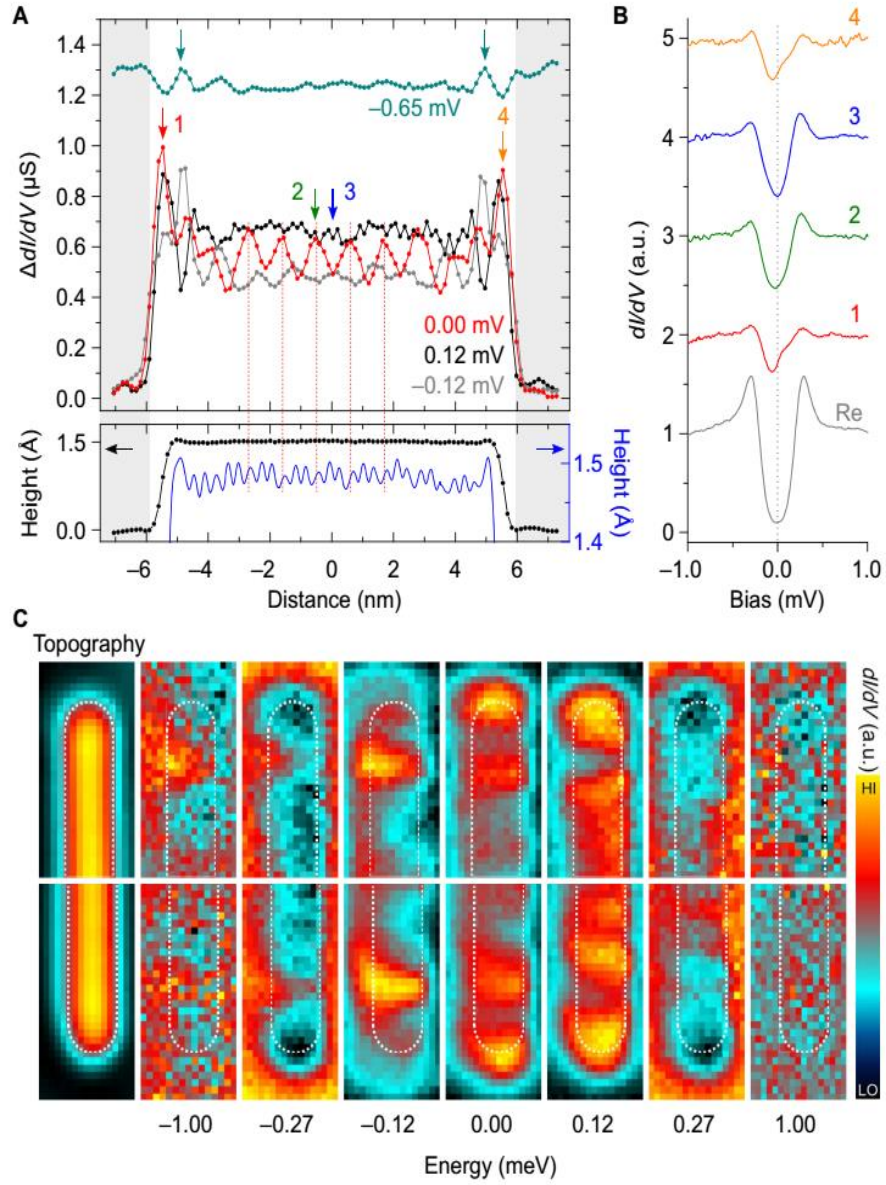

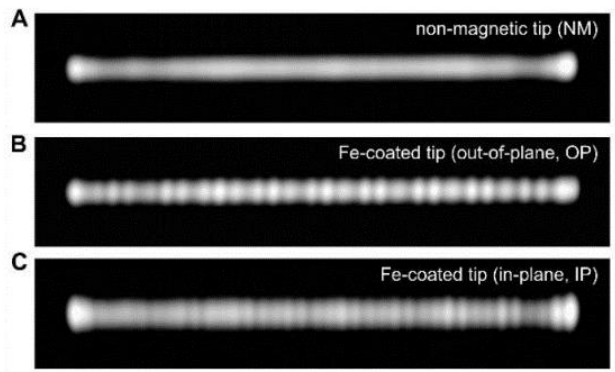

H. Kim, R. Wiesendanger* et al. Sci. Adv. 4, eaar5151 (2018).

RAPID COMMUNICATIONS

PHYSICAL REVIEW B **90**, 100509(R) (2014)

Odd-parity topological superconductor with nematic order: Application to $Cu_xBi_2Se_3$

Liang Fu

Department of Physics, Massachusetts Institute of Technology, Cambridge, Massachusetts 02139, USA

(Received 7 August 2014; revised manuscript received 25 August 2014; published 26 September 2014)

Time-reversal-invariant (T-invariant) topological superconductors in two and three dimensions are a new class of unconventional superconductors which exhibit a full superconducting gap in the bulk and gapless helical quasiparticles on the boundary

We predict that the spin-orbit interaction associated with hexagonal warping plays a crucial role in pinning the two-component order parameter and makes the superconducting state generically fully gapped, leading to a topological superconductor.

$$\Delta^o(\mathbf{k}) = \vec{d}(\mathbf{k}) \cdot \vec{\sigma}, \quad \text{where} \quad \vec{d}(\mathbf{k}) = -\vec{d}(-\mathbf{k}).$$

Odd parity gap

	Δ_{1a}	Δ_{1b}	Δ_2	Δ_3	Δ_{4x}	Δ_{4y}
Irreducible representation	A_{1g}	A_{1g}	A_{1u}	A_{2u}	E_u	
Pairing potential	σ_0	σ_x	$\sigma_y s_z$	σ_z	$\sigma_y s_x$	$\sigma_y s_y$
d-vector	-	-	$\sim (\lambda k_x, \lambda k_y, k_z)$	$\sim (-\lambda k_y, \lambda k_x, 0)$	$\sim (k_z, 0, -\lambda k_x)$	$\sim (\varepsilon k_x, -k_z, \lambda k_y)$
Parity	even	even	odd	odd	odd	
Topo. SC	no	no	yes	yes	yes	
Nematic SC	no	no	no	no	yes	

Schematic d-vector / gap structures

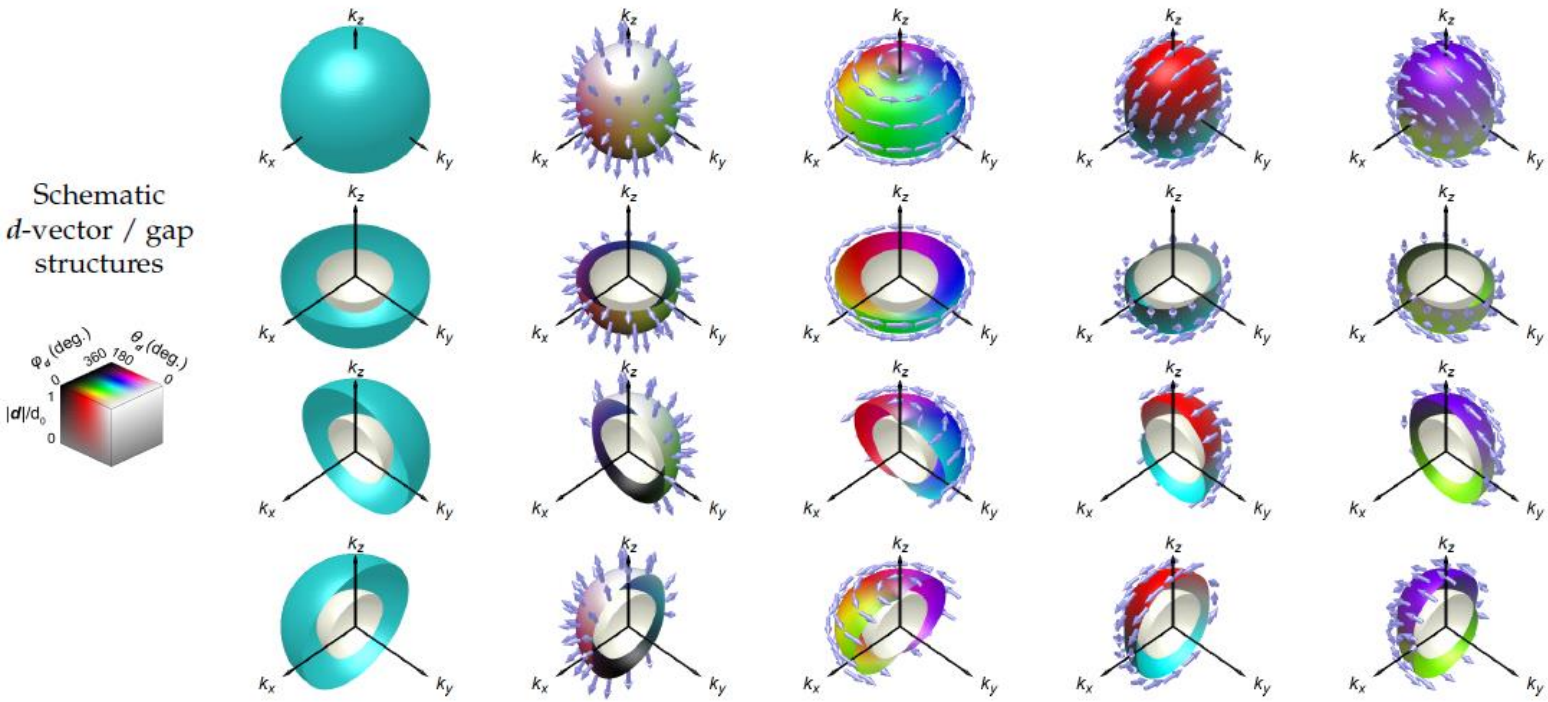

S. Yonezawa et al. Cond. Matt. Physics. 2019

Possible two-fold symmetry in $Cu_xBi_2Se_3$

Theoretical

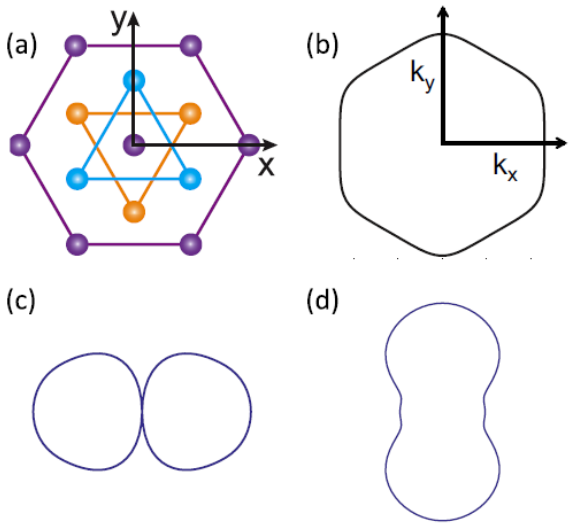

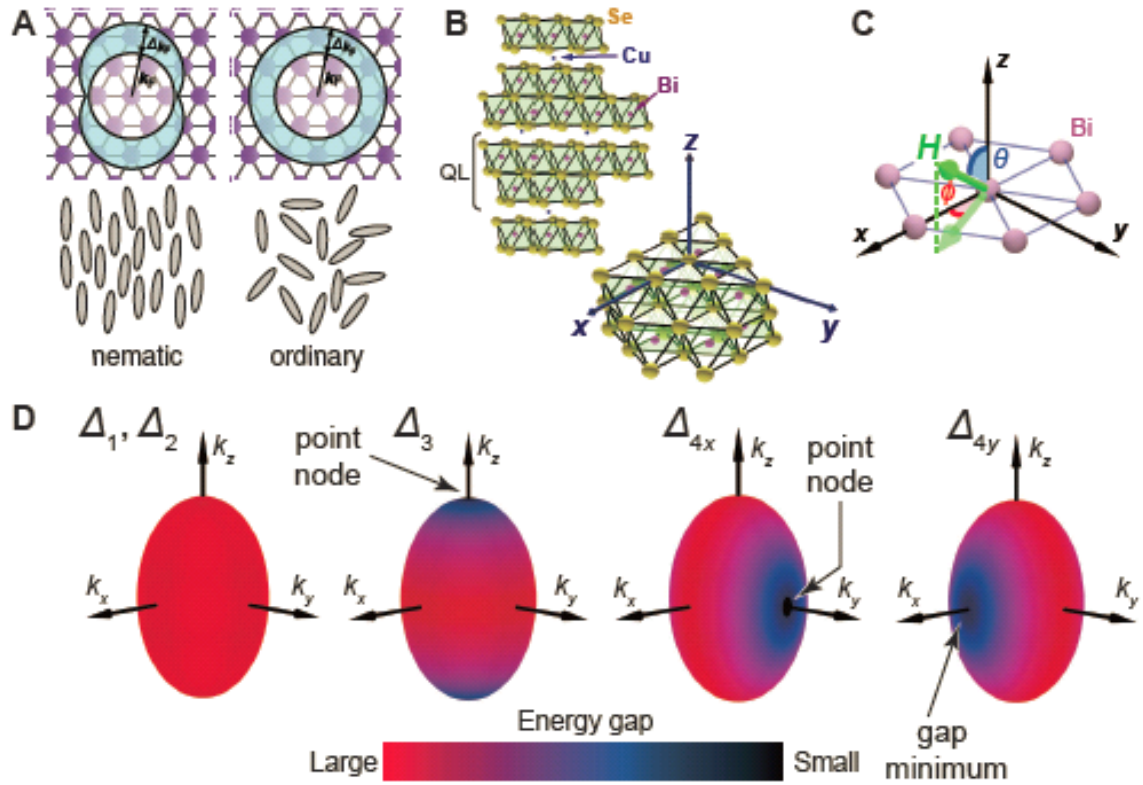

The two-fold superconductivity corresponds to the topological SC phase.

L. Fu, Phys. Rev. B 90, 100509(R) (2014)

NMR

Matano K. , et al. Nat. Phy. doi:10.1038/nphys3781 (2016)

Specific heat

Yonezawa S., et al., *Nat. Phys.* **13**, 123-126 (2017).

How about the bulk superconductivity in $Sr_xBi_2Se_3$?

Superconducting properties of sample 1

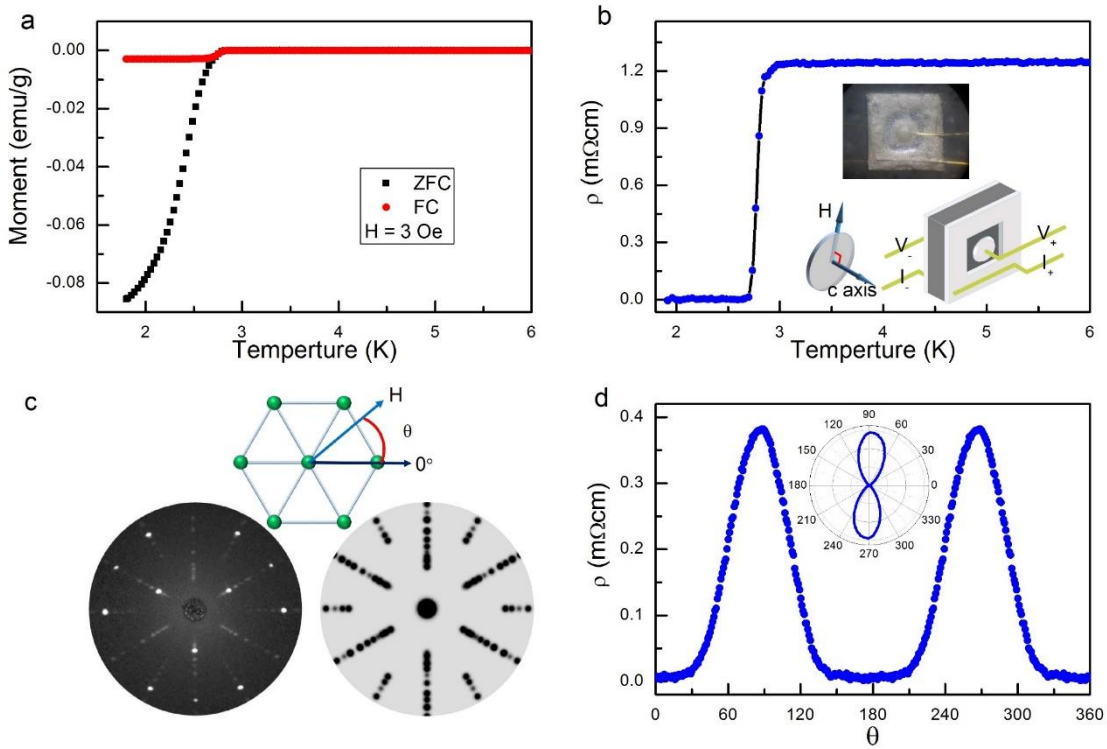

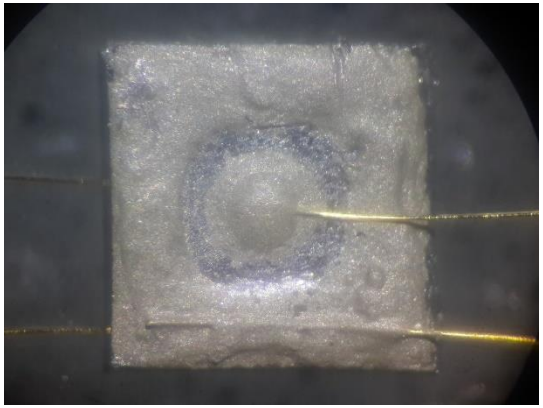

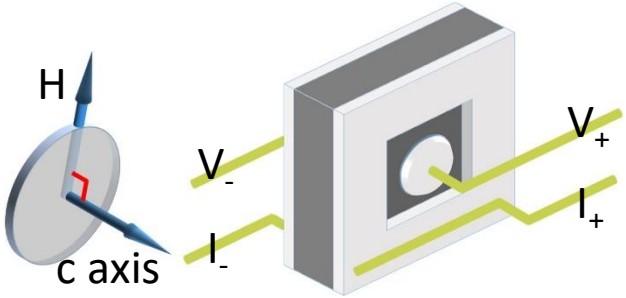

T_c = 2.78 K

Magnetic screening volume is about 92.4%

G. Du, HHW et al.,

Sci. China PMA60, 037411 (2017).

This configuration allows the current flowing always perpendicular to c-axis

The angular dependence of resistivity of sample 1-3 measured at various fields and temperatures.

S1

S2

S3

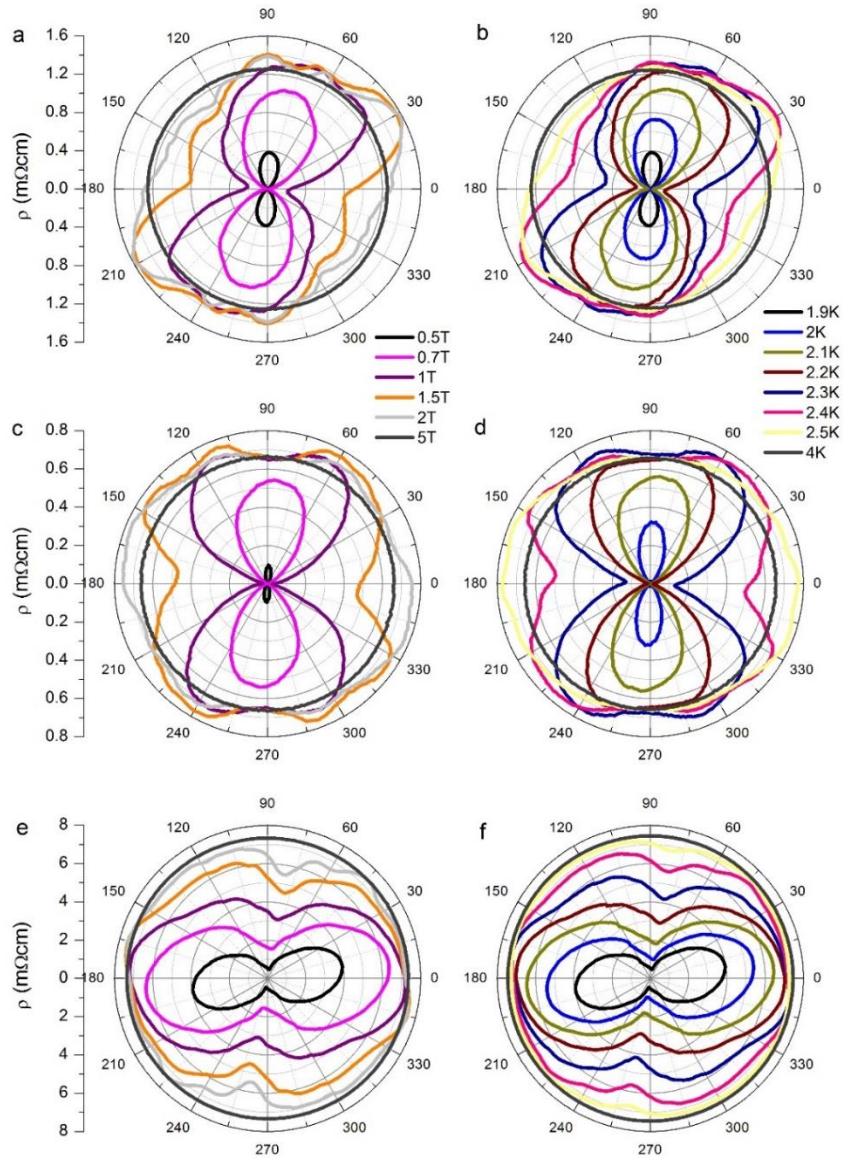

a, c, e are measured at 1.9 K.
b, d, f are measured at 0.5 T.

The maximum resistivity directions at 0.5 T and 1.9 K are defined as θ^{max}. For S1, S2, and S3, θ^{max} values are around 86.3◦, 86.7◦, and 3.9◦, respectively.

The maximum direction of the superconducting gap (θ^{min} for resistivity).

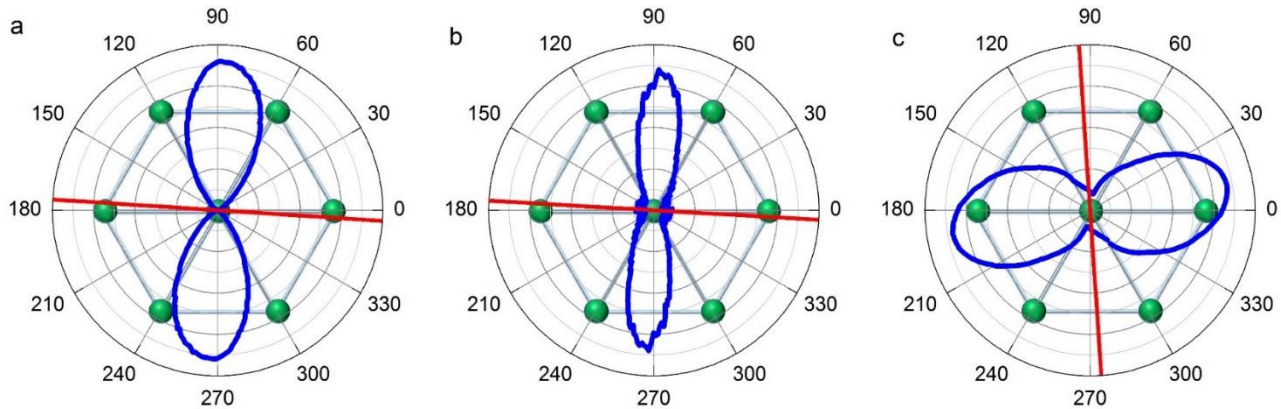

S1 S2 S3

Comparing with former studies:

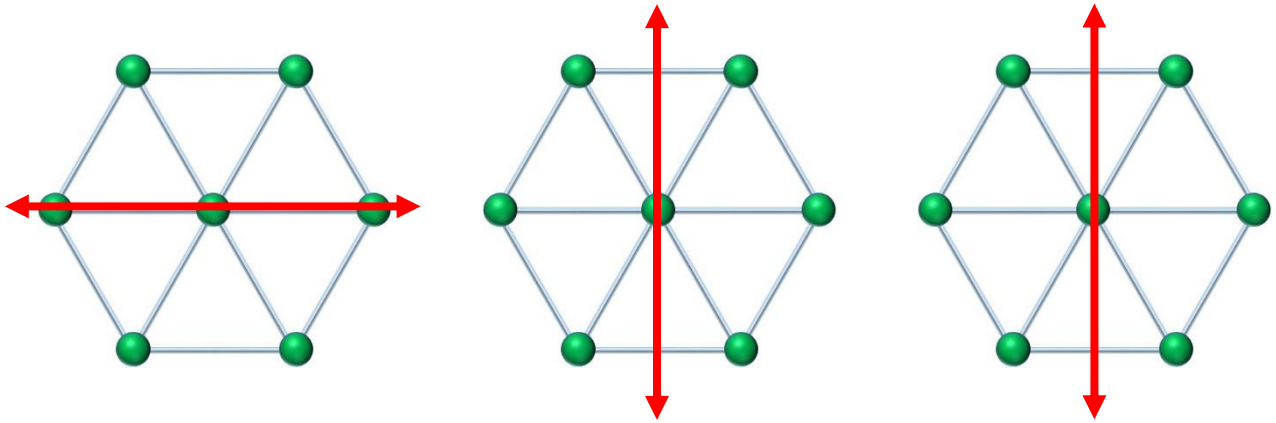

NMR Theoretical Specific heat

The maximum direction of the superconducting gap is either parallel or perpendicular to the main crystallographic axis.

Comparison with an iron based superconductor with isotropic superconductor

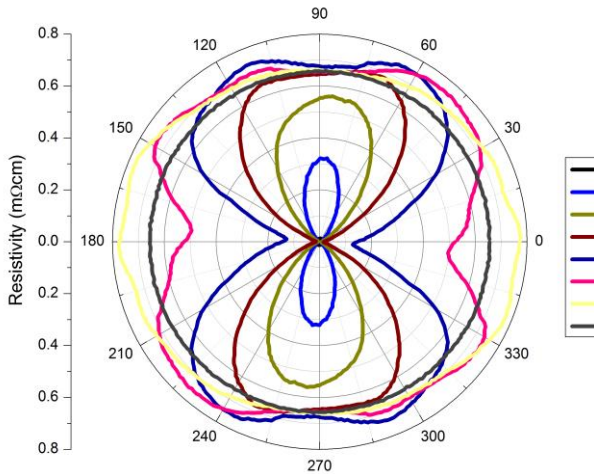

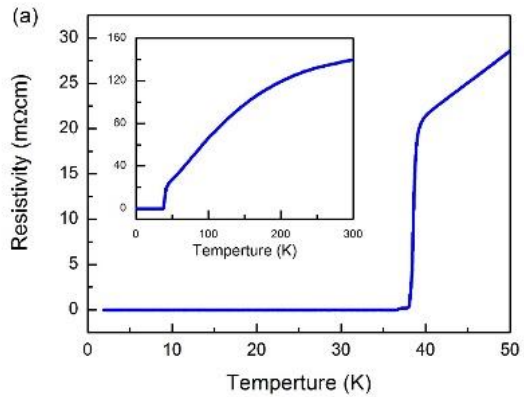

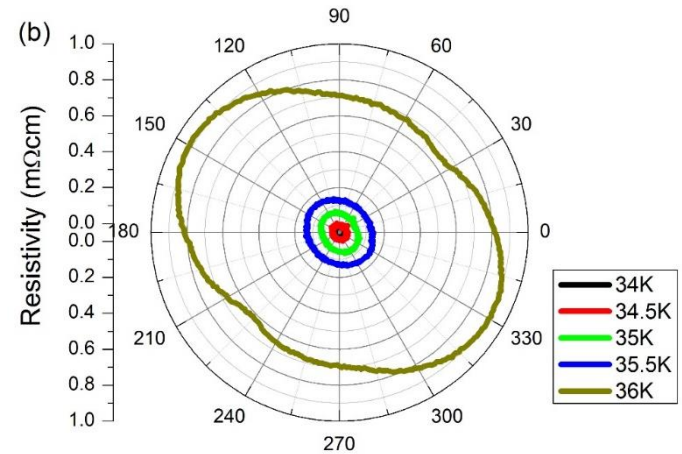

$Sr_xBi_2Se_3$

$Ba_{0.65}K_{0.35}Fe_2As_2$ single crystal in-plane isotropic superconductor

- The resistivity of $Ba_{0.65}K_{0.35}Fe_2As_2$ is zero below 35 K and quickly increase to the value of the normal state above 36 K.
- The simple dumbbell-shaped feature which is observed in the experiment of $Sr_xBi_2Se_3$ is absent in the data of $Ba_{0.65}K_{0.35}Fe_2As_2$.

Drive the Dirac Electrons into Cooper Pairs in $Sr_xBi_2Se_3$

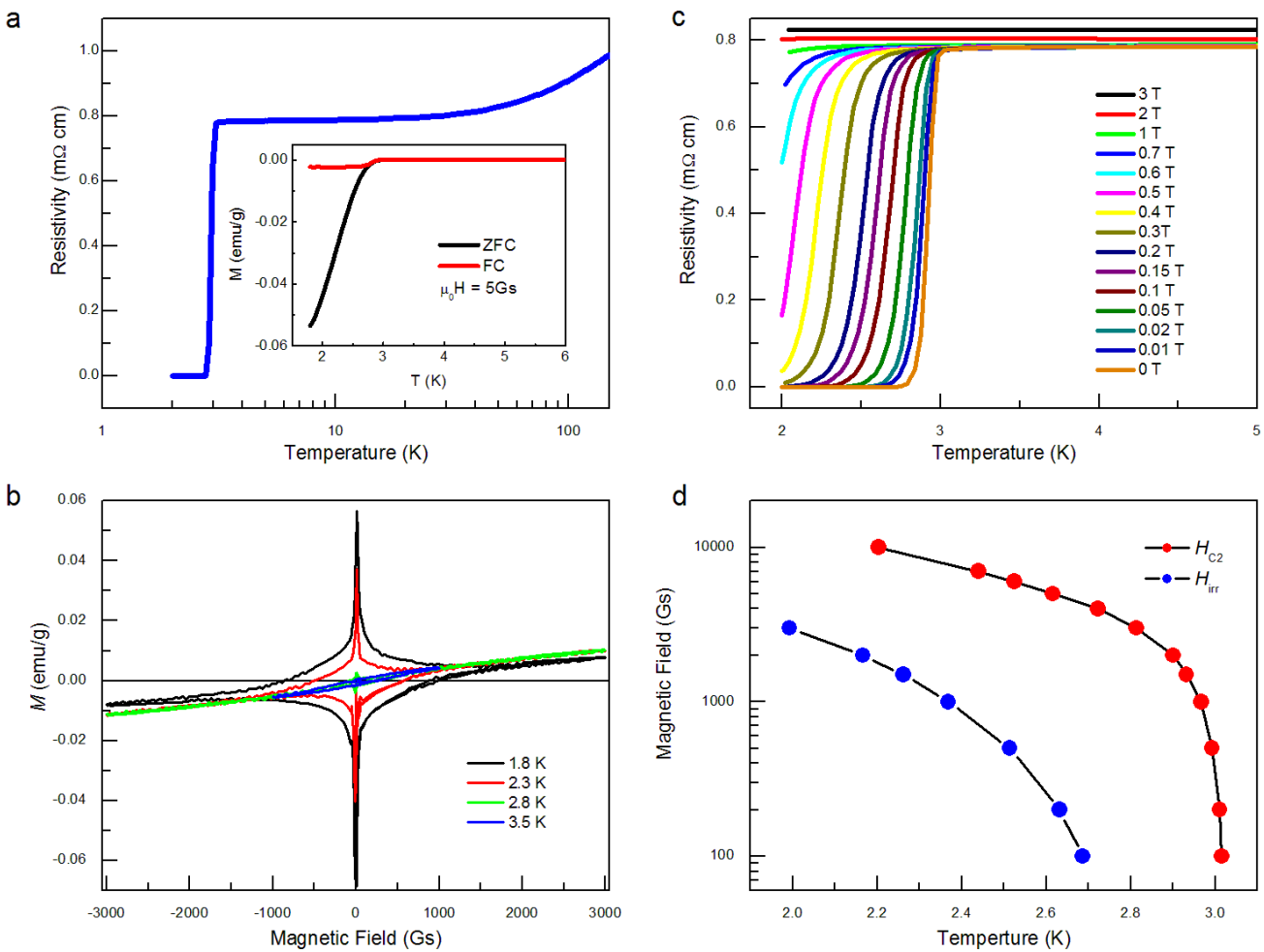

T_c = 3 K.
$\mu_0 H_{c2}$ = 3.5 T.

Magnetic screening volume is about 91.6% at 1.8K.

G. Du, HHW et al., Nat. Commun. **8**, 14466 (2017)

Area with intercalated Sr impurities (Sr clusters)

— STS spectra with superconducting gapped feature

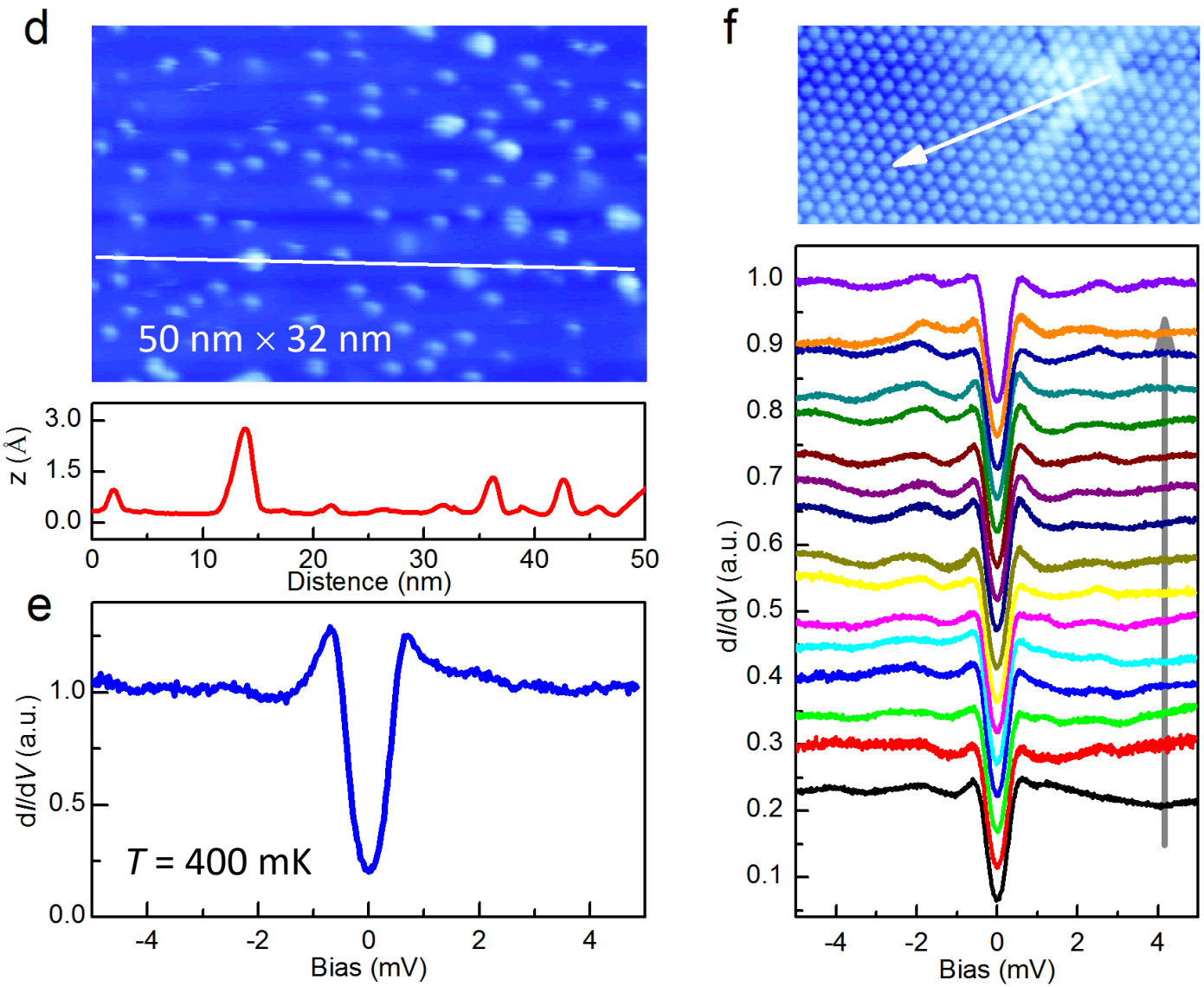

G. Du, Hai-Hu Wen et al., Nat. Commun. **8**, 14466 (2017)

Full superconducting gaps and theoretical fittings

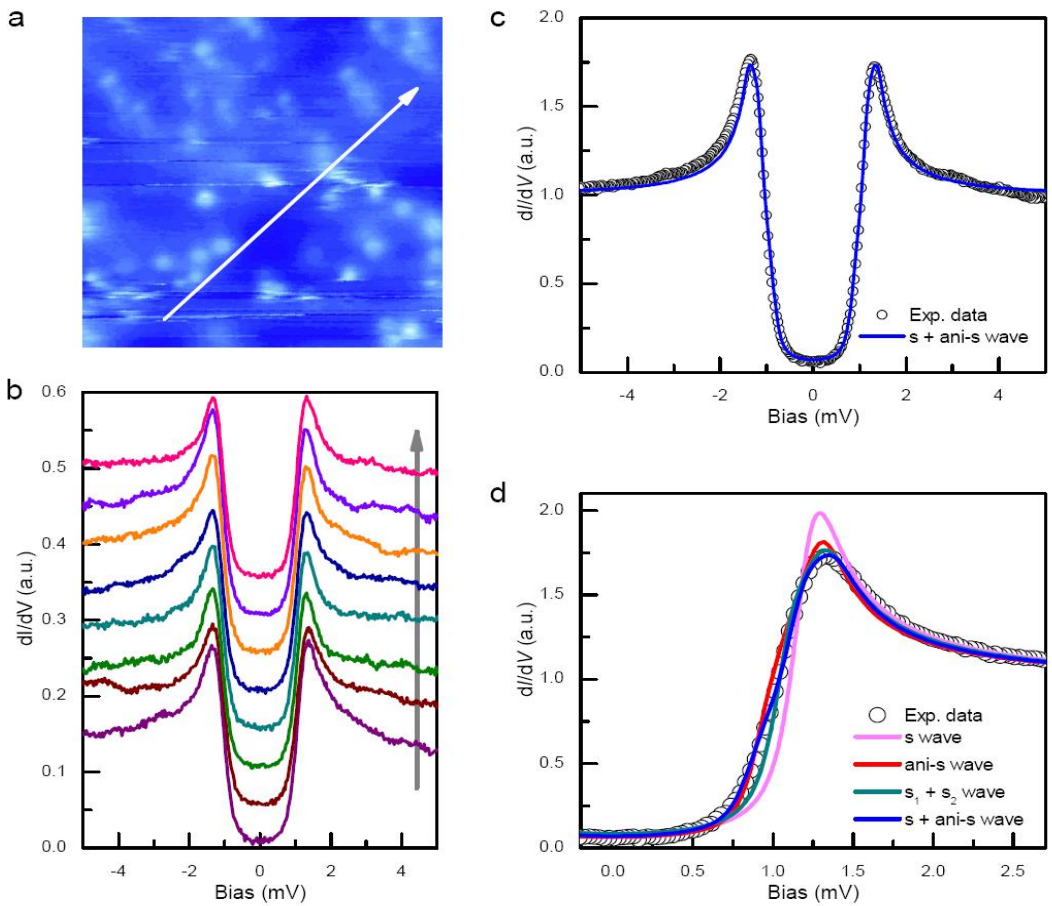

Fitting with two components associating with double gaps (*s* & ani-*s* wave).

A combination of the *s* wave with the weight of 27% and the ani-*s* wave gap with the weight of 73% turns out to give the best fit.

$$I(V) \propto \int_{-\infty}^{\infty} d\varepsilon \int_0^{2\pi} d\theta [f(\varepsilon) - f(\varepsilon + eV)] \times \mathrm{Re}\left\{\frac{\varepsilon + eV - i\Gamma}{[(\varepsilon + eV - i\Gamma)^2 - \Delta^2(\theta)]^{1/2}}\right\},$$

27% S-wave
73% anisotropic S-wave

Temperature and magnetic field dependence of tunneling spectra, and the Landau levels.

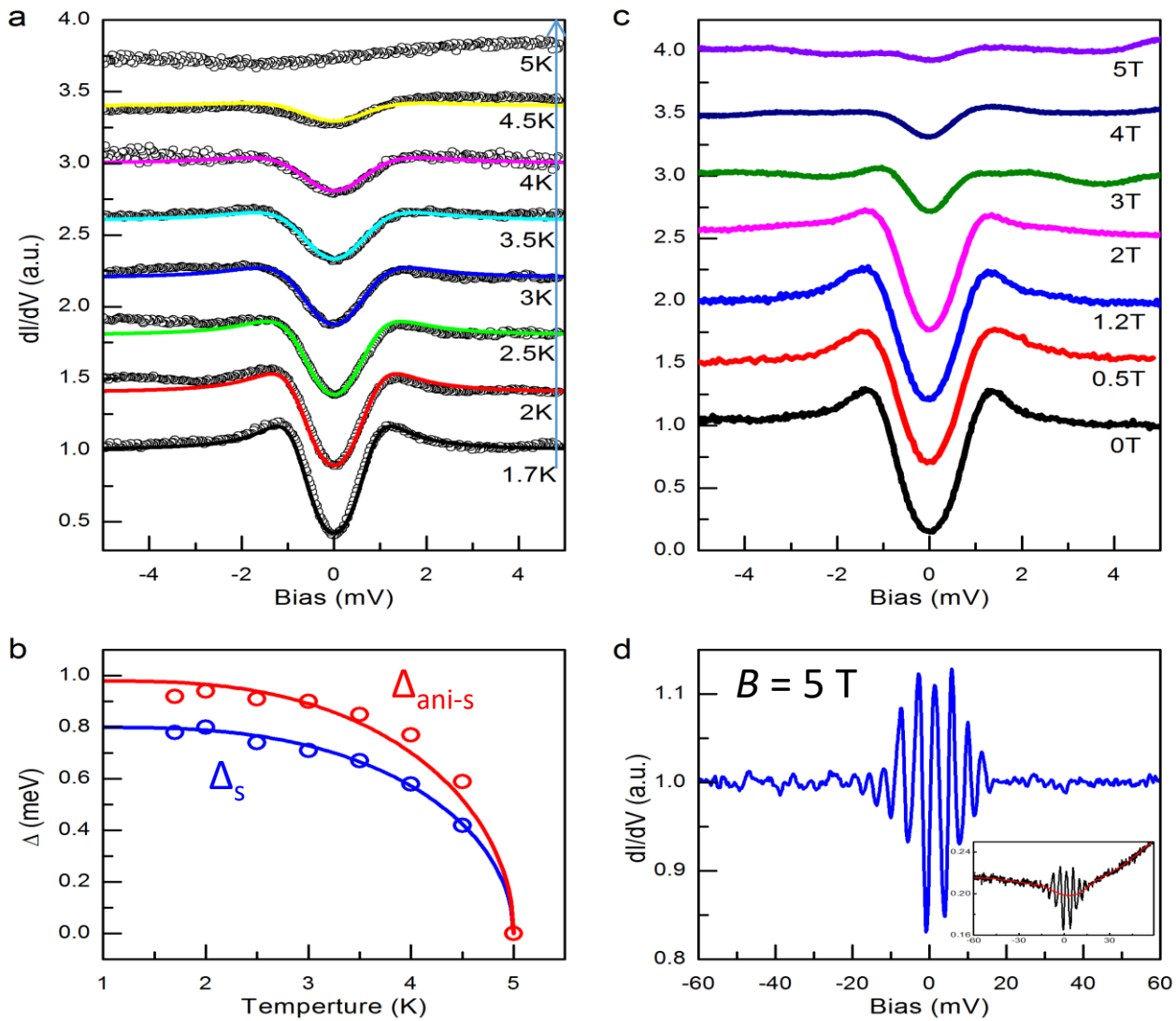

Data averaged over space

Data averaged for STS at the same position

Due to the Landau levels of the Dirac electrons

The variation of LL oscillations with magnetic field.

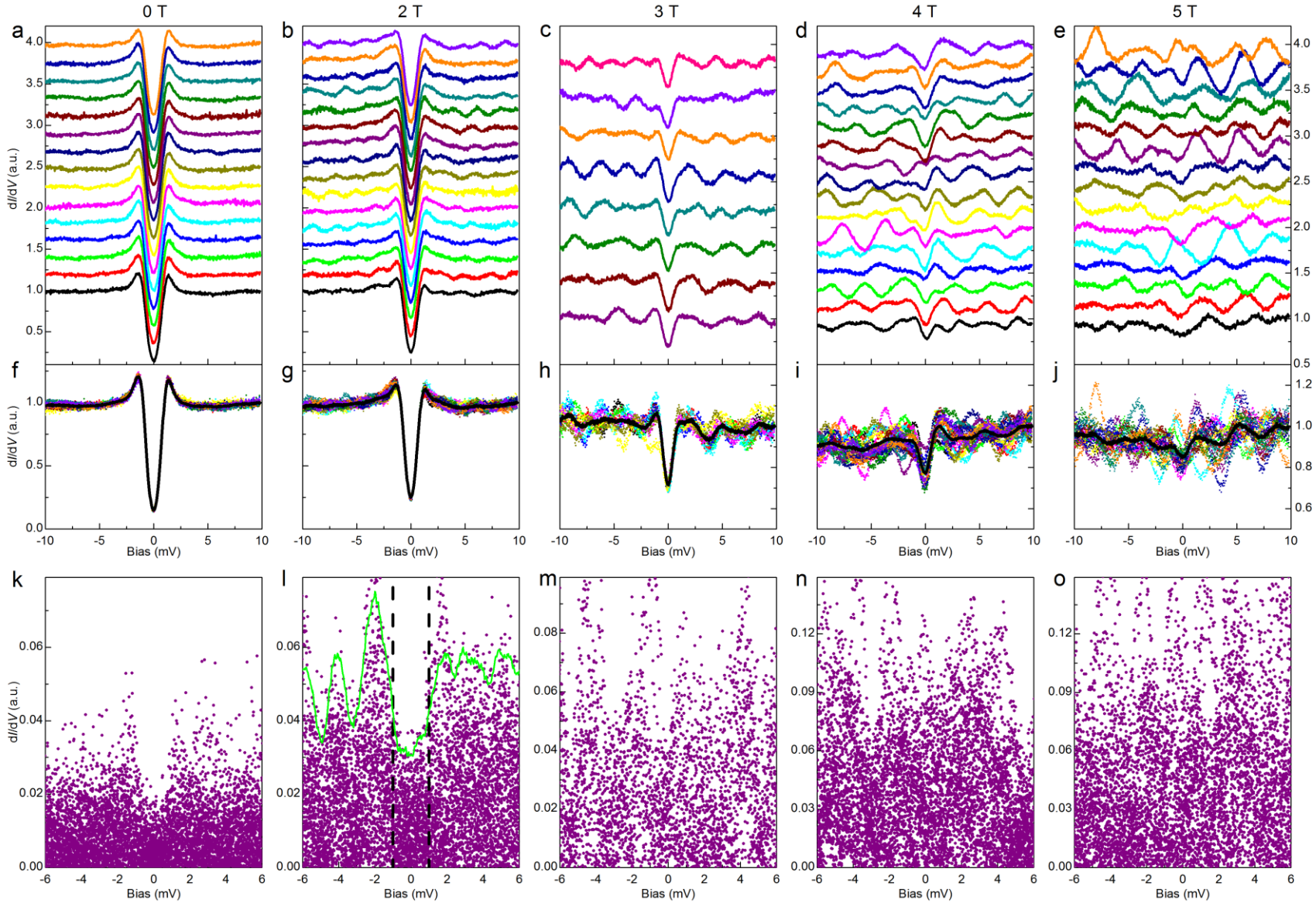

G. Du, HHW et al., Nat. Commun. **8**, 14466 (2017)

Surface Dirac electrons are driven into Coopers by the self-proximity effect. The bulk SC gap has certain anisotropy.

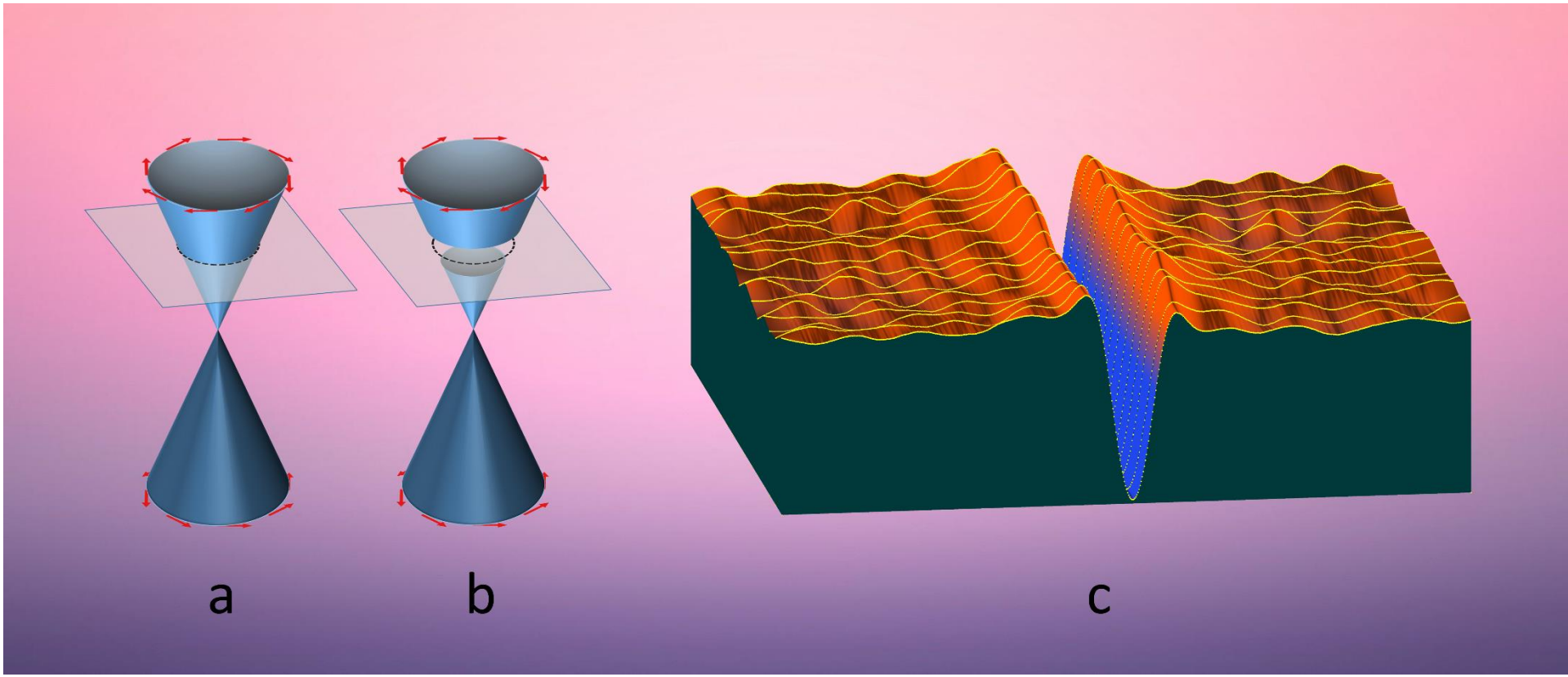

G. Du, HHW et al., Nat. Commun. **8**, 14466 (2017)

Topological insulator/superconductor heterostructure

Jinfeng Jia's group

$Bi_2Se_3/NbSe_2$

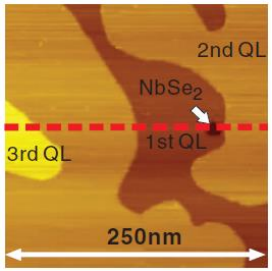

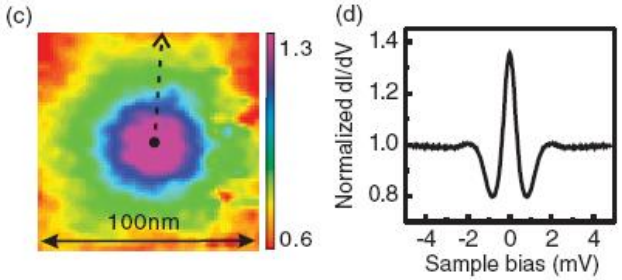

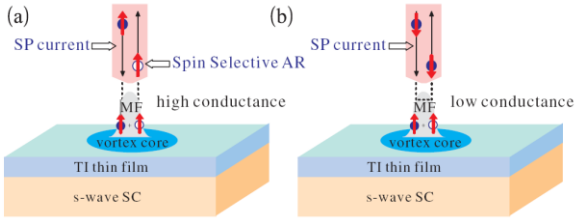

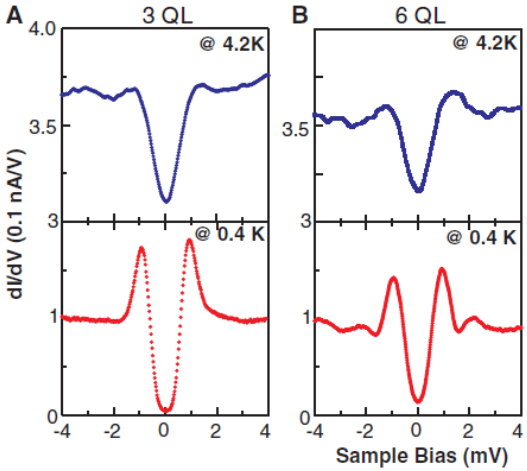

Proximity effect induced superconductivity.

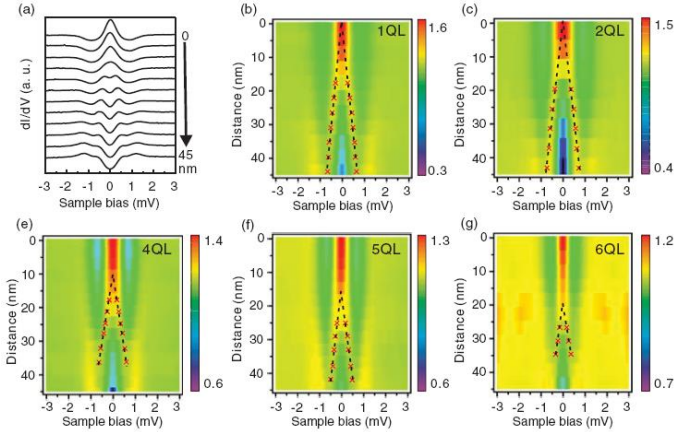

This unusual splitting behavior could be possibly due to the Majorana fermion zero mode.

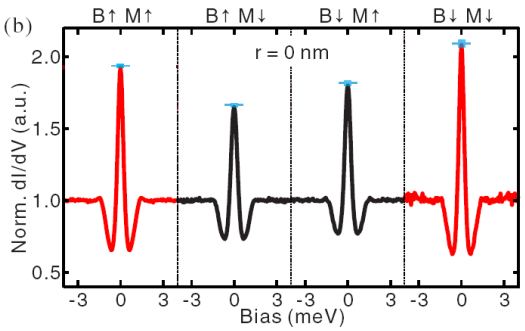

The Majorana mode at the center of vortex core is spin polarized. The spin selective Andreev reflection is observed.

M.X. Wang, *Science* **336**, 52-55 (2012). J.P. Xu, et. al., *Phys. Rev. Lett.* **114**, 017001 (2015). Hao-Hua Sun, et. al., PRL 116, 257003 (2016).

Bi_2Te_3 thin films on the $FeTe_{0.55}Se_{0.45}$

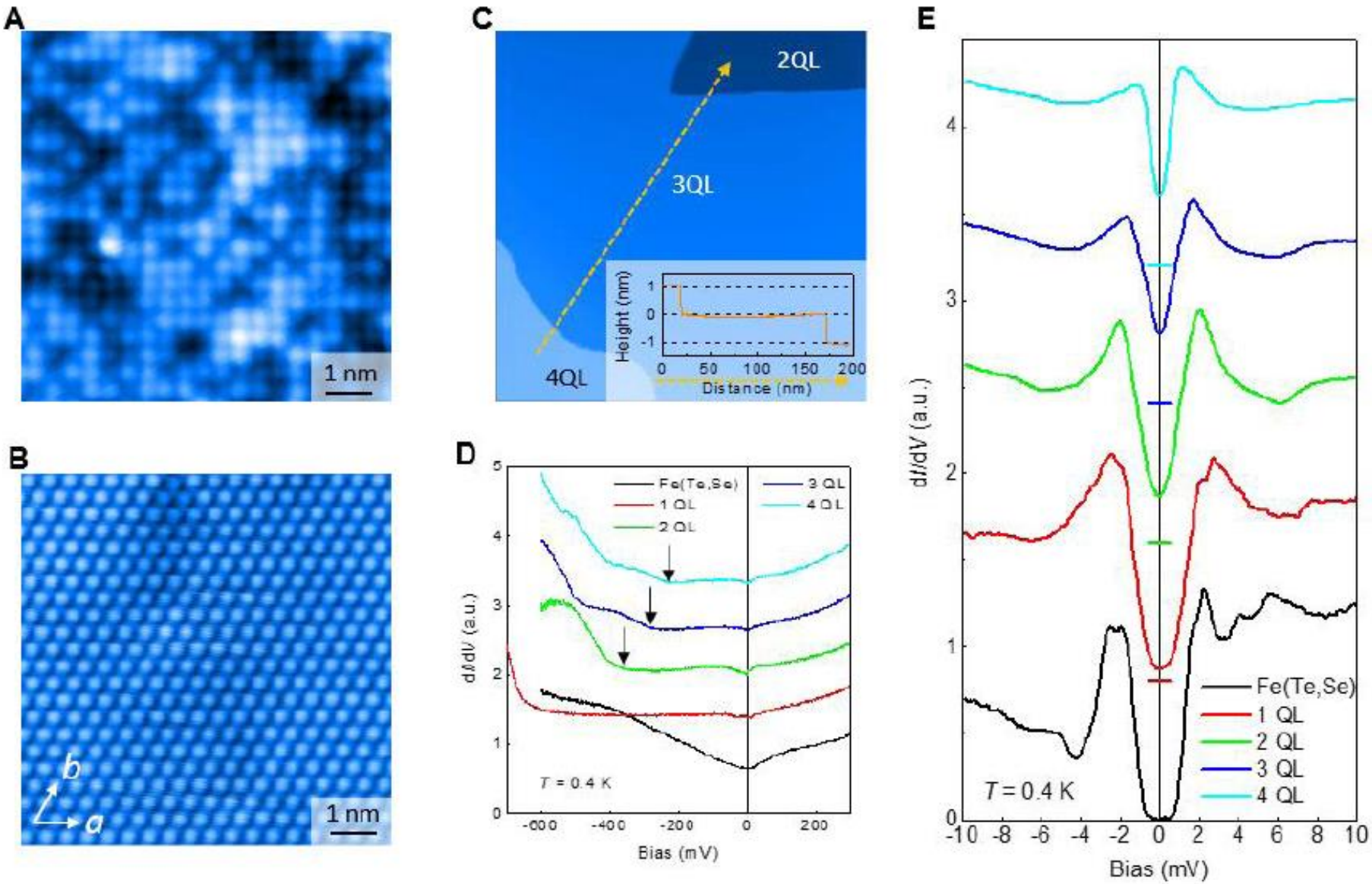

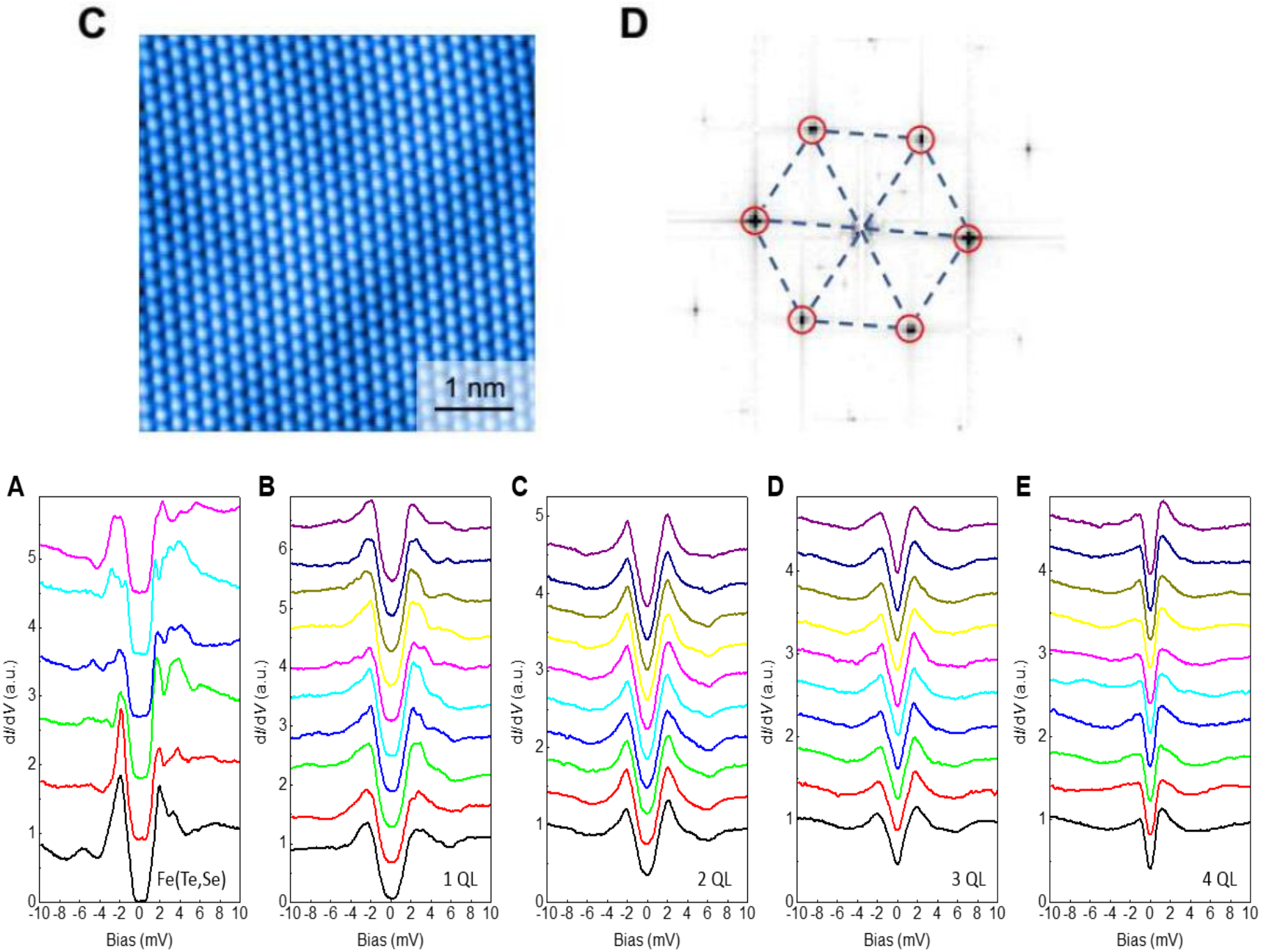
C
1 nm
D
A
Fe(Te,Se)
B
1 QL
C
2 QL
D
3 QL
E
4 QL
dI/dV (a.u.)
Bias (mV)

Quasiparticle Interference (QPI), or FT-STS

QPI in a metal

$$w(i \to f) \propto \frac{2\pi}{\hbar} |V(\vec{q})|^2 n_i(E_i, \vec{k}_i) n_f(E_f, \vec{k}_f)$$

M. Crommie *et al.*, Nature 363, 524 (1993).

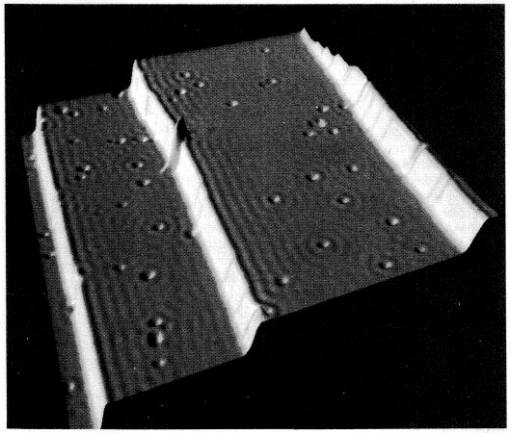

QPI in SC: Bogoliubov QPs

$$E_{\pm}(\vec{k}) = \pm\sqrt{\varepsilon(\vec{k})^2 + |\Delta(\vec{k})|^2}$$

$$w(i \to f) \propto \frac{2\pi}{\hbar} \boxed{\left| u_{k_i} u^*_{k_f} \pm v_{k_i} v^*_{k_f} \right|} |V(\vec{q})|^2 n_i(E_i, \vec{k}_i) n_f(E_f, \vec{k}_f)$$

$$u_k = \frac{\Delta(k)}{|\Delta(k)|} \sqrt{\tfrac{1}{2}\left(1 + \tfrac{\varepsilon(k)}{E(k)}\right)}; v_k = \sqrt{1 - u_k^2}$$

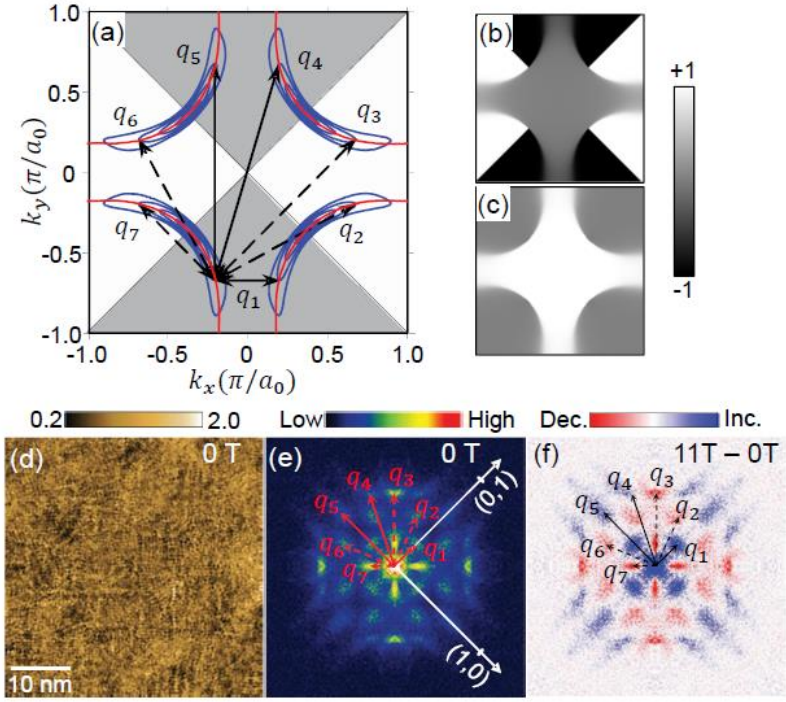

T. Hanaguri et al. Science323, 923(2009).

The QPI intensity appears along one of the Γ-K directions below the gap

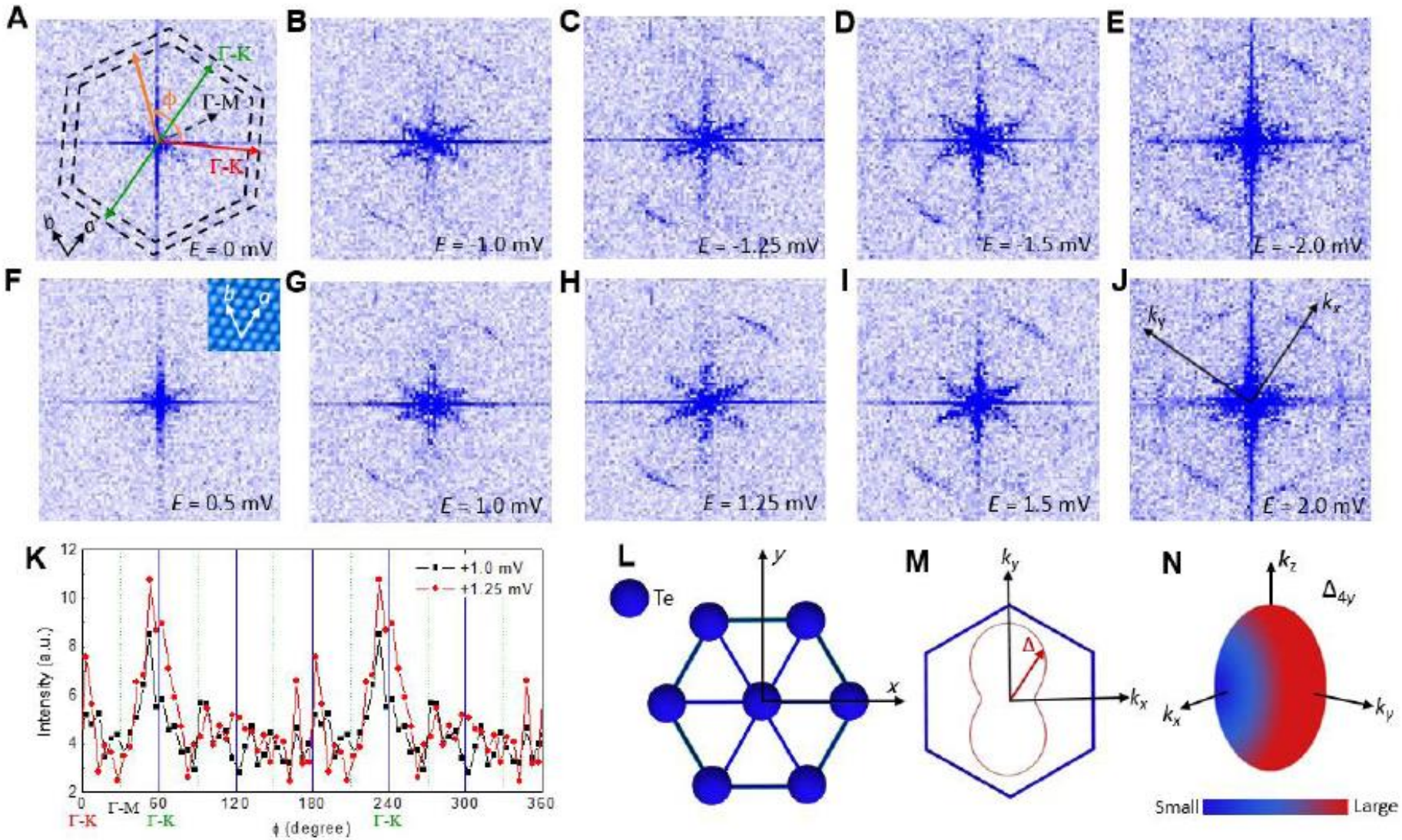

M. Y. Chen, X. Y. Chen, Huan Yang, HHW et al..
Sci. Adv. 4, eaat1084 (2018).

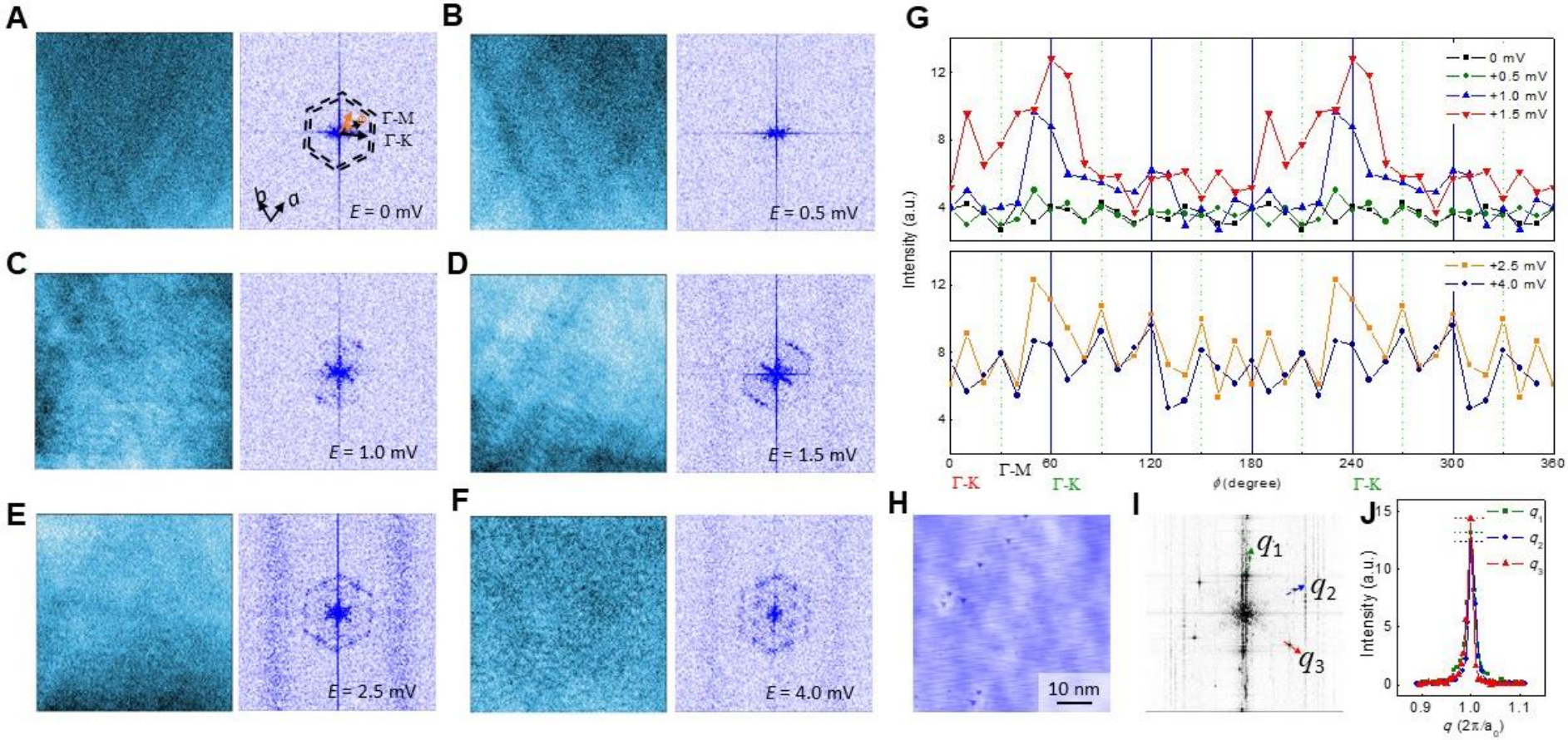

Control experiment: another set of measurements
Fermi surface becomes six-fold beyond the gap.

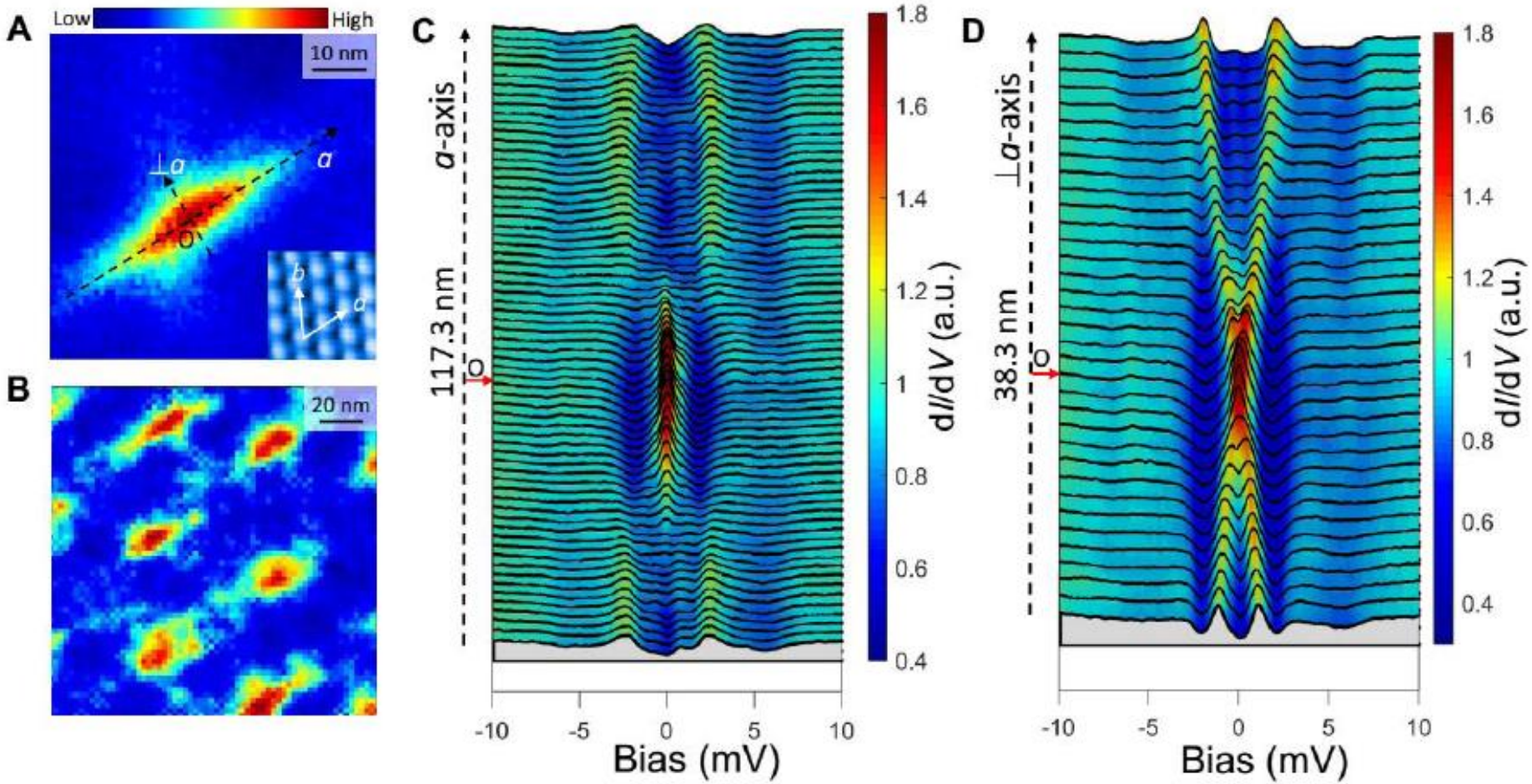

- Elongated vortices, due to two-fold SC gap. The elongated direction is along one of the a-axis.
- Fermi velocity is six-fold or isotropic, not due to the Fermi velocity problem.
- Along a-axis, the core state is always sitting at zero bias, with a small tail of splitting. While along the perpendicular direction, the central peak splits into two, as usual.

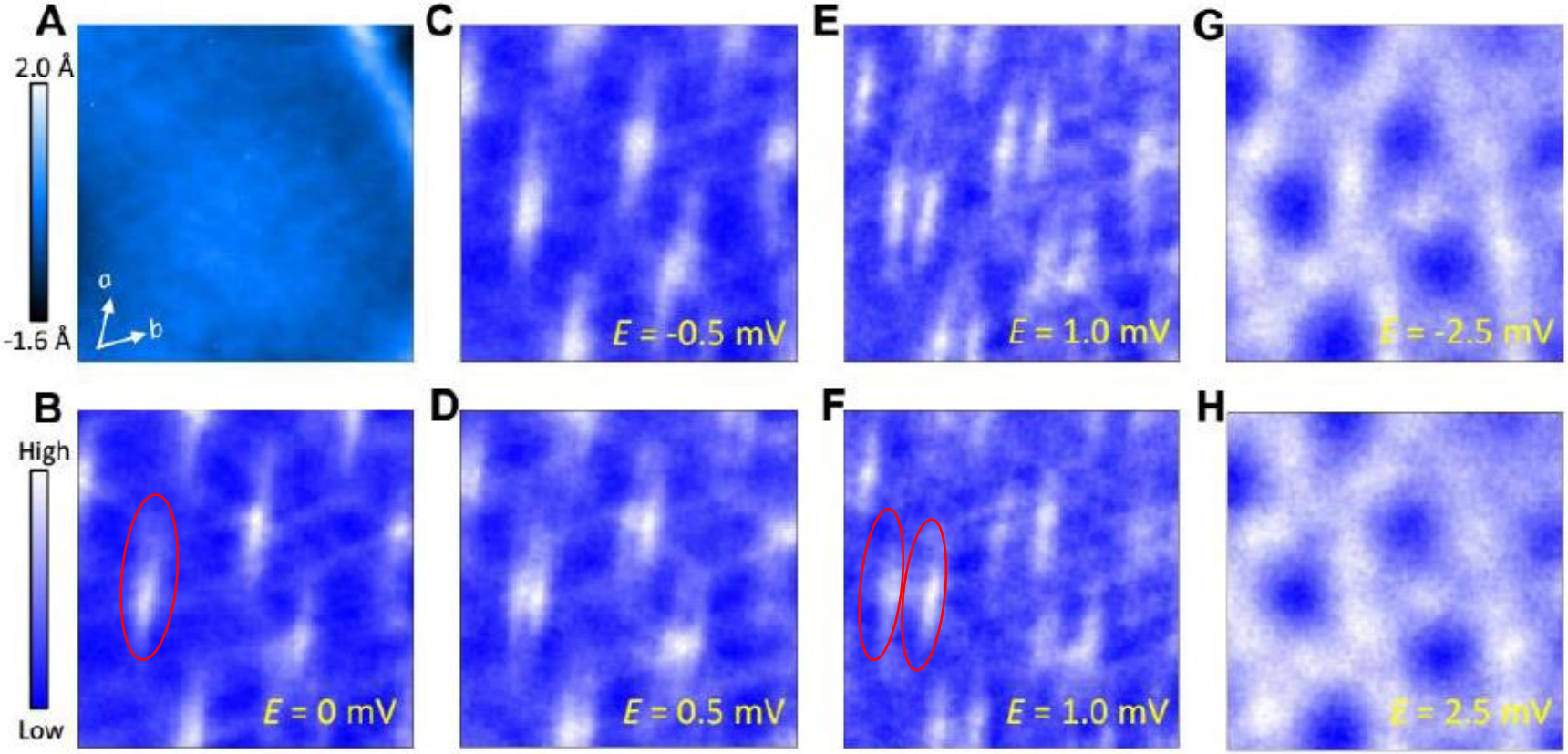

By increasing energy, the vortex image changes from one bar to two within the gap. While the vortex shape becomes roughly round outside the gap region.

M. Y. Chen, X. Y. Chen, Huan Yang, HHW et al..
Sci. Adv. 4, eaat1084 (2018).

Nematic Skyrmions in odd-Parity Superconductors

A. A. Zyuzin, Julien Garaud, and Egor Babaev

Phys. Rev. Lett. 119, 167001 (2017)

$Cu_xBi_2Se_3$

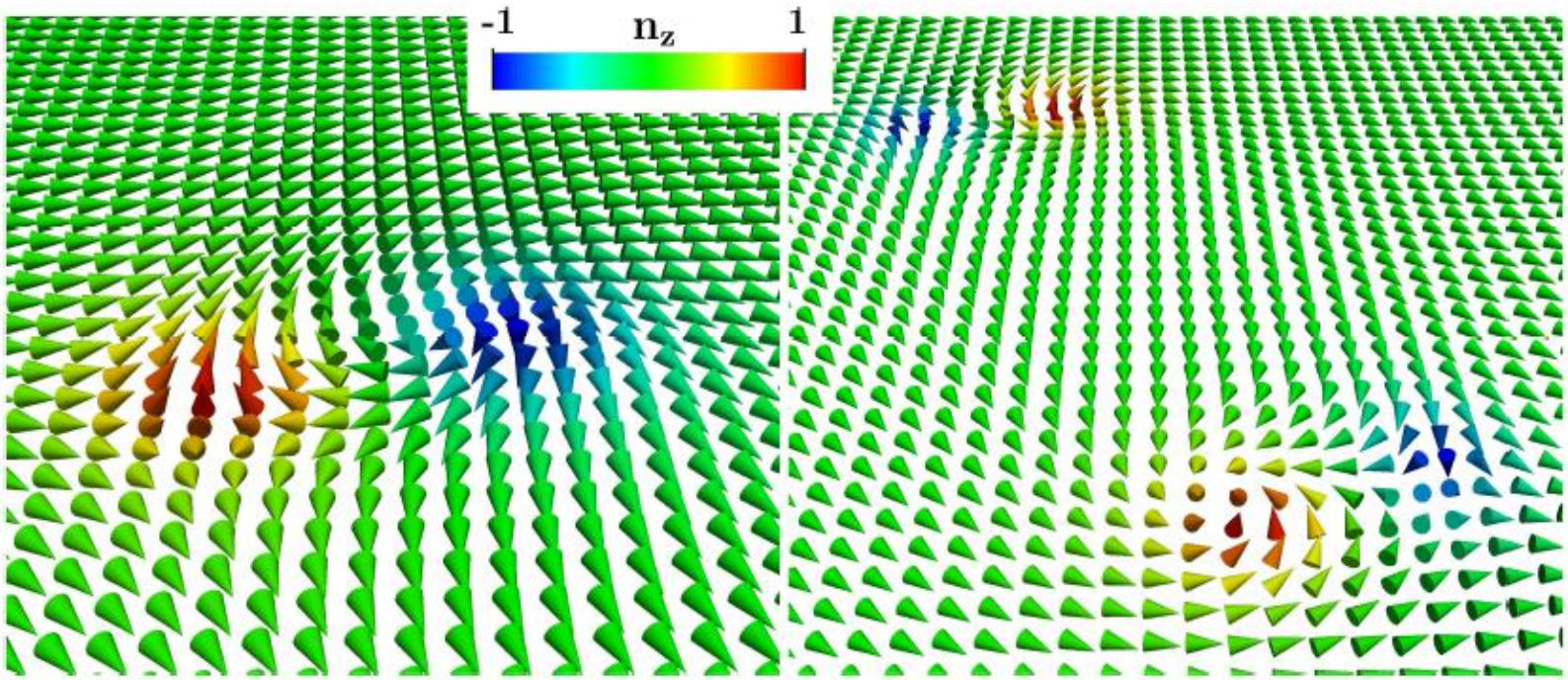

Vortex with two half chiral spin cores?

The spin degeneracy is lifted here.

Concluding Remarks

- Superconductivity has been induced in Bi_2Te_3 thin film deposited on $FeTe_{0.55}Se_{0.45}$ by proximity effect.
- QPI illustrates directly a twofold gap feature with the minimum gap along one of the main axes, supporting the D_{4y} pairing manner.
- Elongated vortex has been observed, supporting the twofold symmetric SC measured by QPI.
- Combining with theory, we believe an uniform SC state with odd pairity has been easily made and proved.

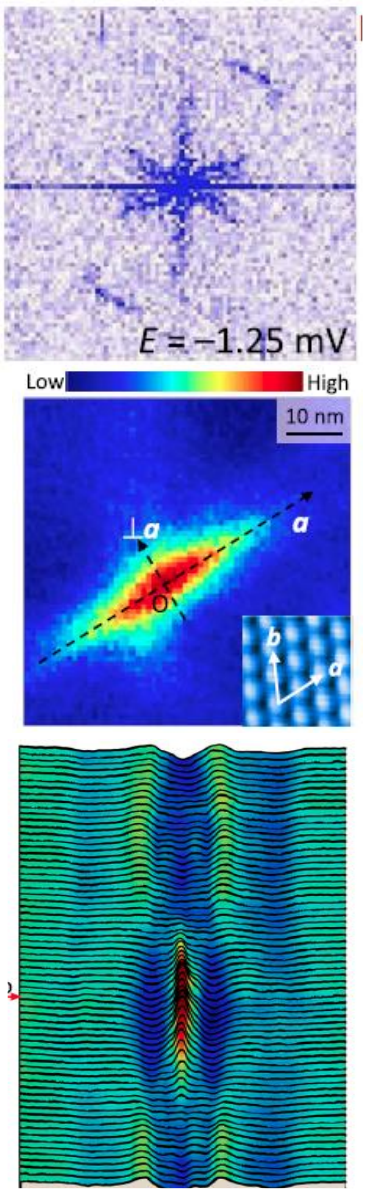

M. Y. Chen, X. Y. Chen, Huan Yang, HHW et al..
Sci. Adv. 4, eaat1084 (2018).

Collaborators

- **Samples, STM, Transport, Laue @ NJU**

Huan Yang

杨　欢

Mingyang Chen

陈明扬

Xiaoyu Chen

陈晓宇

Guan Du

杜　冠

- **Sample growth and characterization:**

Jifeng Shao, Changjing Zhang, Yuheng Zhang @ HF-CHMFL

Kejin Ran, Jingsheng Wen @ NJU

J. Schneeloch, R. D. Zhong, Genda Gu @ BNL

Thank you for your attention!